



**UNIVERSITY *of the***  
**WESTERN CAPE**

**FACULTY OF SCIENCE**  
**DEPARTMENT OF EARTH SCIENCE**  
**ENVIRONMENTAL AND WATER SCIENCE**

**Improving estimation of precipitation and prediction  
of river flows in the Jonkershoek mountain catchment**

*UNIVERSITY of the*  
*WESTERN CAPE*

*A thesis submitted in fulfillment of the requirements for the degree of Magister Scientiae in the  
Department of Earth Sciences, University of the Western Cape.*

**by**

**Siphumelelo Mbali**

Supervisor : Prof D. Mazvimavi

Co-Supervisor : Dr. N. Allsopp

November 2016

## **Key words**

Rainfall estimation

Mountain catchments

Cloud water interception

Streamflow modelling

Langrivier catchment

Jonkershoek

Western Cape

South Africa



UNIVERSITY *of the*  
WESTERN CAPE

## ABSTRACT

### **Improving estimation of precipitation and prediction of river flows in the Jonkershoek mountain catchment**

S. Mbali

MSc thesis, Department of Earth Sciences, University of the Western Cape, Private Bag X17, Bellville 7535, South Africa

Rainfall is the main input into the land phase of the hydrological cycle which greatly determines the available water resources. Accurate precipitation information is critical for mountain catchments as they are the main suppliers of usable water to the human population. Rainfall received in mountain catchments usually varies with altitude due to the orographic influence on the formation of rainfall. The Langrivier mountain catchment, a sub-catchment of the Jonkershoek research catchment, was found to have a network of rain gauges that does not accurately represent the catchment rainfall. As a result, this study aimed to improve the estimation of catchment precipitation and evaluate how improving estimation catchment precipitation affects the prediction of streamflows.

Improving estimation of catchment rainfall in mountain catchments requires that a network of rain gauges that enables accurate estimation of the catchment rainfall is established. Establishment of such a network is problematic in mountainous areas such as Langrivier since some of the locations are not accessible and/or difficult to routinely visit for collecting rainfall data. Furthermore, rainfall is not the only form of precipitation in mountain catchments. Clouds directly contribute to precipitation in mountain catchments through cloud water interception. For most mountain catchments, the contribution of cloud water interception to total precipitation and consequently streamflows is unknown. Therefore, this study expanded the existing rain gauge network in Langrivier to include higher elevation areas of the catchment in order to improve estimation of catchment rainfall. The contribution of cloud water interception to total precipitation was assessed by monitoring cloud water precipitation along an altitudinal transect using Lovred fog screen gauges.

Rainfall results revealed that the rain gauge network that was in place before it was expanded to higher elevation levels was underestimating catchment rainfall. Rainfall measured at 360-800

m.a.s.l altitudinal range in Langrivier is statistically similar at  $p = 0.05$ , with only the rainfall measured at 1214 m.a.s.l being significantly different from the rainfall at the 360-800 m.a.s.l altitudinal range. Cloud water contributes up to 35% to total precipitation at higher elevation areas. Cloud water is critical in the summer season; cloud water contributed over 200 mm to the total precipitation at higher elevations in summer month December 2014. Having improved estimation of catchment precipitation, the ACRU model was used predict streamflow of the Langrivier.

Improving estimation of catchment precipitation led to improved predictions of streamflow for the Langrivier catchment. While streamflow modelling was undertaken with precipitation input either being rainfall only or both rainfall and cloud water interception, the best simulation results were achieved by using rainfall only as precipitation input. Inclusion of cloud water interception to precipitation input led to ACRU over estimating streamflows. Cloud water does not directly contribute to streamflow hydrograph characteristics; cloud water only leads to a reduction of evaporation rates. Configuring the model to be lumped or semi-distributed mode had an effect on modeling results. Ultimately, this study contributed improved understanding of the design of rain gauge networks, importance of cloud water to the Langrivier catchment and hydrological responses of small mountain catchments.

**Keywords:** Rainfall, cloud water, improving estimation precipitation, hydrological responses

## Declaration

I declare that “*Improving estimation of precipitation and prediction of river flows in the Jonkershoek mountain catchment*” is my own work, that it has not been submitted for any degree or examination in any other university, and that all the sources I have used or quoted have been indicated and acknowledged by complete references.

Full name: Siphumelelo Mbali

Date: 24 November 2016

Signed: .....



UNIVERSITY *of the*  
WESTERN CAPE

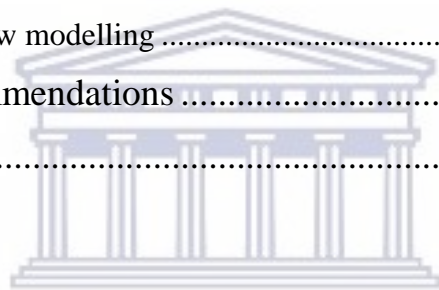
# Table of contents

---

Dedication .....	xiii
Acknowledgements .....	xiv
1 Introduction.....	1
1.1 General background .....	1
1.2 Aim.....	5
1.3 Research Outline .....	6
2 Review on estimation of catchment precipitation and streamflow hydrological modeling.....	7
2.1 Introduction .....	7
2.2 Status of catchment rainfall monitoring .....	8
2.3 Estimation of catchment precipitation.....	9
2.4 Design of rain gauge networks in mountain catchments.....	10
2.5 Estimating catchment rainfall using rain gauges.....	11
2.6 Contribution of cloud water to catchment precipitation.....	12
2.7 Measurement of cloud water interception.....	13
2.8 Prediction of stream flows.....	14
2.9 Application of the ACRU model in streamflow simulation.....	16
2.10 Application of the Pitman model for streamflow simulation.....	17
2.11 Evaluating hydrological model efficiency .....	18
2.12 Hydrological Model calibration .....	19
2.13 Hydrological model validation.....	20
2.14 Prediction of streamflow in small mountain catchments .....	21
2.15 Hydrological responses of small mountainous catchments .....	23
2.16 Summary and Recommendations.....	24
3 Materials and Methods .....	26
3.1 Introduction .....	26
3.2 The study site .....	26
3.3 Data collection.....	30
3.3.1 Rainfall measurements.....	31

3.3.2	Cloud water interception.....	34
3.3.3	Streamflow .....	37
3.3.4	Meteorological elements for estimating evaporation.....	37
3.3.5	Catchment characteristics estimation.....	38
3.4	Infilling of missing rainfall data.....	39
3.5	Data analysis of precipitation.....	41
3.5.1	Testing for normality of rainfall measured by the individual rain gauges.....	42
3.5.2	Comparison of average daily rainfall.....	42
3.6	Comparison of rainfall distribution.....	43
3.6.1	Interpolation of rainfall.....	44
3.6.2	Analysis of cloud water .....	44
3.7	Streamflow modelling.....	44
3.7.1	Streamflow modelling using ACRU.....	45
3.7.2	Model performance evaluation .....	49
3.7.3	ACRU model Calibration and Validation.....	52
3.8	Limitations of the study.....	52
4	Estimation of catchment precipitation.....	53
4.1	Introduction .....	53
4.2	Data quality control and infilling .....	53
4.3	Variation of monthly rainfall with elevation.....	54
4.4	Variation of daily rainfall characteristics .....	56
4.5	Analysis of number of rainfall days .....	57
4.6	Diurnal variation of rainfall.....	59
4.7	Number of wet spells.....	60
4.8	Assessment of the significance of variation of average daily rainfall with elevation....	61
4.9	Cloud water contribution to total precipitation .....	63
4.9.1	Important weather conditions for cloud water.....	63
4.9.2	Cloud water diurnal characteristics.....	69
4.9.3	Cloud water contribution to precipitation at different altitudinal zones.....	71
4.10	Discussion .....	73
5	Streamflow modelling .....	76

5.1	Introduction .....	76
5.2	Model configuration.....	76
5.3	Soil input information .....	78
5.4	Precipitation input .....	79
5.5	Flow routing configuration.....	80
5.6	Evaporation input .....	80
5.7	Vegetation input .....	81
5.8	Model Calibration and Validation.....	81
5.9	Hydrographs characteristics of streamflow modelling.....	83
5.10	Analysis of flow duration curves .....	87
5.11	Statistical results of streamflow modelling .....	89
5.12	Influence of cloud water on evaporation rates .....	91
5.13	Discussion: Streamflow modelling .....	92
6	Conclusions and recommendations .....	95
7	References.....	98



UNIVERSITY *of the*  
WESTERN CAPE



## List of figures

---

Figure 3.1: Location and topography of the Jonkershoek catchment within the ..... Western Cape	28
Figure 3.2: Occurrence of cloud emersion on Langrivier.....	29
Figure 3.3: Illustration of rain gauge station RG360(R360) and R460 (R460) within Langrivier before May 2014 (produced from 1:50 000 (3318DD) map published by the Chief Directorate, Surveying and Mapping, South Africa, 2003).....	32
Figure 3.4: River profile of the Langrivier stream (Google earth, 2015) .....	32
Figure 3.5: Set up with new rain gauge stations within Langrivier after May 2014 (produced from 1:50 000 (3318DD) map published by the Chief Directorate, Surveying and Mapping, South Africa, 2003). .....	34
Figure 3.6: Louvred screen fog (Right) mounted on top of a rain gauge with another rain gauge on the left to assess amount of precipitation falling as rain.....	36
Figure 3.7: Geology map of Langrivier catchment indicating the points of soil properties sampling (Hans, 2015).....	39
Figure 3.8: Structure of the ACRU hydrological model (adopted from Schulze, 1995) .....	47
Figure 4.1:Variation of total rainfall (May 2015- June 2016) with elevation in the Langrivier catchment.....	55
Figure 4.2:Average monthly rainfall for rain gauge 8B for the Wicht et al. 1969 compared to the current study (R360).....	56
Figure 4.3:Diurnal variation of rainfall for rain gauges RG360, RG460, RG500, and RG600....	59
Figure 4.4:Diurnal variation of rainfall for rain gauges RG700, RG800, and DWA1214 .....	60
Figure 4.5:Difference in cumulative rainfall of rainfall when interpolated with and without the inclusion of rainfall monitored at DWA 1214 m.a.s.l .....	62
Figure 4.6a:Wind conditions bringing cloud water precipitation at fog gauge located at 500 m.a.s.l on 10 September 2014.....	64
Figure 4.6b:Wind conditions bringing cloud water precipitation at fog gauge located at 600 m.a.s.l on 10 September 2014.....	64
Figure 4.6c:Wind conditions bringing cloud water precipitation at fog gauge located at 700 m.a.s.l on 10 September 2014.....	65

Figure 4.9d: Wind conditions bringing cloud water precipitation at fog gauge located at 800 m.a.s.l on 10 September 2014.....	65
Figure 4.6 e: Wind conditions bringing cloud water precipitation at fog gauge located at 1214 m.a.s.l on 10 September 2014.....	66
Figure 4.7a: Wind conditions bringing cloud water precipitation at fog gauge located at 500 m.a.s.l on 28 December 2014 .....	67
Figure 4.7b: Wind conditions bringing cloud water precipitation at fog gauge located at 600 m.a.s.l on 28 December 2014 .....	67
Figure 4.7c: Wind conditions bringing cloud water precipitation at fog gauge located at 700 m.a.s.l on 28 December 2014 .....	68
Figure 4.7d: Wind conditions bringing cloud water precipitation at fog gauge located at 800 m.a.s.l on 28 December 2014 .....	68
Figure 4.7e: Wind conditions bringing cloud water precipitation at fog gauge located at 1214 m.a.s.l on 28 December 2014 .....	69
Figure 4.8:Diurnal variation of cloud water (mm) from all the fog gauges. ....	70
Figure 4.9:Contribution of cloud water (mm and %) to total precipitation at the different elevation a=500 m.a.s.l; b=600 m.a.s.l; c=700 m; d= 800 m.a.s.l and e=1214 m.a.s.l. ....	72
Figure 5.1:Langrivier catchment as looking from the mouth of the catchment viewed from upstream with the rock outcrop visible (left), catchment division into the two HRUs. ....	77
Figure 5.2:Simulated vs observed flows for the Langrivier stream with ACRU Lumped + precipitation from old rain gauge network. ....	85
Figure 5.3: Simulated vs observed flows for the Langrivier stream with ACRU Lumped + precipitation from new rain gauge network.....	85
Figure 5.4:Simulated vs observed flows for the Langrivier stream with ACRU Lumped + Precipitation from rainfall and cloud water.....	86
Figure 5.5:Simulated vs observed flows for the Langrivier stream with semi-distri + precipitation from new rainfall network. ....	86
Figure 5.6:Simulated vs observed flows for the Langrivier stream with semi-distri + precipitation from new rainfall network and cloud water.....	87
Figure 5.7: Frequency flow duration curves for dry month (February) in Langrivier using the five different model configurations. ....	88

Figure 5.8: Frequency flow duration curves for wet month (August) in Langrivier using all the five different model configurations ..... 89



UNIVERSITY *of the*  
WESTERN CAPE

## List of Tables

---

Table 3.1: Newly installed rain gauges in Langrivier catchment as from May 2014.....	33
Table 3.2: Newly installed fog gauges for monitoring cloud water interception in Langrivier. ..	35
Table 3.3: Criteria for determining the adequacy of ACRU for simulating streamflow. ....	51
Table 4.1: Non-availability of precipitation data from May 2014- June 2015 for the seven rainfall stations and five cloud water station placed at different elevations .....	53
Table 4.2: Monthly rainfall totals (mm) recorded by the seven rainfall stations at different elevation levels within Langrivier catchment.....	55
Table 4.3: Daily rainfall characteristics of the 7 rainfall stations in Langrivier (May 2014 – June 2015).....	57
Table 4.4: Correlation matrix of daily rainfall totals of the seven rain gauge stations in Langrivier. ....	57
Table 4.5: Number of rainfall days per month for the seven rainfall stations within Langrivier.	58
Table 4.6: Classification of rainy days by magnitude of daily rainfall.....	58
Table 4.7: Number of wet spells for the seven rain gauges within Langrivier.....	61
Table 4.8: Variation of average daily rainfall with elevation in Langrivier. ....	62
Table 5.1: Model configuration with precipitation and model structure. ....	78
Table 5.2: Soil water parameters for a typical South African sandy loam texture as determined by Schulze, 1994 (adopted from new 1999).....	79
Table 5.3: Final ACRU model input parameter values for Langrivier moelling.....	82
Table 5.4: Summary of model evaluation statistics results for the five different simulations.....	91
Table 5.5: Influence of cloud water on evaporation rates in the Langrivier catchment. ....	92

## **Dedication**

This thesis is dedicated to my family who are from the Bhayi clan. My father Mputumi Mbali, my mother Noncedo Mbali and my three sisters Zoliswa Tyelaphantsi, Pinky and Esihle Mbali. I really appreciate their unreserved and unwavering support, more than they would possibly imagine.



UNIVERSITY *of the*  
WESTERN CAPE

## Acknowledgements

I would like to express my sincere gratitude to the South African Environmental Observation network (SAEON). Without the financial support of South African Environmental Observation Network none of this work would have been possible.

I am eternally grateful to my supervisors Professor Dominic Mazvimavi of the University of the Western Cape and Dr Nicky Allsopp of the South African Environmental Observation Network for their guidance and advice throughout this thesis. It has been an exciting but very challenging two and half years.

For technical support, I am greatly indebted to Abri De Buys of South African Environmental Observation Network for assisting in equipment installation, data downloads, and always being available whenever I visited Jonkershoek. I would also like to thank Luvo Dlamini, an intern at South African Environmental Observation Network 2015, with assisted with the equipment installation.

I also wish to acknowledge the support, both intellectually and morally, of my colleagues and friends within the University of the Western Cape notably Thandokazi Maceba, Imelda Haines, Eugene Segwati Maswanganye, Athenkosi Matshini, Nolusindiso Ndara, Qondisa Mbekwa and Siyamthanda Gxokwe.

## List of abbreviations

CWI	Cloud water interception
DWA	Dwarsberg Mountain
HRU	Homogenous hydrological response unit
LSF	Lovred screen fog gauge
m.a.s.l	meters above sea levels
m	meter



UNIVERSITY *of the*  
WESTERN CAPE

# 1 Introduction

## 1.1 General background

Rainfall is the main input into the land phase of the hydrological cycle which greatly determines the available water resources. Thus, accurate information about the spatial and temporal variability of rainfall is necessary for proper water resources management. However, for some catchments, the available rainfall data is not adequate for accurately representing the spatial and temporal variation of rainfall, ultimately leading to inadequate estimation of catchment rainfall. Inadequate estimation of catchment rainfall introduces uncertainty in both the design and management of water resources systems (Mazvimavi, 2003). Therefore, it is imperative to use the best available methods to accurately estimate catchment rainfall.

A rain gauge is the only instrument and method that measures actual rainfall on the earth's surface. As a result, studies that intend to improve the estimation of rainfall should use rain gauges as one of the methods since other rainfall estimation methods such as radar and remote sensing do not directly measure the actual rainfall that falls onto the earth surface (Bitew and Gebremichael, 2010). In addition, the accuracy of rainfall estimates derived from radar and remote sensed data must be assessed using rainfall measured by rain gauges (Kidd et al. 2003; Volkmann et al. 2010).

Accurate estimation of catchment rainfall requires the establishment of a network of rain gauges that realistically captures the spatial variation of rainfall. It is not the density of rain gauge stations that is important, but whether the rain gauge stations represent the spatial variation of rainfall within a catchment. For instance, in the Real Collobrier (71km<sup>2</sup>) catchment in France, 20 rain gauges were not adequate for river flow modeling (AndreÂassian et al. 2001). In contrast 33 rain gauges within the Yonne (10700 km<sup>2</sup>) catchment were found to be adequate for river flow modeling (AndreÂassian et al. 2001). Anctil et al. (2006) found that in a catchment that had 23 rain gauges, flood forecasting was best undertaken using only 12 well-selected rain gauges. Furthermore, rainfall can be highly variable in space such that rain gauges located 300 m apart were found to have recorded significant differences of rainfall totals in a small (4.4 ha) USDA-ARS Walnut Gulch catchment, United States of America (Goodrich et al. 1995). These studies demonstrate the importance of designing a rain gauge network to adequately capture the spatial



variation of rainfall, particularly in mountain catchments where there is generally high spatial variability of rainfall.

Most mountain catchments experience high spatial variability of rainfall mainly due to the orographic effect on rainfall formation (Goovaerts 2000; Buytaert et al. 2006; Cheng et al. 2012). Wicht et al. (1969) found that the low areas (300 m.a.s.l) in the Jonkershoek catchment received an average rainfall of 1187 mm/a, while 3625 mm/a was received at the top (1300 m.a.s.l) of this mountain. Bitew and Gebremichael, (2010) found a coefficient of variation of 15-53% in rainfall recorded by 22 rain gauges in a 6x6 km Beressa mountain catchment, Ethiopia. Apart from the orographic effect, altitude, slope, and aspect have been documented as other important factors that affect the spatial distribution of rainfall in some mountain catchments (Wicht et al, 1969; Bitew and Gebremichael, 2010; Nyssen et al. 2005; Buytaert et al, 2006; Goovaerts, 2000). Thus, an appropriately designed rain gauges networks should account for these factors. Furthermore, although rainfall is the most important form of precipitation for which accurate information is essential in low-lying areas, this may not be the case in some mountainous catchments (Anctil et al. 2006). Cloud water intercepted by plants and rock surfaces has been found to contribute to moisture in some mountainous catchments.

Cloud water contributes between 10-33 % of total summer precipitation in some parts of the world (McJannet et al. 2007; Scholl et al. 2007; Scholl et al. 2011; Gomez-Peralta et al. 2008; Holwerda et al. 2011; Prada et al. 2012; Figuera et al. 2013). In South Africa, cloud water contributed 1000 mm in one month on Table Mountain (Marloth 1903, 1905). Ekerns (1964) found that cloud water contributed a total of 762 mm of water to pine trees over a three-year period in Lunaihale, Hawaii. Such significant quantities of cloud water provide valuable moisture to mountain ecosystems (Prada et al. 2012). In addition, Scholl et al. (2007) report that catchments in tropical montane cloud forests with cloud water interception yielded higher streamflow discharges than from other tropical forest catchments with similar rainfall without frequent cloud. The finding of Scholl et al. (2007) suggests that cloud water interception may contribute directly to streamflows quantities. However, there is limited information on the direct contribution of cloud water to streamflows. Thus, there is a need to include cloud water in the monitoring of precipitation of some mountainous catchments as cloud water may influence streamflow hydrographs and ultimately water management.

Accurate precipitation information is critical for mountain catchments as mountain catchments are the main suppliers of usable water to the human population. In humid regions, mountain catchments supply between 20-50% to total stream discharge while for semi-arid and arid regions mountain catchment contribute between 50-90% to total stream discharge (Viviroli and Weingartner, 2004). In South Africa surface water is the most important source of water, as 83.3 % of water used in south Africa comes from surface water (mainly rivers) while groundwater contributes 17.7 % per annum (Colvin, et al. 2013). Moreover, accurate precipitation information is necessary for accurate prediction of climate change scenarios.

One catchment that is important for the supply of water to the downstream areas and has a dam reservoir is the Jonkershoek catchment. The Jonkershoek, which has five smaller sub-catchments that monitors rainfall has been found to have rainfall varying spatially and increasing with altitude (Wicht et al. 1969). The spatial rainfall patterns of Jonkershoek catchment have not changed in almost 40 years (Moses, 2008). Moreover, rainfall within the small sub-catchments of Jonkershoek has been found to vary significantly. For instance, the Swartboskloof catchment, a sub-catchment of Jonkershoek catchment 1, has significant rainfall depth increase with altitude (Britton, 1991). The Langrivier catchment (2.45 km<sup>2</sup>) which is also within Jonkershoek has two rain gauges located at elevation levels that are not representative of the top of the mountain. New (1999) and Manamathela (2012) suggested that the existing rain gauges did not always accurately represent the catchment rainfall.

The rain gauges in Langrivier catchment currently monitor rainfall up to an elevation level of 460 m.a.s.l., while the maximum elevation point in the catchment is 1423 m.a.s.l. (Scott et al. 2000). New (1999) found that for the period of 11<sup>th</sup> June 1985 to 1<sup>st</sup> July 1985 the observed streamflow was more than the estimated precipitation by nearly 50%. Similarly, Manamathela (2012) found that mean monthly flows were consistently higher than mean monthly rainfall. Therefore, the current Langrivier rain gauge network needs to be improved in order to improve the estimation of catchment rainfall. Furthermore, clouds are frequently observed to be intercepted by the land surface at high elevations in the Langrivier catchment. The extent to which interception of cloud influences the catchment water balance has not been established. Hence, the aim of this study is to establish whether the accuracy of estimating catchment precipitation (rainfall and cloud water) in the Langrivier catchment will be improved by

expanding the precipitation monitoring network to locations representative of the various elevation levels.



UNIVERSITY *of the*  
WESTERN CAPE

## 1.2 Aim

To contribute towards an improved understanding of the spatial and temporal variation of different forms of precipitation in the Langrivier and Jonkershoek mountain catchment and their influence on hydrological responses.

## 1.3 The objectives of this thesis are the following:

- 1.3.1 To determine whether the establishment of additional rain gauges to representing the elevation levels improves the estimation of event based and daily catchment rainfall
- 1.3.2 To establish if cloud water interception significantly affects the total precipitation in Langrivier catchment
- 1.3.3 To assess if the establishment of additional rain gauges and inclusion of cloud water interception improve the prediction of river flows in the Langrivier catchment.



UNIVERSITY *of the*  
WESTERN CAPE

### 1.3 Research Outline

The thesis has the following chapters:

- **Chapter 1** presents the context within which the study was undertaken. It also attempts to show that a need exists to improve estimation of catchment precipitation especially in a mountain catchment such as the Jonkershoek catchment in Western Cape, South Africa.
- **Chapter 2** reviews the literature about patterns of precipitation in mountain catchments. It also outlines the most important aspects of improving estimation of catchment precipitation.
- **Chapter 3** presents a description of the study area. Information is presented on topography, the spatial location of rain gauges, geology, and vegetation of the catchment. The methods for data collection and analysis are presented in this chapter.
- **Chapter 4** presents the results about the expansion of the rain gauge network and inclusion of cloud water with regard to improved estimation of total precipitation.
- **Chapter 5** assesses how the improvement of estimation of catchment precipitation (Rainfall and Cloud water) affects the prediction of river flows using the ACRU hydrological model.
- **Chapter 6** concludes the research with a brief discussion on its implications for catchment rainfall estimation in mountainous catchments and recommendations for further research.

## **2 Review on estimation of catchment precipitation and streamflow hydrological modeling**

### **2.1 Introduction**

The scientific method is a practice by which scientists, collectively and over time, attempt to construct an accurate representation of the world. This process requires a review of previous literature in order to distinguish what has been done, seek new lines of inquiry and gain methodical insights to avoid fruitless approaches, with the goal of improving understanding of the world. This chapter presents a review of the literature dealing with factors and aspects related to the improvement of estimation of catchment precipitation in mountain catchments.

It is important to identify the main reasons for the lack of accurate information on catchment precipitation. This may be caused by technical limitations in methods (rain gauges, radar, and satellite derive rainfall estimates) used for estimating catchment rainfall. While the accuracy of actual rainfall measured by a rain gauge may negatively influenced by wind speed, aspect, and slope (Lents et al.1995; Nesper and Sevruk, 1998, Nyssen et al. 2005), one of the main causes of inaccuracy in the estimation of catchment rainfall using rain gauges is a rain gauge network that is not non-representative of spatial rainfall differences. Furthermore, not accounting for other precipitation types' (such as clouds and snow) contribution to total precipitation in mountain catchments that are frequently under cloud emersion or have the presence of snow may cause inaccurate estimation of catchment precipitation. Accurate precipitation information is necessary for predicting streamflows, which is a critical aspect of water resources management. Prediction of streamflow is done using hydrological models (Xu and Singh 1998; Sanborn and Bledsoe, 2006).

The chapter is structured such that it first discusses critical aspects with regards to improving estimation of catchment precipitation, specifically rainfall and cloud water contribution to mountain catchments moisture. Secondly, hydrological models as a tool used for streamflow modeling including model calibrations and validations are discussed. Lastly, a discussion on important hydrological processes in small mountain catchments like the Langrivier is discussed,

with the view to further enhance the understanding of the Langrivier Catchment in order to select the appropriate methods for addressing the study objectives.

## **2.2 Status of catchment rainfall monitoring**

Rainfall has been monitored around the world for a relatively long time, with the first record of rainfall data being over 750 years old (Strangeways, 2010). However, consistent precipitation monitoring records with acceptable accuracy, which offer values that are applicable to the requirements of modern applications, rarely ever extend for periods longer than 70 years (Berndtsson and Niemczynowicz, 1988). Inadequate rainfall data increases uncertainty to projected water availability under prevalent levels of climate variability and for climate change scenarios.

Rainfall monitoring spatially and temporally has improved significantly over the years. New monitoring methods (radar and remote sensing) have been developed and can monitor rainfall over thousands of square kilometers and over the sea, and the accuracy of measuring equipment (rain gauges) and estimation techniques (interpolation) have also improved. This has led to improved quality of rainfall data for catchment management. However, the challenge in monitoring rainfall has been determining the appropriate scale of monitoring. Rainfall is stochastic in nature and rainfall variability differs from catchment to catchment, as a result, determining the appropriate scale of rainfall monitoring is critical for accurate estimates of catchment rainfall (Wicht et al. 1969; Goodrich et al. 1995; Buytaert et al. 2006; Cheng et al. 2012).

Rain gauge networks in many parts of the world do not adequately represent the spatial variation of rainfall and while radar and remote sensing can monitor rainfall on a large scale they require ground validation sites (Cheng et al. 2008; Bitew and Gebremicheal, 2010). In the case of rain gauges, the main causes of inadequate representation of rainfall is deteriorating rain gauge networks (particularly in African countries), lack of commitment to funding hydro-meteorological gauging networks in countries that have many more immediate economic issues, high cost of maintenance of rain gauge networks; inaccessibility of sites of interest, and uneven distribution of rain gauges (Mazvimavi, 2003; Buytaert et al. 2006; Hughes, 2006; Beyene and

Meissner, 2010). As a result, satellite rainfall estimates are being used widely in place of rain gauge observations (Beyene and Meissner, 2010).

### **2.3 Estimation of catchment precipitation**

Catchment rainfall is traditionally estimated from point measurement which introduces errors due to rain gauges not always being representative of the spatial variation of rainfall (Buytaert et al. 2006; Cheng et al. 2012; Ndiritu, 2014). A rain gauge measures rain that falls in a few square centimeters in a catchment (Bitew and Gebremichael, 2010). That single point is used to estimate the total rainfall amount for the catchment. This point may not be representative of a large area, particularly in mountain catchments as rainfall is stochastic (Bitew and Gebremichael, 2010). Efforts are being made to improve the estimation of aerial precipitation by using rainfall data derived from remote sensing and radar estimates.

Estimating rainfall from remote sensing and radar estimates is advantageous as rainfall can be estimated for large areas, at a low cost, and in real time (Ciach and Krajewski, 2006). Remote sensing products estimate rainfall using infrared, visible satellite imagery and passive microwaves (Kidd et al. 2003). Infrared (IR) and visible satellite (VIS) provide information about cloud tops characteristics (e.g. temperature, brightness) which are used to estimate rainfall. Passive microwave on other hand uses observations of the hydrometeor (i.e. ice particles and droplets) (Kidd et al. 2003). However, satellite products have deficiencies such as inappropriate spatial and temporal resolution.

Passive microwave products such as Special Sensor Microwave Imager (SSM/I), Microwave Imager (TMI), and Tropical Rainfall Measuring Mission (TRMM) are more accurate than IR and VIS (Kidd et 2003) but have a small temporal sample size. Passive microwave provides rainfall estimates for up to six samples a day, while VIS and IR samples rainfall 48 times a day (Kidd et al. 2003). Although both IR and VIS sensors have high daily sampling sizes, VIS suffers from day-night bias as it does not monitor precipitation at night (Bellerby et al. 2005). On the other hand, IR relates cloud temperature thresholds (eg.  $-38.15^{\circ}\text{C}$ ) to rainfall rates. However, factors such as high level of cirrus and other non-precipitating cloud forms interfere with the statistical



relationship of cloud water temperature (Bellerby et al. 2005). Thus, a cloud top with a temperature of  $-38.15^{\circ}\text{C}$  which supposedly leads to a certain amount of rainfall may end up not leading to precipitation. Moreover, satellite derived rainfall have limited resolution for small spatial scale monitoring (highest resolution being  $1 \times 1 \text{ km}$  for Climate Hazards Group Infra-Red Precipitation with Station data (CHIRPS) to  $3 \times 3 \text{ km}$  for Multi-Sensor Precipitation Estimate (MPE), and even so such resolutions may be coarse for catchments such as Langrivier catchment which is  $2.45 \text{ km}^2$ . A critical drawback of all satellite products is that they do not measure rainfall directly and ultimately need rain gauges to validate their accuracy. As a result, the need to validate their accuracy by rain gauges limits their applicability in studies that attempt to further improve estimation of catchment rainfall.

Weather radar observations are also averaged over areas ranging from about  $1 \text{ km}^2$  to  $25 \text{ km}^2$ , at 5–15 min temporal resolution (Ciach and Krajewski, 2006). Thus, the spatial resolution may also be too coarse for the small Langrivier Catchment. In addition radar-based rainfall estimates, like satellite rainfall estimates, suffer from uncertainties and biases due to the combined effects of limitations in representations of the underlying rainfall processes, poor parameter estimation, and inaccuracy in mountainous topography (WMO, 2008; Volkmann et al, 2010). Thus, for the Langrivier catchment which already has two rain gauges, an expansion of the current rain gauge network is the best option to improve estimation of catchment rainfall as it would allow for a comparison of rainfall estimation before and after the rain gauge network expansion.

#### **2.4 Design of rain gauge networks in mountain catchments**

Appropriate design of rain gauge networks in mountain catchments, which are important for providing clean water for the human population, is difficult mainly because of the expense of maintaining such networks in mountain catchments that are generally remote and have inaccessible areas (AndreÂassian et al. 2001; Buytaert et al. 2006). The expenses of maintaining a rain gauge network in mountain catchments lead to rain gauges being placed and installed at accessible points (Cheng 2008), which may not be representative of the rainfall patterns. As has been discussed in Chapter 1 and the presiding sections in this Chapter, the main factors that influence the spatial distribution of rainfall in mountain catchments are aspect, slope, and

altitude. As a result, an appropriate design of rain gauges in mountain catchments requires placement of rain gauges at locations representative of different slopes, aspects, and altitudes within a particular catchment.

## **2.5 Estimating catchment rainfall using rain gauges**

A rain gauge has over the years been shown to accurately measure actual rainfall depth (Bitew and Gebremichael, 2010). Using point measurements from one rain gauge or more, catchment rainfall can be estimated with reasonable accuracy using interpolation. There are three main interpolation methods commonly used for estimating catchment rainfall, namely the Inverse Distance Weighted, Thiessen polygons, and kriging approaches.

Each of the aforementioned interpolation methods uses different assumptions and mathematical formulations to obtain the results. Kriging is a geostatistical interpolation method estimates rainfall based on weighted average of available data and analyzes the spatial correlation between the data recorded at several weather stations for interpolation (Vicente-Serrano et al. 2003). Kriging, unlike the other two interpolation methods named above accounts for elevation which is an important factor in determining rainfall characteristics and produces a prediction error value (Goovaerts, 2000). Buytaert et al. (2006) used kriging with success, to examine the spatial and temporal variability of the rainfall in a mountainous area of Ecuador, South America. However, inverse distance weighted and Thiessen polygons are simple to use.

Thiessen polygon interpolation method is described as simplest interpolation method to use (Goovaerts, 2000; Vicente-Serrano et al. 2003). Thiessen Polygon method, which demarcates a catchment into small polygons, estimates rainfall at an un-sampled location (polygon) by taking the value of the nearest rainfall value (Goovaerts, 2000; Vicente-Serrano et al. 2003). On the other hand, in the inverse weighted distance approach, rainfall at an un-sampled area is estimated using a distance-weighted average of surrounding rain gauges (Vicente-Serrano et al. 2003). Chen and Liu (2012) highlights that the Inverse Distance Weighted approach performed better than kriging in most rainfall studies around the world and was more easy to use with spatially dense rain gauge networks. Moreover, Goovaerts (2000) reports that for high-resolution

networks (e.g. 13 rain gauges over a 35 km<sup>2</sup> area), all of the three interpolation methods produce similar results.

## **2.6 Contribution of cloud water to catchment precipitation**

Cloud water precipitation is due to the concurrent presence of persistent cloud cover, the wind, and dense vegetation cover (Prada et al, 2009). According to Scholl et al. (2007) and Bruijnzeel et al. (2005) clouds require a substrate (e.g. vegetation, soil/rock surfaces) to coalesce on in order to reach the earth surface. Cloud water interception (CWI) quantities depend on wind speed, fog liquid water content, duration, air temperature, relative humidity, geometry and surface area of vegetation (Holwerda et al. 2011; Figuera et al. (2013). The presence of vegetation is critical in determining the quantity of CWI to total precipitation. For instance, the absence of vegetation leads to cloud water interception quantities into the soil not exceeding 0.2mm/day (Prada et al. 2009). Apart from CWI providing moisture to plants in mountainous catchments other processes of the hydrological cycle are also influenced by this form of precipitation.

Cloud water presence decreases evapotranspiration rates of mountain catchments. Figuera et al. (2013) reported that the presence of orographic clouds and fog increases the relative humidity, decreases the insolation and temperature, thereby decreasing water use by plants. This has important implications for the water resources of an area as it will result in low soil moisture loss rates through evaporation; rivers and groundwater have higher water levels as a result of low water use by the plants and decreased rates evapotranspiration.

Apart from a 33% contribution to total precipitation in summer months in the Madeira Islands, Portugal (Prada et al, 2009; Figuera et al, 2013), cloud water contributes to groundwater recharge in the water balance of forest ecosystems (Prada et al, 2009). Holder (2003) suggested that conservation of cloud forests in the Sierra de las Minas in Guatemala was important, as cloud water interception from the forest is a critical input to the water resources of surrounding arid valleys of Sierra de las Minas.

Cloud water interception also improves plant survival and soil moisture content of mountain catchment. In California mountain catchment, 34% of the hydrological input of the soil content

was as a result of cloud water interception by the California redwood forest, while the absence of trees led to only 17% of the hydrological input coming from clouds (Dawson, 1998). In Chile, a *loma* forest vegetation survives exclusively on fog precipitation (Bruijnzeel et al. 2005). In summer, cloud water uptake within trees and plants species of the California redwood forest ranged between 19-66%. Additionally, *S.sempervirens* a species of the California redwood forest, 13–45% of its annual transpiration was from fog water input (Dawson, 1998).

Most studies (McJannet et al. 2007; Scholl et al. 2007; Scholl et al. 2011; Gomez-Peralta et al. 2008; Holwerda et al. 2011; Prada et al. 2012; Figuera et al. 2013) on CWI focus on the contribution of clouds to mountain catchments with regards to moisture supply to these forests and soil moisture but do not explicitly examine the impact of cloud water on water resources (groundwater and surface water). Cloud water contribution to streamflow may also be critical. Furthermore, a vast amount of available literature (Scholl et al. 2007; Scholl et al. 2011; Gomez-Peralta et al. 2008; Holwerda et al. 2011; Prada et al. 2012; Figuera et al. 2013) on CWI is limited to tropical forest and limited information is available on CWI in fynbos vegetation catchments such as the Langrivier catchment (Marloth 1903, 1905).

## **2.7 Measurement of cloud water interception**

Cloud water interception (CWI) is measured and quantified using throughfall collectors or fog collectors, and can be estimated from an assessment of the wet canopy water budget, and isotopic analysis of water intercepted by plants and streamflows (McJannet et al. 2007; Scholl et al. 2007; Gomez-Peralta et al. 2008; Holwerda et al. 2011). The decision regarding which method to use depends on the research objectives, the expertise needed, and the financial resources.

Fog collectors are accurate, relatively easy and inexpensive methods for measuring cloud water interception. There are various types of fog collectors used to quantify cloud water such wire harp, Juvik louvered shade screen, and tunnel gauge. The fog droplets condense on the surfaces of these instruments and drip down to a collecting rain gauge at the bottom of the fog collector. In essence, the fog collectors' behave like plant surfaces wherein nature clouds and fog coalesce on the leaves. The fog collection efficiency of most fog collectors is largely influenced by the

wind speed and cloud droplet sizes. For instance, at low wind speed (2 m/s) and small drop size it was found that a single strand of the Juvik louvered shade screen is more efficient for fog droplet collision than the wire harp and tunnel gauge (Framau et al. 2006), while at higher wind speeds and larger droplet sizes the Juvik louvered shade screen and tunnel gauge performed better than the wire harp. Overall, the Juvik louvered shade screen generally performs better than the other two fog collector instruments.

## **2.8 Prediction of stream flows**

Prediction of streamflow can be achieved using hydrological models. A hydrological model is defined as an abstract of a real world catchment using mathematical relationships to simulate hydrological processes (Viessman et al. 1989; Lewarne, 2009). Hydrological models are used to predict the behavior of the hydrological system and have the potential to provide reliable information for water resource planning and management (Sawunyama, 2008). There are different types of hydrological models, which vary mainly in the representation of processes or the level of complexity. Hydrological models can be classified into two main types namely conceptual and physically based models (Viessman et al, 1989). The two mentioned types of models can further be classified as either lumped or distributed models.

Lumped models treat a catchment as a single unit, and assume catchment homogeneity (New, 1999). In lumped models, the spatial variations of hydrological response characteristics such as climate, soils, slopes and land cover within a catchment are assumed not to have significant effects on streamflow (Ncube, 2006). On the other hand, distributed models attempt to represent the spatial variations of catchment characteristics and hydrological processes (Beven, 2001; Jayakrishnan et al. 2005). In a distributed model, a catchment is divided into different homogeneous hydrological response units (Reed et al. 2006). The ability of hydrological models to simulate a catchment in distributed mode was shown to improve simulations. For example, the ability of a model to account for non-uniform catchment characteristics (distributed modeling) led to relatively better simulation results of Xinanjiang conceptual model in comparison to the Pitman, NAM, and SMAR conceptual models (Gan et al. 1997).

A conceptual model conceptualizes the concepts of important processes within a catchment and simulates internal variables, such as soil moisture, by various types of explicit mathematical

relationships (Viessman et al, 1989 and Beven, 2001). Conceptual models use a mixture of physically measurable and empirically estimated parameters (Ncube, 2006). The Pitman model and Xinanjiang model are examples of conceptual models (Gan et al. 1997). The Pitman model is the most widely used monthly time step rainfall-runoff model in Southern Africa and utilises two inputs, monthly precipitation in terms of mean annual percentage and monthly potential evapotranspiration to simulate monthly runoff (Hughes et at, 2006).

Physically based models attempt to represent the spatial variation of processes and model parameters should ideally be measured directly in the field (Lewarne, 2009). Physically-based models are based on the laws of thermodynamics, conservation of mass, momentum and energy (Beven, 2001). MIKE SHE is one of the best examples of physically based models (Ncube, 2006). MIKE SHE is a distributed-parameter, fully integrated model for three-dimensional simulation of hydrological systems that simulates hydrological processes on a catchment scale (Abbott et al. 1986; Ncube, 2006). The SWAT model, which can operate both on distributed and lumped mode, may also be considered as a physical, semi-distributed model as it requires measured information about weather, soil properties, topography, vegetation, and land management practices occurring in the catchment (Lewarne, 2009; Arnold et al 2012). The SWAT model is also conceptual in the sense that it uses existing mathematical equation to approximate the physical behavior of the hydrological system (Lewarne, 2009).

Physically based models in principle should simulate hydrological responses better as they are processes based, theoretically more exact and thus, in principle, require little calibration of parameters (Bergstro and Graham, 1998). However, Reed et al. (2006) found that conceptual models often outperformed physically based models. The cost of setting up a simulation for physically based models is high (Dye and Croke, 2003; Reed et al. 2006). Additionally, the high data demand and high level of calculation in physically based model often lead to complex solutions that may disturb the main focus of the modeling processes (Beven, 2001). Reed at al. (2006) highlights that model formulation, parameterization, and the skill of the modeler may have a bigger impact on simulation accuracy than simply whether or not the model is conceptual or physical.

Choosing the appropriate model depends on the nature of the problem being investigated and model availability. Important aspects to consider when choosing a specific model for a

catchment are the nature of the problem being investigated, the spatial and temporal scale of the model, and the data requirements (Beven, 2001; Lewarne, 2009). In terms of the present study objectives and model availability, two models that have been developed in South Africa, namely the Pitman Model and ACRU model and as such may be suitable in this study and are thus discussed below. Afterward, model calibration and validation will be discussed.

## **2.9 Application of the ACRU model in streamflow simulation**

The ACRU model was first designed and used in the 1970s, on a distributed catchment for an evapotranspiration based study in the Natal Drakensberg (Schulze, 1995; Forbes et al. 2011). The ACRU model is a daily time step, physical conceptual model (Schulze, 1995). ACRU is conceptual in that it conceives of a system in which important processes and couplings are idealised and physical to the degree that physical processes are represented explicitly (Schulze, 1995). The model is well suited for use in southern Africa, with links to appropriate local land use, soil, and climate (Schulze, 1995; New 1999). The conceptual aspect, the daily time scale and links to South African climatological data of this model is advantageous for a catchment like the Langrivier that has limited soil and groundwater dynamics information, thus soil and groundwater values can be based on suggested values from the ACRU database. The ACRU model is applied to solve various problems which include water resource assessment, design flood estimation, crop yield estimation (Schulze, 1995). The daily time scale aspect of the model is favourable for assessing cloud water contribution on daily streamflows as CWI may not be clearly detectable at monthly and yearly scales.

The equations that are incorporated in the ACRU model that represent specific hydrological processes include a wide range of potential evapotranspiration routines, the Green–Ampt equation for infiltration, the Richard’s equation for soil water redistribution, a radiation-based snowmelt equation, seasonal plant transpiration coefficients, the von Hoyningen– Huene equation for canopy interception, and the modified soil conservation services equation for runoff generation (Kienzle, 2011). The modeller needs to understand the catchment characteristics and processes that operate in that particular catchment, in order to activate the right components in the model. The ACRU agrohydrological model has worked well in South African catchments and other parts of the world with modelling results that have a correlation ( $r$ ) over 0.75 between

observed and simulated streamflows (Butterworth et al. 1999; Everson, 2001, Forbes et al. 2011) but has some limitations.

The ACRU model is predominately an overland flow model. Rainfall falling on impervious areas is routed directly to streamflow if adjacent to a river (Schulze, 1995). Baseflow is represented as a function that releases groundwater contribution at a constant rate, albeit groundwater contribution to streamflow is not always constant (Schulze, 1995). The constant release function may lead to over/underestimation of total streamflow as groundwater contribution is not constant throughout the year. In the Langrivier, the linear representation of groundwater contribution was identified as potentially the cause of a 10% underestimation of summer low flows (New, 1999). In Cathedral Peak, South Africa the ACRU model simulated streamflow well ( $r = 0.80$ ) with good quality precipitation and potential evaporation data available except in wet years (Everson, 2001).

## **2.10 Application of the Pitman model for streamflow simulation**

The Pitman model was first developed in the 1970s at the University of Witwatersrand, South Africa (Hughes et al. 2006; Kapangaziwiri and Hughes, 2008). The Pitman model is a conceptual model and can operate as a semi-distributed model (Kapangaziwiri and Hughes, 2008). The model was originally developed to simulate Hortonian overland flow and has three conceptual storages namely rainfall interception by plants, soil moisture, and groundwater (Gan et al. 1997; Kapangaziwiri and Hughes, 2008). Over the years the model has been consistently modified. The prominent modifications of the Pitman Model are the ability of the model to account for land use change in order to better integrate human land use change and use sub-catchments in distributed modelling approach, with groundwater routines being explicitly represented (Hughes, 2004; Kapangaziwiri, 2007). The Pitman model was originally developed as a monthly time scale model and recently a daily time scale version of the Pitman that generates daily flow simulations from existing monthly simulations has been developed (Hughes and Slaughter, 2015). The monthly version of the Pitman model is not ideal for a study that attempts to assess daily flow characteristics and the daily model has been found to be less useful for peak flow analysis (Hughes and Slaughter, 2015). As a result, the Pitman model would not be ideal for the current study which attempts to assess daily flow characteristics.



## 2.11 Evaluating hydrological model efficiency

As there are various types' hydrological models, modelling results of each model and simulation need to be evaluated. As such there are various specific statistics and performance ratings which have been developed and used to assess model performance (Moraisi et al. 2007). According to Krause et al. (2005) hydrological model evaluation of model performance is required to provide a quantitative estimate of the model's ability to reproduce historic and future Catchment characteristics, to provide a means for evaluating improvements to the modeling approach through adjustment of model parameter values, model structural modifications, the inclusion of additional observational information, and representation of important spatial and temporal characteristics of the catchment; and compare current modeling efforts with previous study results. While there are various specific statistics and performance ratings for hydrological models, such performance ratings are mostly model and project specific (Moraisi et al. 2007). Nonetheless, there are common statistics that are used to evaluate model performance.

There are common statistics and performance ratings which are generally used in model performances and have defined acceptable ranges. The statistics and performance ratings can be qualitative (e.g visual) and quantitative. Model qualitative assessments generally involve visually assessing the observed streamflow and simulated streamflow hydrographs (Kapangaziwiri, 2007). There are a large number of quantitative statistics and performance ratings depending on the specific model and as such cannot all be described in this section. Quantitative assessment can be divided into three major categories namely standard regression (Pearson's correlation coefficient ( $r$ ) and coefficient of determination  $R^2$ ), dimensionless (Nash-Sutcliffe efficiency, Persistence model efficiency) and error index (Percent bias, Root Square Mean Error) (Moraisi et al. 2007). All of the name quantitative statistics have defined acceptable ranges, for instance the Nash-Sutcliffe efficiency measure which goes up to 1.0 for a perfect match (Moraisi et al. 2007; Gumindoga et al. 2015). According to Gumindoga et al. (2015) a value between 0.6 and 0.8 indicates that the model performs reasonably, while values between 0.8 and 0.9 indicate that the model performs very well and values between 0.90 and 1.0 indicate that the model performs extremely well. As such when assessing the performance of a particular model, the modeller should assess model performance using the generally defined acceptable ranges for each performance statistic.

## 2.12 Hydrological Model calibration

Most hydrological models require calibration for a particular catchment. Calibration is a process used to better parameterize a model to a given set of local conditions (Arnold et al. 2012). Model calibration is performed by carefully selecting and adjusting model input parameters to achieve an adequate fit between simulated model output and observed values (e.g.. simulated streamflow vs observed streamflow) (Kapangaziwiri, 2007; Arnold et al. 2012).

According to Madsen (2000), the objective of performing model calibration is “selection of model parameters so that the model simulates the hydrological behaviour of the catchment as closely as possible”. In the case of calibrating a model for streamflow simulations, as is the case for this study, Madsen (2000) states that streamflow calibration should be performed to obtain an adequate agreement between the average simulated and observed catchment runoff volume (i.e. a good water balance), an adequate overall agreement of the shape of the hydrograph, adequate agreement of the peak flows with respect to timing, rate and volume and adequate agreement for low flows. The definition of “Adequate” streamflow simulations, is different for different models, research objectives and data availability. Thus, it is important to set criteria for the simulations before the start of simulations (Moriassi et al. 2007). Model calibration can be performed manually or automatically.

In manual calibration, the modeller adjusts the parameters (on a trial and error basis) based on visual assessment of the observed streamflow and simulated streamflow (Kapangaziwiri, 2007). Manual calibration results depend on the modeller’s experience of the specific hydrological model used, knowledge of the hydrological processes of the catchment (Mandsen, 2000). Thus, an experienced modeller is likely to obtain hydrological meaningful results. Drawbacks of this method are subjectivity and it is a time-consuming exercise, especially for an inexperienced hydrologist (Mandsen, 2000; Kapangaziwiri, 2007). Nonetheless, manual calibration can be favourable for areas with data scarcity and eliminate obtaining adequate results for the wrong reason, as the parameters can be adjusted within meaningful hydrologically sound values (Kapangaziwiri, 2007).

Automatic calibration, based on the optimization theory, adjusts model parameters automatically according to specified search schemes and numerical measures of the goodness-of-fit between the simulated and observed hydrographs (Madsen, 2000; Kapangaziwiri, 2007). Automatic calibration was partly developed to address the drawbacks (time consuming, experienced modeller, subjectivity) of manual calibration (Kapangaziwiri, 2007). However, automatic calibration has issues including having parameters being insensitive beyond certain threshold values which is not the case in a hydrological system (Kapangaziwiri, 2007). The process of model calibration also aids in identifying sensitive parameters of a certain model and the identified sensitive parameters can be examined for their hydrological importance in a particular catchment (Arnold et al, 2012). After model calibration, the model must be validated.

### **2.13 Hydrological model validation**

Model validation is the process of demonstrating that a given site-specific model is capable of making accurate simulations beyond the data used for calibration (Refsgaard, 1997). Model validation is performed by running a model using parameters that were deemed suitable during the model calibration process, and comparing the predictions of the model to observed data not used during calibration (Refsgaard, 1997; Kapangaziwiri, 2007; Arnold et al. 2012). The model is supposed to be validated if its accuracy in the validation period has been proven to lie within acceptable limits (Refsgaard, 1997). Often validation performance statistics are poorer than calibration statistics, which may be because of model over- parametrization (Kapangaziwiri, 2007).

Model validation is mostly performed by splitting a dataset into two periods for calibration and validation. In model validation process, it is important to ensure that the dataset to be used are similar to the dataset used in the calibration process i.e. wet, moderate, and dry years occurs in both periods (Arnold et al. 2012). However, in some cases, the data available may not be long enough to allow the aforementioned situation. In such instances, data at a given monitoring location are used for the calibration phase and validation performed at one or more other gauges within the same particular catchment (Arnold et al. 2012).

## 2.14 Prediction of streamflow in small mountain catchments

Accurate representation of evapotranspiration, infiltration, groundwater contribution, soil characteristics generally lead to improved streamflow predictions (Bonell, 1998; Anderson et al, 2009). Topography, soils, rainfall which varies spatially in mountain environments are noted as being the main factors causing runoff heterogeneity at different catchments (Singh, 1997; Koren et al. 1999). Moreover, one issue that comes up particularly in mountain catchment modelling is the ability of hydrological models to consider scale variability of the important site-specific hydrological processes (Seyfried and Wilcox, 1995). Therefore, a challenge in the prediction of streamflows in small mountain catchments is a selection of a model that appropriately represents catchment processes at appropriate scales. Below only a few examples are presented to illustrate the challenge of scaling hydrological processes in mountain catchments which ultimately influence the accuracy of streamflow modelling.

Hydrological processes (infiltration, evaporation, soil moisture, temperature) are variable at different spatial scales (Didszun and Uhlenbrooke, 2008). For instance, Didszun and Uhlenbrooke, (2008) reports that in Neversink River catchment (United States of America) physical water parameters differed significantly only at a scales above 3 km<sup>2</sup> while significant differences in runoff characteristics occurred at scales of 8-21 km. Thus, the measurement scale and averaging values measured at different scales is a challenge in mountain catchment modelling. This is evident in the challenge of transferring modeling results obtained on small representative catchments to larger catchments (Koren et al. 1999).

Efficiency modelling streamflow in mountain catchments is influenced by spatial and temporal rainfall variability. For instance, the KINEROSR distributed hydrological model was sensitive to variable spatial rainfall input in the USDA-ARS Walnut Gulch Experimental catchment (Goodrich 1990, Goodrich et al 1995). Using the radar (NEXRAD) estimated rainfall, the Sacramento model, was sensitive to spatial rainfall variability, with the change from broad to small resolutions of spatial averaging of rainfall leading to less surface and total runoff generation (Koren et al 1999). In contrast, the sensitivity of TOPMODEL to spatial rainfall patterns for the Real Colobrier catchment (71 km<sup>2</sup>) reveals that the primary reason for evaluating spatial variability was to accurately estimate the total volume of the model input; and beyond

that knowledge of the spatial pattern did not appear to improve the predictive performance of TOPMODEL (Shah et al. 1996). The Langrivier catchment, simulated using the ACRU model in lumped mode, underestimated flows possibly as a result of underestimation of catchment rainfall (New, 1999). Thus, the current study attempts to accurately represent the total volume of rainfall for model input.

Physiographic catchment characteristics such as topography, which is directly linked to rainfall residence time, are also challenging to accurately represent. The TOPMODEL developed specifically to generate streamflow based on topography, using the topographic index, as the main control of rainfall routing (Beven, 2001). However, Franchini et al (1996) found that the sensitivity of the topographic index is dependent on the size of a digital elevation model (DEM). Scaling soil properties, important for runoff generation and timing of peak flow, is also challenging to accurately represent in hydrological modelling (Zehe and Bloßchl, 2004). Thus, modelling streamflow in mountain catchments requires selection of a model that will account for important site-specific catchment characteristics. The scale challenges to modelling mountain catchments processes have led to the development of the Representative Elementary Area method (REA).

The Representative Elementary Area method determines a certain threshold area beyond which an 'average' hydrologic response can be found (Seyfried and Wilcox, 1995). This method was developed to address extensive sampling in space and time that would be required for process understanding for water resources predictions at larger scales (Didszun and Uhlenbrooke, 2008). Zehe and Bloßchl, (2004) highlight that no matter what the spatial resolution of the field measurements, there would always be some fine-scale detail not captured by the measurements, thus REA is needed in hydrological modelling. Deciding on the appropriate REA is challenging as REA can be catchment specific (Zehe and Bloßchl, 2004; Didszun and Uhlenbrooke, 2008), and consequently hydrological models require calibration. Therefore, selection of a hydrological model in mountain catchments, apart from the model being representative of the main catchment processes, requires an understanding of the sensitivity of the particular model to the spatial and temporal variation of hydrological processes that are dominant to a particular catchment.

## 2.15 Hydrological responses of small mountainous catchments

Understanding the main hydrological characteristics of a catchment is essential in the prediction of streamflow. Accurate estimation of catchment characteristics significantly affects the quality of modelling results in mountainous catchments (Gurtz et al, 2003). Thus, a conceptual model of Langrivier's critical runoff components and flow paths to is needed, in order to adequately represent important runoff controlling and generating hydrological processes. The discussion in this sections aims to identify the main fluxes and hydrological flow characteristics of small mountainous (<10 km<sup>2</sup>) catchments, including those that have been investigated in Langrivier. Ultimately, this sections aims to facilitate the selection process of the appropriate hydrological model and appropriate model parameters ranges to use to predict streamflows in Langrivier.

It is important to note that different climatic zones (e.g. Tropical climate, Mediterranean climate) have different dominant processes. For instance, soil water content variability is influenced by the depth to water table in humid environments while this is not the case in arid to semi-arid areas (Gomez-Plaze et al. 2001). As such, certain models developed in different parts of the world are generally structurally suited for the regions they were developed in.

Energy and water fluxes dictate the flow of water to and from a mountain catchment (Bales et al, 2006). Variable mountain physiography (topography, vegetation, geology) leads to non-systematic distributions of conditions that control the energy fluxes of latent heat, sensible heat, solar radiation and terrestrial radiation (Bales et al, 2006). Invariably, such non-systematic distribution of energy fluxes naturally leads to variable water fluxes within catchments. The most critical energy flux is net radiation, as it is the main supplier of energy required to drive the evapotranspiration process (Teixeira et al. 2008)

In many mountains, the greatest flux of water out of the system is evapotranspiration (Bales et al, 2006; Teixeira et al. 2008). Evapotranspiration is either controlled by atmospheric demand or by soil hydraulic properties (Zehe and Bloßschl, 2004). Evaporation estimated using meteorological elements (solar radiation, wind speed, relative humidity, and air temperature) generally decreases with an increase in elevation for most mountainous areas (Nullet and Juvik, 1994). Evaporation rates vary hourly as a result of daily variation of the meteorological elements. In the Langrivier, the highest daily evaporation rates occur between 14:00 and 16:00 (Whicht, 1941).

The dominant runoff generation pathways are different in small mountain catchments than in larger catchments. A 0.015 km<sup>2</sup> Dreisam headwater catchment (Germany), the dominant flow generation mainly by pre-event hillslope water with only a small fraction of new rainfall contributing to runoff generation (Didszun and Uhlenbrooke, 2008). Steep hillslopes are dominated by preferential flow particularly in humid catchments (Anderson et al, 2009). In Langrivier, an isotope study revealed that only 5% of the streamflow was made of surface runoff, while 95% of the runoff generating rainfall reached the stream as baseflow (Midgley and Scott, 1994). Additionally, the Langrivier has a high run-off ratio, with 75% of annual rainfall becoming runoff (Booyesen and Tainton, 1984). A fast response characteristic to rainfall has been observed in catchments dominated by subsurface flow because of a well-developed preferential flow network (Anderson et al, 2009). Bonell (1998) notes that although forested catchments may have preferential flow as the dominant runoff generation mechanism, in topographically convergent areas, the overland flow may occur albeit their importance to storm hydrograph depends on their connectivity to organized drainage. There are a few topographically convergent areas in the Langrivier that may give rise to overland flow in the catchment and contribute to the fast response of the catchment.

There is limited information on groundwater flow dynamics, aquifer properties, and groundwater recharge rates in Jonkershoek catchment as a whole. The soils have a low bulk density, high infiltration capacity and are well-drained (Scott et al. 2000). Soil depths range from roughly 1 to 2 m but are underlain by unconsolidated or decomposed material that allows free drainage of water which would lead to a quick response from the stream even if most (95%) of rainfall reaches the stream as baseflow. However, Hans (2015) found that the A-Horizon depth varied 0.16 to 0.80 m, and the depths decreased with an increase in altitude, with gentle slopes having low soil stoniness. In Arna's mountainous catchment, an extensive soil depth study revealed that soil depth decreased with an increase in altitude, slope steepness albeit the catchment was once used for cultivation (Navas et al. 2005).

## **2.16 Summary and Recommendations**

This chapter highlighted various aspects and challenges of estimating catchment rainfall and cloud water. Factors such orography and topographic feature such altitude, slope, aspects were

identified as aspects that influence the spatial distribution of rainfall in mountain catchments. As a result of the aforementioned factors, monitoring rainfall for accurately estimating catchment rainfall is a challenge and possibly leads to inaccurate precipitation information. Developing of monitoring equipment has drastically improved the accuracy of rainfall estimation. Although there have been drastic advances in the development of new equipment/techniques to estimate catchment rainfall, rain gauges are still one of the most suitable methods to measure rainfall as they are accurate and other methods directly depend on rain gauges for estimation of rainfall. Furthermore, cloud water is an important precipitation source in mountain catchments such as Langrivier. As a consequence, when a catchment has precipitation underestimated, cloud water interception should be considered as one of the precipitation forms that may be causing the precipitation underestimation.

For the current study, underestimation of catchment rainfall was determined by streamflow records showing more streamflow output than rainfall. As a result, after improving catchment precipitation for Langrivier, the improved estimation precipitation should be examined by predicting streamflows for the catchment. This chapter revealed that hydrological models are an appropriate tool to predict streamflows. In terms of hydrological modeling, accurate representation of catchment characteristics was identified as an important factor that determines streamflow modelling success particular in small mountain catchments. As a consequence, a hydrological model that is selected for streamflow modeling in this catchment has to be able to represent the main catchment characteristics.



## 3 Materials and Methods

### 3.1 Introduction

The assessment of the contribution of cloud water to total precipitation, significance of including high altitude rainfall stations in improving rainfall estimation was achieved by evaluating whether (a) the establishment of additional rain gauges to cover the different elevations improves the estimation of event based and daily precipitation, (b) improve the estimation of catchment precipitation by including cloud water interception. Thereafter, rainfall estimated using the expanded precipitation network was used for prediction of streamflows of the Langrivier catchment. Monitoring of cloud water and rainfall was for a one-year period from May 2014 to June 2015.

The selection of an appropriate study area with necessary characteristics in line with the study objectives was essential. The appropriate study site had to have a marked difference in elevation, and with long rainfall and streamflow data, in order to evaluate whether the establishment of additional rain gauges improves estimation of catchment rainfall and prediction of hydrological processes. In addition, the site should have frequent observable clouds being intercepted by the land surface.



### 3.2 The study site

In South Africa, there are various study areas that meet the aforementioned characteristics of an appropriate study site. Mountain catchments such as Cathedral Peak in Kwazulu Natal Province, the Berg River catchment in the Western Cape Province could fulfill the requirements for a study of this nature. However, the Langrivier catchment a sub-catchment of Jonkershoek River was selected for this study. The Jonkershoek catchment is located north-east of Stellenbosch in the Western Cape Province, South Africa. The Langrivier catchment has marked elevation difference varying from 360 m.a.s.l to 1423 m.a.s.l, and over 70 years of rainfall and streamflow data, and frequent presence of clouds near the surface.

The Jonkershoek research site (Figure 3.1) was established in 1935 (van Wyk, 1987), for interdisciplinary research examining the ecological and hydrological effects of replacing indigenous fynbos vegetation with forestry pine plantations (Bennett and Kruger, 2013). The climate of the study area is Mediterranean and rainfall is the main form of precipitation. There are five sub-catchments whose rainfall, temperature, and streamflow is continuously monitored. These catchments are Bosboukkloof, Biesievlei, Tierkloof, Lambrechtsbos A and B, and Langrivier. The Jonkershoek catchment is enclosed on three sides by mountains with the highest elevation ranging from 792 to 1525 meters (van Wyk, 1987). A previous study (Wicht *et al.* 1969) reveal that the Jonkershoek catchment has a steep rainfall gradient increasing south-east towards the Dwarsberg mountain. The Dwarsberg has the highest rainfall ever recorded in South Africa (3620 mm/year) (Wicht *et al.*, 1969). The open side of the catchment is to the north-west, from which the prevailing rain-bearing winds blow, with the Dwarsberg acting as an effective rain-trap (van Wyk, 1987, Wicht 1940).



UNIVERSITY *of the*  
WESTERN CAPE

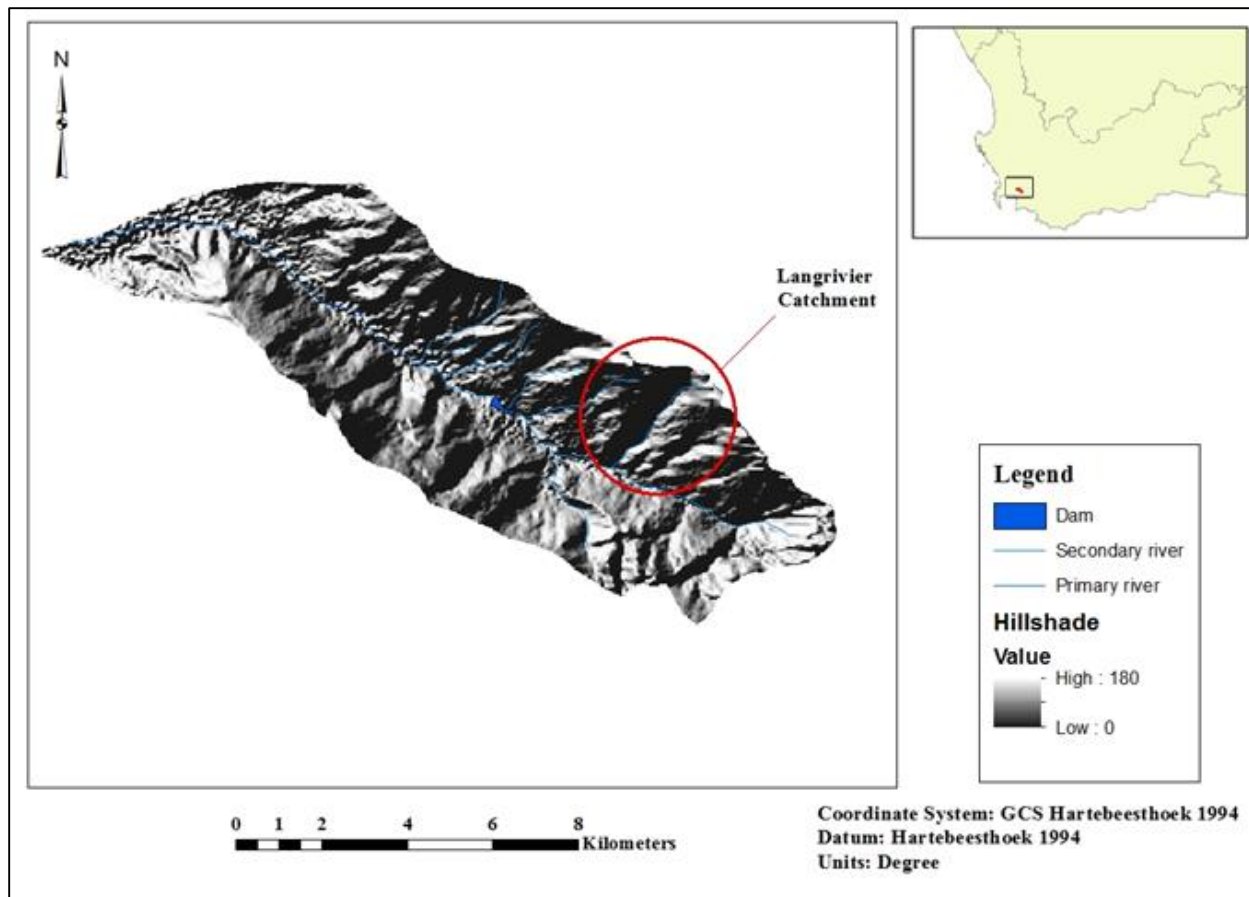


**Figure 3.1: Location and topography of the Jonkershoek catchment within the Western Cape**

According to Wicht (1940), the prevailing winds are relatively dry during summer (October to March). These dry summer winds only cause orographic rains on the mountain-tops. The mountain-tops experience hail and snow two or three times every winter. According to Van Wyk (1987), the Jonkershoek catchment has 85% of the rainfall falling between the months of April to September, with yearly average rainfall for Langrivier catchment being 1600–1800 mm/year (Wicht et al. 1969). The mean annual temperature is 16.1 °C, with a yearly average maximum temperature of 38.1 °C and a yearly average minimum temperature of 0.7 °C (Van Wyk, 1987). The Langrivier catchment has fynbos vegetation, ranging in height between 2-3 meters when mature, and dominated by *Protea nerrifolia*, *Protea repens*, *Brunia nodiflora* and *Widdringtonia nodiflora* (Van Wyk, 1987). Fog frequently occurs to 450-600 m.a.s.l ground levels within the Langrivier (Figure 3.2).



**Figure 3.2: Occurrence of cloud emersion on Langrivier**

The geology of the Langrivier catchment consists mainly of fractured Table Mountain Sandstone outcrop, Cape Granite on the low areas (van Wyk, 1987; Midgley and Scott, 1994; Scott and

Prinsloo, 2008). The Langrivier is dominated by structureless, low organic matter, and mostly deep rocky soils with a large water holding capacity (New, 1999; Scott and Prinsloo, 2008). The soils have infiltration capacities well in excess of prevailing rainfall intensities (Midgley, 1994; Dye and Croke, 2003). The soils are mainly derived from quartzitic sandstone talus. According to New (1999), most locations have shallow soil depths which can be up to several meters in depth.

The main runoff generating mechanism in Langrivier catchment is throughflow or “push-through” (Midgley and Scott, 1994; New, 1999). In the upper part of the catchment ( $\geq 850$  m.a.s.l) which has bare rock outcrop is likely to have overland flow as the dominant runoff generating mechanism. This rock outcrop in Langrivier may be important for streamflow hydrograph characteristics. For instance, a rock outcrop which occupied a third of 10 hectare Maimai research catchment in New Zealand contributed 50-55% to peak flows after a single rainfall event and similarly a 3.6 hectare outcrop in a 41 hectare catchment significantly affected streamflow hydrograph (McGlynn and McDonnell, 2003). The area below 850 m.a.s.l in the catchment is highly vegetated with fynbos vegetation (graminoids, shrubs), and afrotemperate forests along streams and on slopes. The abundance of vegetation coupled with increased water holding capacity leads to increased infiltration rates, which favour interflow and baseflow in Langrivier. Furthermore, the steep slopes with small tributaries facilitate a fast response to rainfall events. One prominent feature that might alter the hydrological responses (flow) for the current study within the Langrivier catchment is fire. The Jonkershoek catchment has recently had two wildfires, in 2009 and in March 2015.

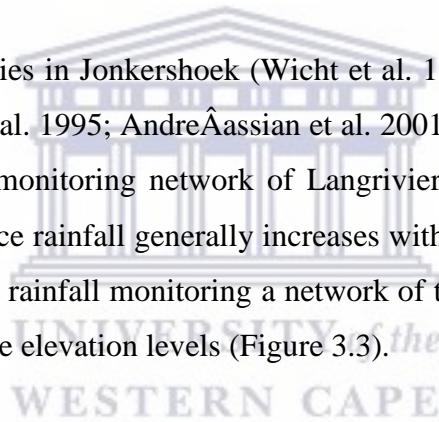
### **3.3 Data collection**

This thesis deals with improving estimation of catchment precipitation for predicting streamflows. Data is required for precipitation (rainfall and cloud water), streamflow, evaporation, and catchment physiographic characteristics for improving hydrological parameter estimation. As objective one of this thesis aims at improving estimation of catchment rainfall at a daily scale, other meteorological data types that were used in this study were also required at daily time scale. The methods used to collect data for all the variables are described below.

### 3.3.1 Rainfall measurements

As stated in Chapter 1, the Langrivier catchment (2.45 km<sup>2</sup>) has a marked difference in elevation with only two rain gauges (Davis tipping bucket) located at historical monitoring sites of 8B (from now on referred to as R360) and 14B (from now on referred to as R460) m.a.s.l located 700 meter as way from each other (Figure 3.3). A recent weather station was erected by SAEON at 1214 m.a.s.l in 2013 (called DWA 1214 from here onwards) near the site of a historic rain gauge that monitored rainfall on a monthly basis. The DWA 1214 weather station monitors weather elements on an hourly based including cloud water. The river profile of Langrivier stream shows the sharp change in elevation over a short distance (3 km length), with a change in elevation of 652 m over the 3 km distance from the lowest to the highest point (Figure 3.4). The Langrivier has an aspect facing south-west, with a slope range of 0.05-0.8 and average slope of 0.43% (New, 1999).

Based on previous rainfall studies in Jonkershoek (Wicht et al. 1969; Moses 2008) and in other parts of the world (Goodrich et al. 1995; AndreÂassian et al. 2001; Anctil et al. 2006; Buytaert et al. 2006), the current rainfall monitoring network of Langrivier catchment is likely to underestimate catchment rainfall, since rainfall generally increases with altitude. Therefore, to address the objectives of this thesis, the rainfall monitoring a network of the Langrivier was expanded to monitor rainfall at representative elevation levels (Figure 3.3).



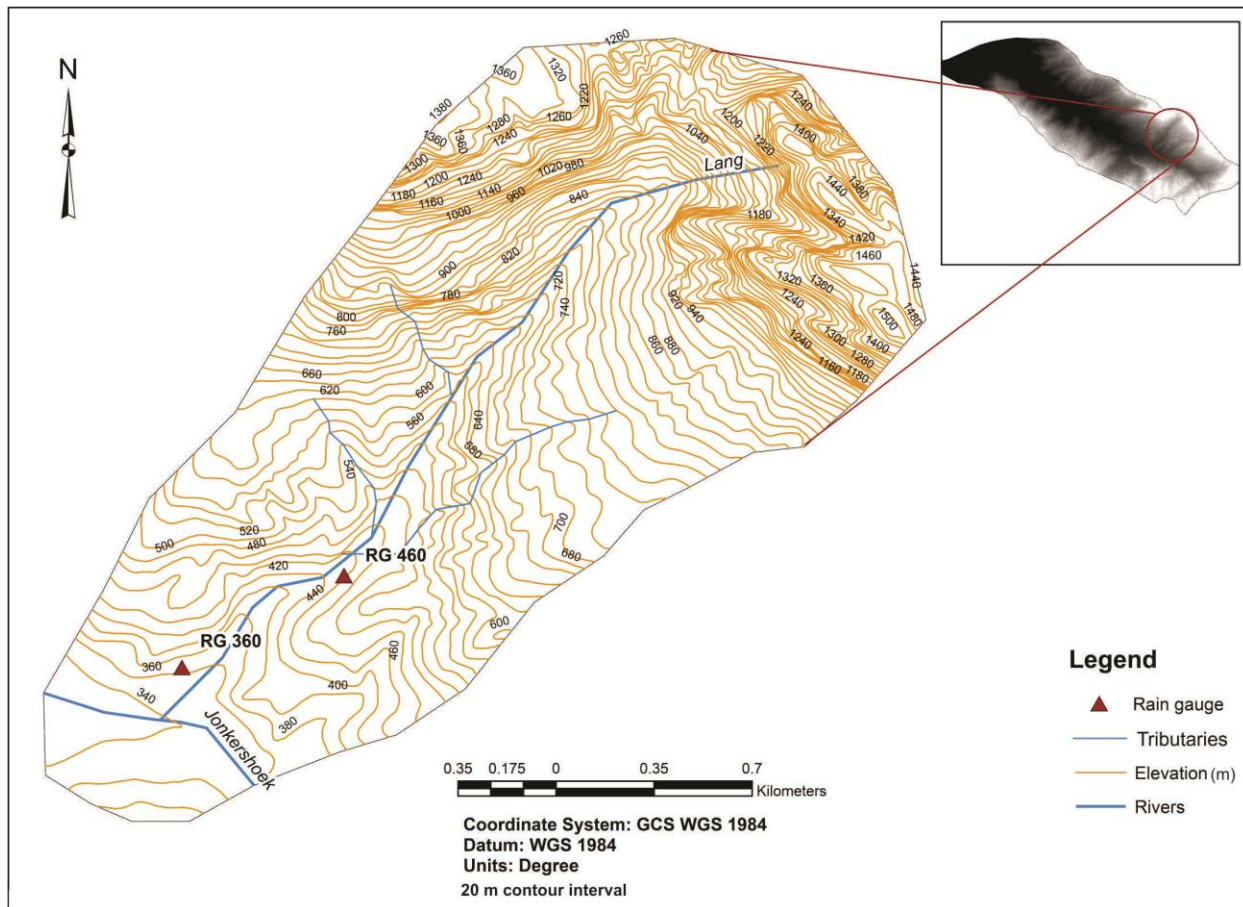


**Figure 3.3: Illustration of rain gauge station RG360 (R360) and R460 (R460) within Langrivier before May 2014 (produced from 1:50 000 (3318DD) map published by the Chief Directorate, Surveying and Mapping, South Africa, 2003).**

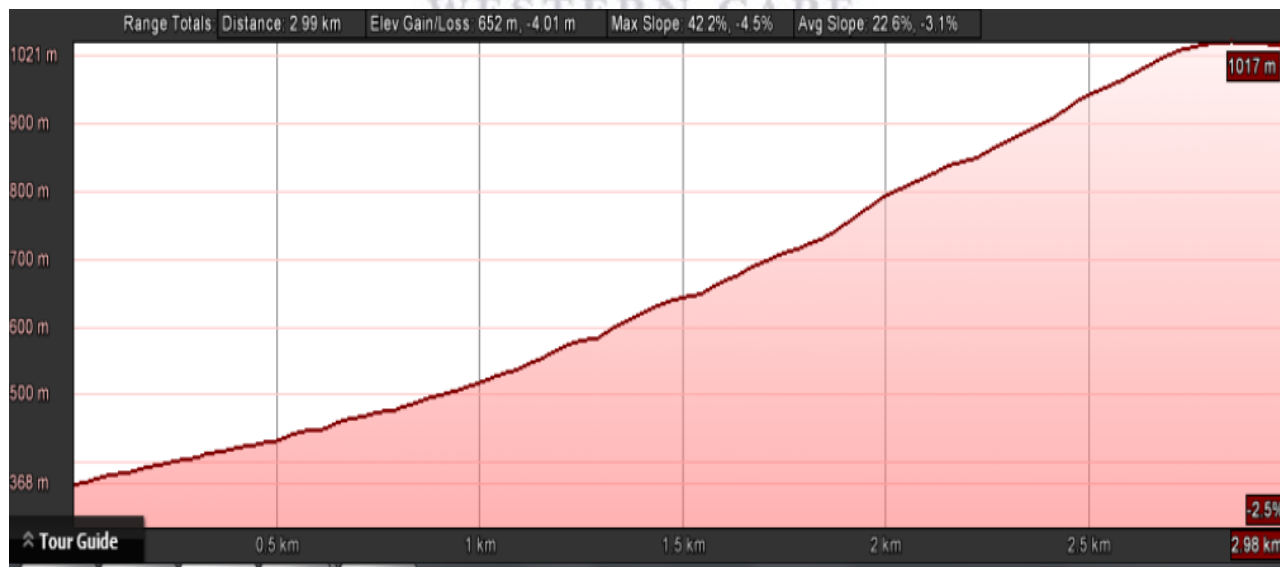


**Figure 3.4: River profile of the Langrivier stream (Google earth, 2015)**

Four additional rain gauges were installed by SAEON in the Langrivier catchment at different altitudes (Figure 3.5 and Table 3.1). The rain gauges were installed at altitudinal intervals of 100 meters from 500 to 800 m.a.s.l in order to examine the variability of rainfall with altitude. The 100 meter elevation interval was used as rainfall has been shown to vary by as much as 14% over 100 meter distance (Goodrich et al. 1995). The lateral distance between the rain newly installed rain gauges was not constant. For instance, the rain gauge at 500 m.a.s.l is 165 meters away from the rain gauge at 600 m.a.s.l while the rain gauge at 700 m.a.s.l is 785 meters away from the rain gauge at 800 m.a.s.l. In total, there were seven rain gauges (i.e RG500 with the RG standing for rain gauge while 500 stands for elevation above sea level in meters) when including the three already existing rain gauges in the catchment. All the newly installed rain gauges were Texas electronic tipping bucket rain gage model TR-525I with a tipping resolution of 0.254 mm. All the rain gauges were programed to produce rainfall totals at one-hour intervals and sum to daily totals at midnight (the monotoring period was from May 2014 to June 2015). Additionally, all the rain gauges were placed at the height of 1.25 m above the ground.

**Table 3:1: Newly installed rain gauges in Langrivier catchment as from May 2014**

Elevation (m.a.s.l)	Rain gauge
500	RG 500
600	RG 600
700	RG 700
800	RG 800



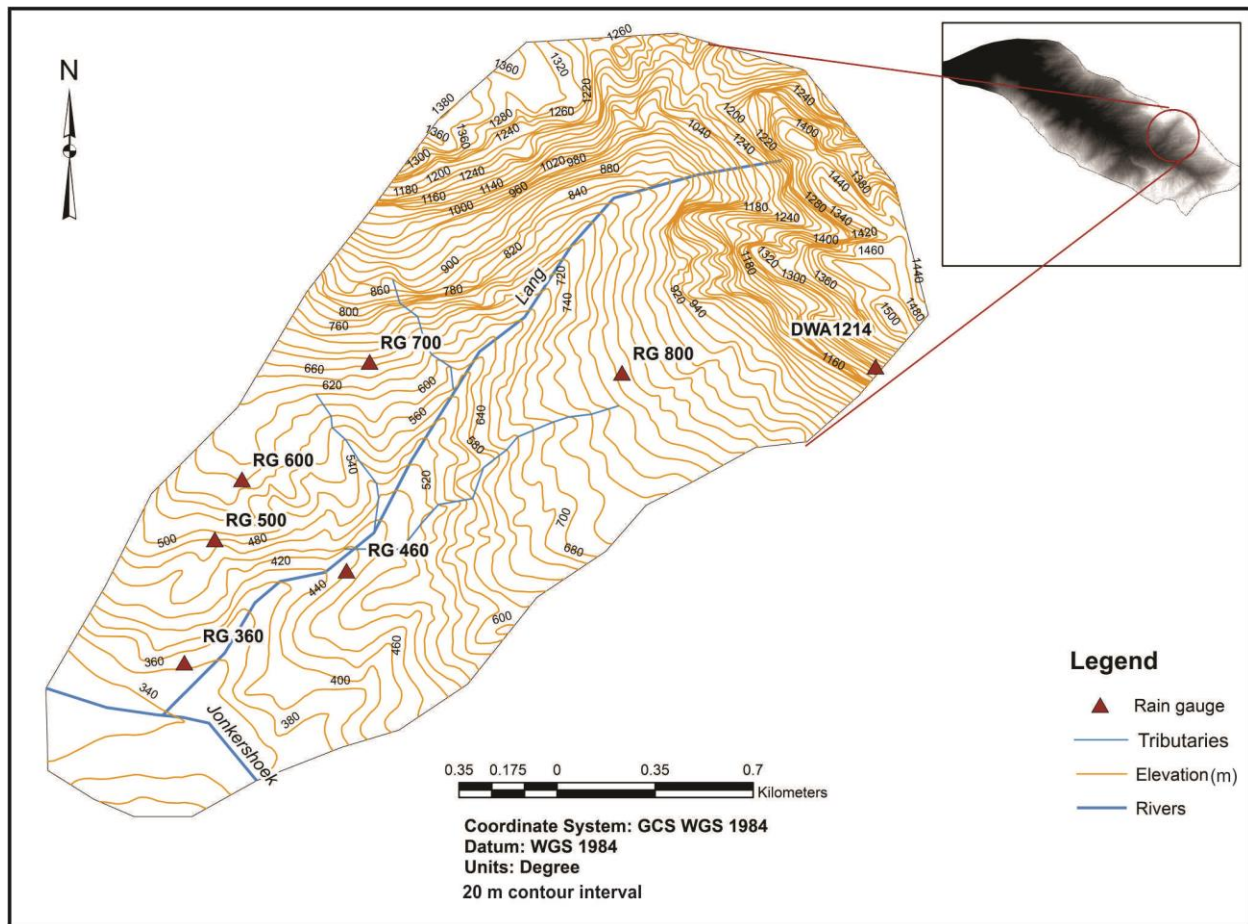


**Figure 3.5: Set up with new rain gauge stations within Langrivier after May 2014 (produced from 1:50 000 (3318DD) map published by the Chief Directorate, Surveying and Mapping, South Africa, 2003).**

The exact locations of the rain gauges were partly selected based on accessibility as the slopes can be very steep and the presence of short vegetation. All the rain gauges were placed in similar aspects (south-west) and surrounded by short vegetation less than 1 meter. However, a challenge in mountainous catchments is that the topography is relatively steep which rarely presents the ideal environmental setup (a relatively flat area clear of vegetation) required for rain gauge locations. This is not always available particularly in mountainous areas as was the case with Langrivier.

### 3.3.2 Cloud water interception

The main aim of collecting cloud water data is to quantify cloud contribution to total precipitation of the Langrivier catchment. To achieve this, the variation of cloud water was assessed by placing fog gauges along an elevation gradient. Assessing the variation of fog along

the elevation gradient within the Langrivier catchment was conducted using a Louvred screen fog (LSF) gauge also known as Juvik collector.

Four Louvred screen fog gauges were installed by SAEON in collaboration with UWC along an elevation gradient and installed adjacent to tipping bucket rain gauges that were installed for rainfall estimation (Table 3.2). The Louvred screen fog (LSF) catcher is 25.4 cm in diameter, with a 54.3 cm mesh height, and the circumference is 76.2 cm connected to Texas Electronics model TR-525I tipping bucket gauges with a resolution of 0.254 mm (Figure 3.6). All the TR-525I tipping bucket gauges recording cloud water were programmed to produce rainfall totals at one-hour intervals and sum to daily totals at midnight (the monitoring period was from May 2014 to June 2015). The LSF has a cylindrical configuration which enables interception of fog irrespective of the direction from which fog originates. The LSF gauge has a semi-rigid structure with the definable surface area and high collection efficiency (Framau, et al 2006), and is relatively inexpensive to assemble. The LSF was placed 1.5 meters above ground. The surface area of the LSF collector is used to quantify fog contribution to total precipitation. A correction of 5.8 was used as the LSF collector has a cross-sectional area that is 5.8 times greater than that of a rain gauge. The LSFs were installed with wind direction and speed sensors, in order to examine how wind direction and speed influence the cloud water quantity.

**Table 3:2: Newly installed fog gauges for monitoring cloud water interception in Langrivier.**

Elevation (m.a.s.l)	Fog gauge
500	LSF 500
600	LSF 600
700	LSF 700
800	LSF 800

LSF stands for Louvred screen fog gauge while the number stands for the elevation of the LSF.



**Figure 3.6: Louvred screen fog (Right) mounted on top of a rain gauge with another rain gauge on the left to assess amount of precipitation falling as rain.**

The limitation of using a LSF is that when it rains the quantity of fog collected cannot be determined with confidence as there is a possibility of rainfall being captured by the fog gauge especially if there are strong winds accompanying the rainfall. Therefore, cloud water can only be estimated when there is no rainfall. In addition, LSF has less than 100% efficient collection either due to a fractional sampling of the air passing the gauge or by flow distortion around the gauge. As such fog during precipitation-free periods is underestimated especially for short intermittent fog events due to losses by wetting of the gauge surface and evaporation from the gauge surface (Framau et al 2006). On the other hand, such short periods of fog precipitation are

unlikely to add to the system's water balance since it is likely to evaporate off the surfaces of plants or rock on which it may precipitate.

### 3.3.3 Streamflow

Streamflow records were needed for calibration and validation of the prediction of streamflow modelling. Streamflow data were obtained from a gauging station on the Langrivier, that has a combination of a 90° V-notch for low flows and a rectangular sharp crested weir, established in 1938 by the Jonkershoek Forestry research Centre, connected to an automated Belfort streamflow recorder and Orpheus mini Hach/OTT to monitor streamflow within the Langrivier. The weir records streamflow at average hourly intervals. The streamflow data for simulation is from March 2013 to June 2015.

### 3.3.4 Meteorological elements for estimating evaporation

Potential evaporation can be estimated using various approaches. In South Africa the Hargreaves and Samani approach has been shown to estimate evaporation successfully (Bezuidenhout, 2005). Warburton et al. (2012) used the Hargreaves-Samani equation and the ACRU hydrological model to successfully predict streamflow in three catchments located in different climatic regions within South Africa. However, the most appropriate method to calculate evaporation should be a physically based approach (New, 1999; Teixeira et al. 2008). The Penman-Monteith equation is one approach that is physically based and is widely used and is recommended by the by various authors (Allen et al. 2006; Teixeira et al. 2008). The Penman-Monteith requires data on temperature, radiation, relative humidity, and wind speed.

The Penman equation (Allen et al. 2006) can be written as:

$$ET = \frac{\Delta(R_n - G) + \rho_a c_p (e_s - e_a) / r_a}{(\Delta + \gamma (1 + \frac{r_s}{r_a})) \rho_w \lambda} \quad (3.1)$$

Where ET is the evapotranspirative flux expressed as depth per unit time,  $\Delta$  the slope of the saturation vapor pressure versus temperature curve,  $R_n$  the net radiation flux density at the surface,  $G$  the sensible heat flux density from the surface to the soil (positive if the soil is warming),  $\rho_a$  the air density,  $c_p$  the specific heat of moist air at constant pressure,  $e_s$  the

saturation vapor pressure at air temperature,  $e_a$  the actual vapor pressure of the air,  $r_a$  the aerodynamic resistance to turbulent heat and/or vapor transfer from the surface to some  $z$  height above the surface,  $\gamma$  the psychrometric constant,  $r_s$  the bulk surface resistance that describes the resistance to flow of water vapor from inside the leaf, vegetation canopy or soil to outside the surface,  $\rho_w$  the density of liquid water, and  $\lambda$  is the latent heat of vaporization.

Weather data for estimating evaporation was collected on an hourly basis. Wind speed was measured using wind sentry anemometer and vane (W/Crossarm) Model 03002. Temperature and relative humidity were measured using CS215 temperature and relative humidity probe from Campbell scientific. Net radiation was collected using an NR lite 2 net radiometers. The Penman-Monteith equation estimates reference evaporation. The reference surface used for calculation ET is standard hypothetical grass reference crop with an assumed crop height of 0.12 m, a fixed surface resistance of  $70 \text{ s m}^{-1}$  and an albedo of 0.23 as suggested for estimating daily ET (Allen et al, 2006). The monitoring period was from May 2014 to June 2015, identical to the rainfall and cloud water interception.

### **3.3.5 Catchment characteristics estimation**

Accurate representation of catchment characteristics aids in improving prediction of streamflow. Catchment characteristics such as infiltration rates, A and B soil horizon depths, vegetation cover, soil porosity and texture, and slope are important in improving simulation of streamflow. These can be estimated or measured directly in the field. Field measurements of soil characteristics i.e soil depth, hydraulic conductivity, bulk density, infiltration were done by (Hans, 2015). Soil characteristics from Hans (2015) we collected at various elevation levels within the catchment as indicated as a-f in Figure 3.7, thus are representative of the catchment soils.

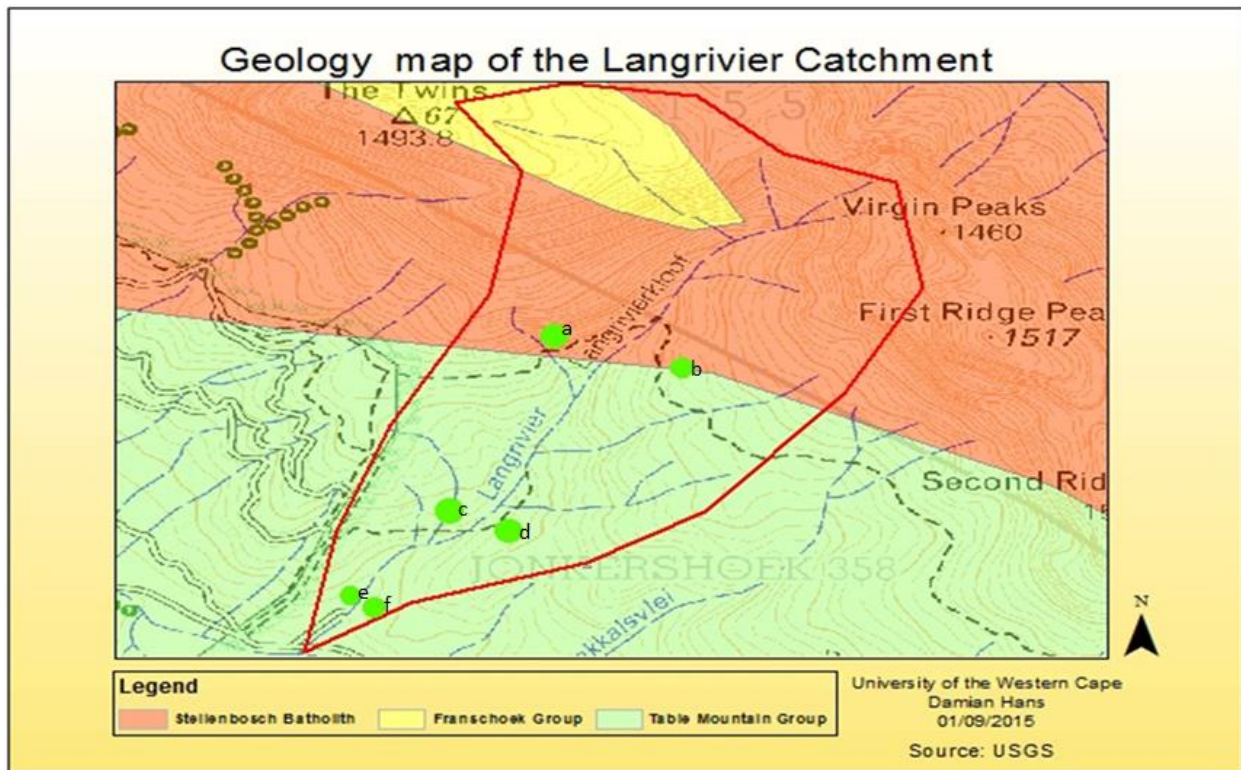


**Figure 3.7: Geology map of Langrivier catchment indicating the points of soil properties sampling (Hans, 2015)**

### 3.4 Infilling of missing rainfall data

Hydrological time series data rarely have complete data (Helsel and Hirsch, 2002). Rain gauge R360 and R460 measured rainfall in 0.2 mm increments, while rain gauges RG 500, RG 600, RG 700, RG 800, DWA 1214 measured rainfall in 0.254 mm and totaled at 1 hour intervals. Therefore, missing data may be found in either increments (R360 and R460) or hourly rainfall data with the other five rain and fog gauges. As a result of operational problems and malfunctioning of the instrumentation, missing data were found in hourly and daily records of precipitation data.

Missing rainfall data was in-filled using linear regression model (equation 3.7). Howerda et al (2010) used linear regression with success to fill in missing rainfall data between individual rain gauges. The reference variables can be the same (e.g. rainfall vs rainfall) or different (rainfall vs flow) (Bogaard, 2010). For missing rainfall data, the same reference variable were used, any two

rainfall stations that had a high correlation coefficient were used to calculate the missing values in between them using equation 3.7.



UNIVERSITY *of the*  
WESTERN CAPE

$$Y = a + bX \quad (3.7)$$

Where: Y= is the dependent variable

X= independent variable

a = intercept

b = slope or regression coefficient

Linear regression tends to limit data variability (Tennant and Hewitson, 2002; Bogaard, 2010). The y-intercept is a constant and causes limited variability as a value of 0 for the independent variable (X) always leads to the value of the dependent variable (Y) value being equal to the value of the y-intercept. To overcome this limitation, the substituted rainfall amounts were multiplied by the ratio of the variance of the daily rainfall of the two stations. According to Tennant and Hewitson (2002) the multiplication of adjusted substitute rainfall by the variance ratio ensures that adjusted station keeps its original climatological variance. The ultimate goal of the data quality process is to use a reliable, continuous long-term set of meteorological data measurements for the study area. Streamflow was in filled using different reference variables (rainfall vs streamflow) while Meteorological variables were in filled using same reference variables as there were numerous measuring stations within the catchment.

### **3.5 Data analysis of precipitation**

The data from the seven rain gauges was assessed on a daily and monthly basis. The most important aspect for analysis of rainfall data for the objectives of this study is to determine whether an increased array of rain gauges to monitor rainfall at different elevation levels improves the estimation of catchment rainfall. If any of the new rain gauges receives statistically different rainfall totals from R360 and R460, it will therefore, demonstrate that R360 and R460 were not representative of catchment rainfall totals. So the increased rain gauge network would have improved catchment rainfall estimation. An important rainfall characteristic to prove that rainfall is underestimated for the catchment is average daily rainfall of each rain gauge. Thus, the rain gauges were analyzed by comparing their average daily rainfall, to determine whether the expansion of the rain gauge network to monitor rainfall at different elevation leads to an



improved estimation of catchment rainfall. Rainfall will firstly be described using descriptive statistics to determine rainfall characteristics such as the rainfall intensities, diurnal rainfall variability, number of dry and wet spells we only read them in the results section. Furthermore, the contribution of cloud water interception to precipitation was quantified.

### **3.5.1 Testing for normality of rainfall measured by the individual rain gauges**

There are numerous normality tests, testing whether daily rainfall is normally distributed. The most commonly used test being the Shapiro-Wilk test. The Shapiro-Wilk test is sensitive to a wide range of distributions and detects departures due to either skewness or kurtosis or both (Razali and Wah, 2011). Razali and Wah (2011) found the Shapiro-Wilk test to have more power when compared with other popular normality tests. Thus, the Shapiro-Wilk test was used to test the normality. The Shapiro-Wilk test was used by comparing the daily rainfall totals of a particular rainfall station (e.g RG 360) against the other six rain gauge stations rainfall totals to determine whether there are significant rainfall differences. The process was repeated until all the rainfall stations have been cross compared with each other and presented in comparison matrix.

### **3.5.2 Comparison of average daily rainfall**

To determine whether an increased array of rain gauges to monitor rainfall at different elevation levels improves the estimation of catchment rainfall, a t-test was used. The t-test is a parametric test that is widely used for testing if two means are significantly different. The null hypothesis for this test is  $H_0$ : the daily average rainfall does not significantly differ between the two stations while the alternative hypothesis is  $H_a$ : the daily average rainfall between the two stations is significantly different. The t-test assumes that both groups of data are normally distributed, and have the same variance. The two groups, therefore, are assumed to have identical distributions which differ only in their central location (mean). Although hydrological data is rarely normally distributed and have the same variance, Stonehouse and Forrester (1998) report that for large samples  $n > 25-30$ , the t-test can be used with good accuracy. The t-test was used by comparing the daily average rainfall of a particular rainfall station (e.g RG 360) against the other six rain gauge stations average daily rainfalls to determine whether there are significant rainfall

differences. The process was repeated until all the rainfall stations have been cross compared with each other and presented in comparison matrix.

An important aspect in rainfall analysis for variability is analyzing the difference in sample characteristics (mean, median and distributions) on rainfall days only. For the purpose of this study, a rainy day for the catchment is defined as a day when at least one of the seven rain gauges has recorded at least of 0.2 mm of rainfall because the rain gauges have a maximum resolution of 0.2 mm. Nandargi and Mulye (2012) defined a rainy day as a day on which a station has recorded 0.1mm or more rainfall. Consequently, analysis of the difference between daily rainfalls recorded at different elevations was carried out only, when at least one of the seven rain gauges recorded rainfall as per definition is given for this study. This approach of analyzing rainy days only aims to remove the influence of the days without rainfall on the variation of mean daily rainfall.

Helsel and Hirsch, (2002) report that the main limitation of the t-test is a lack of power when applied to non-normal data. However, because of the objectives of the study and the type of data being collected (independent and a large sample  $n > 100$ ) the t-test is an appropriate test as compared to Wilcoxon Rank Sum Test which works well with smaller samples and dependent samples (Sawilowsky, 2005). Therefore, the t-test was selected to test if the average daily rainfall received at stations in Langrivier differed significantly.

### **3.6 Comparison of rainfall distribution**

The cumulative distribution of rainfall between the seven rain gauges may be different because of their different locations. Information on rainfall distribution further aids in the assessment of effects of altitude on rainfall and ultimately improvement in the estimation of catchment rainfall. The Kolmogorov–Smirnov test (K–S test or KS test) is a nonparametric test of the equality of continuous, one-dimensional probability distributions. The Kolmogorov–Smirnov test compares the distance between the empirical distribution function of the sample and distribution function of the reference distribution, or between the empirical distribution functions of two samples (Young, 1977). The null hypothesis is that the samples are drawn from the same distribution. For

the current study, the K-S test was used to test if the seven rain gauges used are drawn from the same distribution.

### **3.6.1 Interpolation of rainfall**

As highlighted in Chapter 2, in a small catchment with a dense rain gauge network all the interpolation methods are successful. For this study, Thiessen polygons interpolation method which is the simplest interpolation method was used to interpolate rainfall for the catchment as the rain gauge network is considered dense with the addition of four rain gauges to the 2.45 km<sup>2</sup> catchment. In the interpolation process, weighting was through dividing the catchment into three equal grids and assigning each grid the value of the rain gauge closest to it. Total rainfall for the catchment was then interpolated by summing the rainfall provided by these grids proportionally using the grid sizes.

### **3.6.2 Analysis of cloud water**

There is a need to quantify the cloud water contribution particularly in this catchment as previous studies (New, 1999; Manamathela, 2012) reveal underestimation of catchment precipitation. Monitored cloud water in Langrivier was quantified for daily totals and percentage contribution to total precipitation. With the altitudinal transect design of the cloud water monitoring network in Langrivier, it was also possible to identify altitudinal zones where cloud water interception is prominent. To assess whether cloud water contributes to streamflow; a hydrological model was used to predict streamflow using (a) rainfall and cloud water as precipitation input (b) using only rainfall as precipitation input. Additionally, the possible influence of cloud water interception on evaporation rates was examined by comparing ET values for days differing only in the presence or absence of cloud water.

### **3.7 Streamflow modelling**

To assess whether improved estimation of catchment precipitation leads to the improved prediction of streamflows, a hydrological model was used. There is a criteria that a model has to meet, in order to be deemed adequate to assess whether improved estimation of catchment precipitation leads to improved predictions of streamflows.

The model has to meet the following criteria:

- a) The selected model has to be on a fine scale (hourly or daily) time scale to enable the detection of non-linear hydrological response to precipitation (rainfall and contribution of cloud water) that might not be clearly visible at monthly and yearly time scales; and
- b) The model chosen must operate in distributed mode to be capable of responding to spatially variable input of precipitation, soil and runoff processes that are likely to be different for the Langrivier catchment; and
- c) The model chosen must be able to account for important hydrological processes that operates in Langrivier such as flow dynamics that have baseflow/throughflow as the main flow mechanism.

### **3.7.1 Streamflow modelling using ACRU**

ACRU model, with outputs that include daily stormflow and baseflow contributions, was chosen for simulating the streamflows in this catchment (Schulze, 1995; Mugabe et al, 2011). ACRU can operate in lumped mode for smaller catchments, or as a distributed cell type model (homogenous hydrological response units) for areas with more complex physiography (Schulze, 1995; New, 1999). Simulated streamflow values can be requested individually for each homogeneous hydrological response units (which may be different to those of other homogeneous hydrological response units). In this section, the structure and critical model parameters of the ACRU model is described. The model set up, calibration and validation are described in Chapter 5 to improve readability.

ACRU has five important input variables which are precipitation, evapotranspiration, soil types, land use, and temperature and radiation. When some required variable/s are not available, they are estimated within physically meaningful ranges based either on the literature or on local expert knowledge (Schulze, 1995). Spatial variation of rainfall, soils, and land cover is captured by operating the model in a distributed mode. In a distributed mode, ACRU is divided into smaller hydrological response units (HRU). The ability to create different HRU's is critical for the current study, as the upper parts of the Langrivier catchment has bare rock surfaces. They are likely to have low infiltration rates than the lower parts.

The general structure of the ACRU model (Figure 3.8) is such that gross rainfall received by pervious areas is subjected to interception and initial abstractions (Schulze, 1995; New, 1999). In ACRU, net rainfall is routed to streamflow via infiltration-excess and infiltration into the topsoil horizon, using either the Green-Ampt approximation of Darcy's law or a modified Soil Conservation Services equation (New, 1999). Access water from the top horizon (A-horizon) drains to the B-horizon at a rate determined by soil textural properties (Schulze, 1995). The ACRU version used in this study uses the Soil Conservation Services equation.

In ACRU, evaporation takes place from previously intercepted water, as well as from the various soil horizons (Schulze, 1995). Evaporation may be estimated as two components which are soil water evaporation (from the topsoil only) and plant transpiration (from all horizons in the root zone), and these can be modelled separately or jointly as total evaporation (Figure 3.8) (Warburton et al. 2010). Soil water evaporation for a day can either occur at the maximum rate (if a minimum threshold of soil water content is exceeded), or below the maximum rate once soil water content has dropped below this threshold. Evaporation from vegetation cover is estimated from a reference potential evaporation, and a plant water use coefficient (i.e. consumptive water use by the plant) of which reflects, *inter alia*, the growth stage of the vegetation. Plant roots absorb soil water in proportion to the distributions of root mass density in the respective horizons, except when conditions of low soil water content prevail. In such cases, the relatively wetter soil horizons provide higher proportions of soil water to the plant in order to obviate plant stress for as long as possible.

# ACRU - Agrohydrological Model

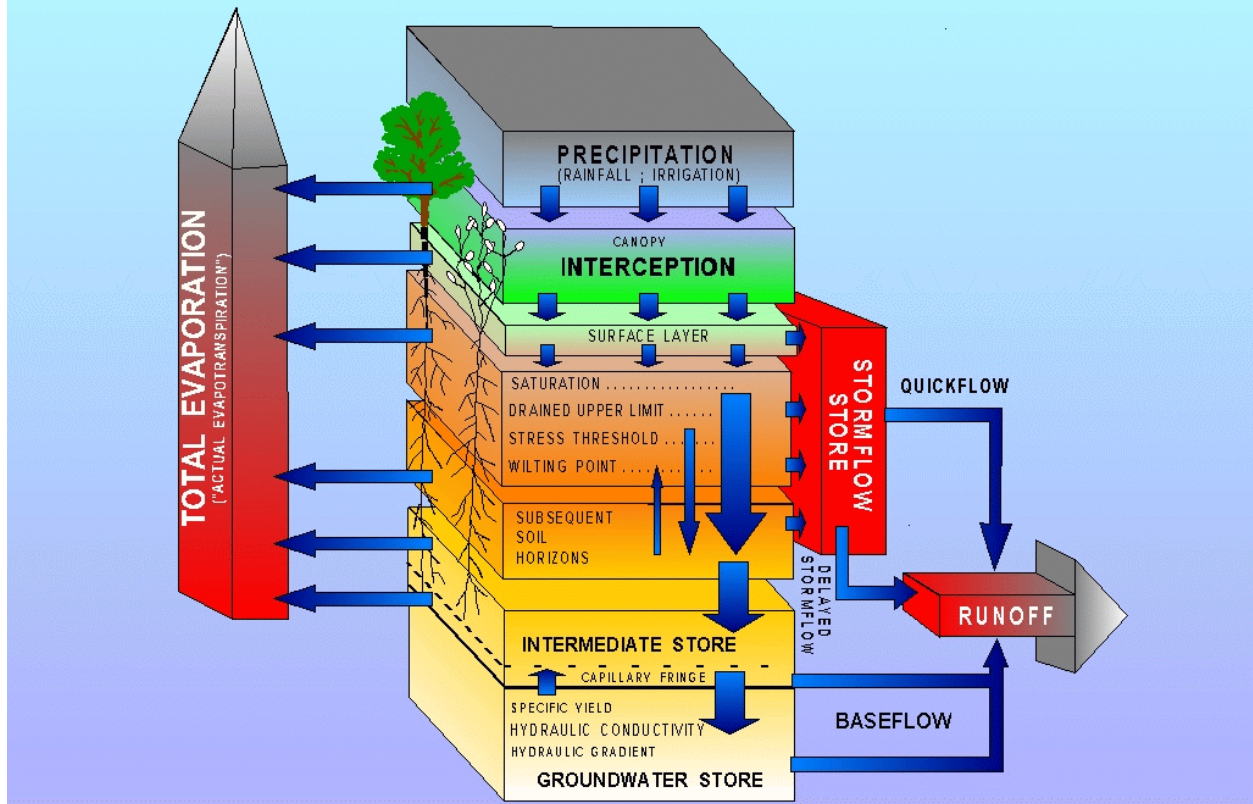


**Figure 3.8: Structure of the ACRU hydrological model (adopted from Schulze, 1995)**

The ACRU model is based on modifications to the equation derived by the Soil Conservation Services, where the daily runoff depth is proportional to the antecedent soil moisture content (equation 1) (Schulze, 1995). For a given amount of rainfall, runoff depth is proportional to the antecedent soil moisture content (New, 1999).

$$Q = \frac{(Pn - cS)^2}{Pg + S(1 - c)} \quad (3.2)$$

Where:  $Q$  = runoff depth (mm)

$Pn$  = net daily rainfall (mm); i.e gross rainfall less canopy interception; plus contribution from pervious areas

$S$  = Potential maximum retention

=  $SWD * SMDDEP$

Where  $SWD$  = the soil water deficit

$SMDDEP$  = is the critical run-off response soil depth

$c$  = coefficient of initial abstraction

The potential maximum retention of the soil,  $S$ , is considered as a soil water deficit and is taken as the difference between water retention at porosity and the actual soil water content just prior to the rainfall event (Schulze, 1995).  $c$  is a regression coefficient, relates  $S$  to initial abstractions due to depression and other storages (Schulze, 1995; New, 1999). The default value of the regression coefficient in ACURU is 0.2 (Schulze, 1995). The critical soil depth,  $SMDDEP$ , attempts to account for different dominant runoff-producing mechanisms that prevail in different climates, catchment conditions and for different soil properties. Thus, the  $SMDDEP$  parameter may need to be calibrated to be deeper than the A-horizon for this particular catchment.

The critical soil depth ( $SMDDEP$ ) in which soil moisture deficit is calculated for stormflow generation is critical for this catchment that is dominated by a "push through" mechanism for runoff generation.  $SMDDEP$  for short vegetation, a default value equal to the depth of the topsoil (A-horizon) may be used (Schulze, 1995), while for a catchment with a dense canopy cover such as forest plantations, or has a deep litter or an organic layer, or contains highly leached soils resulting in relatively high infiltrability (like Langrivier), the critical depth for calculating the soil water deficit may be deeper than the topsoil horizon because stormflow on such catchments may be perceived as being produced more by a "push through" mechanism.

Streamflow generated by the ACURU model comprises baseflow and stormflow, from both pervious and impervious areas (Schulze, 1995). Stormflow from pervious areas consists of a quickflow response that is released into the stream on the same day as the rainfall event and a delayed stormflow response which represents a surrogate for post-storm interflow. Baseflow is derived from the groundwater store that is recharged by drainage out of the lower active soil horizon when its water content exceeds the drained upper limit (Schulze, 1995).

With regard to baseflow estimation, two response coefficients have been incorporated into the model (Schulze, 1995). The first coefficient relates to the drainage rate of water out of the

bottom soil horizon (B-horizon) when its soil water content exceeds the drained upper limit also known as field capacity. The A-horizon soil layer response coefficient (ABRESP) determines the rate at which excess water drains from the A- to B-horizon while B-horizon soil layer response coefficient (BFRESP) controls the rate of saturated drainage from the B-horizon to the intermediate groundwater store (Schulze, 1995). Suggested values drainage rate for BFRESP for different soil texture classes are given in Schulze (1995). In Schulze (1995), Sandy loam soils such as the one found in Langrivier, the suggested value drainage rate for BFRESP is 0.65

The second coefficient is baseflow response, COFRU, which controls the release of water as baseflow from the intermediate and groundwater store into the stream per day. Factors influencing baseflow release include geology, catchment area and slope (Schulze, 1995). In small and large catchments a 0.5-5% per day is suggested as a starting value (Schulze, 1995). COFRU, by definition, may be considered a baseflow recession constant. However, baseflow is not constant, but rather a function of the magnitude of the previous day's groundwater store (Schulze, 1995). Represented as:

$$F_{bff} = F_{bfi} \left[ \frac{(S_{gwp})^2 + S_{gwp}}{1000 \cdot 1.3} \right]^{11} \quad (3.3)$$

where

$F_{bff}$  = final baseflow release coefficient

$F_{bfi}$  = input baseflow release coefficient and

$S_{gwp}$  = magnitude of previous day's intermediate/groundwater store (mm)

### 3.7.2 Model performance evaluation

There are various criteria for evaluating model performance. It is important to specify criteria of how the model results will be the evaluated before the start of the simulation exercise. Flow duration curves (FDC) analysis is one of the common methods to assess if a model simulates observed flows well. Flow-duration curve can be defined as a cumulative frequency curve that shows the percent of time during which specified discharges were equaled or exceeded in a given period (Searct, 1969). Flow duration curves may be used to compare if a model simulates streamflow discharges frequencies closely to observed streamflow discharges. Apart from FDCs,



the Nash-Sutcliffe coefficient of efficiency (NSE), correlation coefficient ( $r$ ) and coefficient of determination ( $R^2$ ), Root Square Mean Error (RSME), percentage difference between simulated and observed simulated and performance bias (PBIAS) are critical for assessing if a particular model simulates streamflow successfully (Moriasi et al. 2007).

The above mentioned model evaluation statistics have specific values that qualify the model results as successful or not. Correlation coefficient ( $r$ ) measures how two objects are associated, while correlation of determination describes the proportion of the variance in measured data explained by the model (Moriasi et al. 2007). PBIAS (represented by equation 3.4) measures the average tendency of simulated data to be larger or smaller than their observed counterparts; with a positive PBIAS indicating that the model under estimates streamflow and a negative PBIAS indicates that the model over simulates streamflow (Moraisi et al. 2007).

$$PBIAS = \left[ \frac{\sum_{i=1}^n (Y_{obs, i} - Y_{sim, i}) * 100}{\sum_{i=1}^n (Y_{obs, i})} \right] \quad (3.4)$$

- Where :
- $Y_i^{obs}$  is the  $i$ th observation for the component being evaluated
  - $Y_i^{sim}$  is the  $i$ th simulated value for the component being evaluated
  - $n$  is the total number of observations

NSE (represented as equation 3.5) indicates how well the plot of observed versus simulated flow fits 1:1 plot (Singh et al. 2004; Moraisi et al. 2007). In literature, values of  $\geq 0.5$  for NSE are generally accepted as adequate (Moraisi et al. 2007).

$$NSE = 1 - \left[ \frac{\sum_{i=1}^n (Y_{obs, i} - Y_{sim, i})^2}{\sum_{i=1}^n (Y_{obs, i} - \bar{Y}_{obs, i})^2} \right] \quad (3.5)$$

- Where :
- $Y_{obs, i}$  is the  $i$ th observation for the component being evaluated
  - $Y_{sim, i}$  is the  $i$ th simulated value for the component being evaluated
  - $\bar{Y}_{obs, i}$  is the average of observed data for the component being evaluated
  - $n$  is the total number of observations

RMSE (equation 3.6) indicates error in squared units of the constituent of interest and the desired value is 0 (Moraisi et al, 2007). RMSE is considered low when its value is less than half the standard deviation of the measured data (Singh et al, 2004).

$$RMSE = \left[ \sqrt{(Y_{obs, i} - Y_{sim, i})^2} \right] \quad (3.6)$$

- Where :
- $Y_{obs, i}$  is the  $i$ th observation for the component being evaluated
  - $Y_{sim, i}$  is the  $i$ th simulated value for the component being evaluated

For this study, the criteria for qualifying the simulation of streamflow in the catchment using ACRU as adequate is given in table 3.3. As the objective of this study was to improve streamflow simulation after improving precipitation input, the above mentioned values were set according to the general guide as in Moriasi et al 2007.

**Table 3:3: Criteria for determining the adequacy of ACRU for simulating streamflow.**

Statistic	Desired value	Statistic range
NSE	0.6	0-1
r	>0.70	-1 to 1
R <sup>2</sup>	>0.70	0 to 1
PBIAS	25	0% to 100%
RSME	Less than standard dev	
% difference in Mean simulated vs Mean Observed	10%	0% to 100%

### **3.7.3 ACRU model Calibration and Validation**

For this study, manual calibration was chosen as the calibration method. As stated in the aforementioned sections, the Langrivier catchment has the “push-through” process as the main streamflow generation method where most of the daily rainfall reaches the stream as interflow/throughflow and baseflow (Midgley and Scott, 1994; New, 1999). However, there has not been a through field study of the through flow process or groundwater dynamics in the catchment. Thus, a challenge in using a hydrological model for streamflow simulations in the catchment is the issue of throughflow dynamics that is not fully understood. Thus, manual model calibration albeit subjective will be able to identify hydrological meaningful parameters and adjust such parameters used within hydrologically meaningful ranges.

### **3.8 Limitations of the study**

The one-year data in the newly extended rain gauge network may not be long enough to give the full extent of the rainfall variability. One year data may limit the level of confidence in findings as it may be a dry or wet year which may be starkly different from long term averages. In addition, the one year data will limit the calibration and validation periods. A key hydrological process for this catchment i.e groundwater has limited information and as such calibrating the model for this parameter will be challenging as there is no available data on groundwater characteristics.

## 4 Estimation of catchment precipitation

### 4.1 Introduction

This chapter presents results that address the first objective of this thesis which attempts establish if rainfall monitored at higher elevations in the catchment significantly influences the accuracy of estimating catchment rainfall. This chapter first presents rainfall descriptive statistics. Thereafter, statistical analyses for addressing the first objective are presented. In addition, results on the contribution of cloud water to total precipitation to address the second objective which aimed at establishing if accounting for the contribution of cloud water interception improves the estimation of total precipitation in Langrivier catchment are presented. The third objective which assesses how the expanded precipitation network for estimation of catchment precipitation (Rainfall and Cloud water) improves prediction of streamflows will be presented in Chapter Five.

### 4.2 Data quality control and infilling

Both rainfall and cloud water had some missing data over the study period (May 2014 to June 2016). The missing data amongst the different stations were caused either by battery failure or damage to the equipment by fire. Although rainfall, cloud water, and streamflow all had missing data, there were no instances where all the rain gauges and fog gauges failed at the same time even for the period of the fire 9-16<sup>th</sup> of March 2015. Most of the missing data for rain gauges RG500, RG600, RG700, RG800 occurred during and after the fire. As stated in Chapter 3, linear regression was used for data infilling using data from a rain gauge station with the highest correlation coefficient (to the gauge with missing data). Missing precipitation data at different elevations is presented in Table 4.1.

**Table 4:1: Non-availability of precipitation data from May 2014- June 2015 for the seven rainfall stations and five cloud water station placed at different elevations**

	Elevation levels (m)						
	360	460	500	600	700	800	1214
Number of days with missing data	74	32	7	75	12	8	0
% missing data	18.55	8.02	1.75	18.8	3.01	2.01	0

The number of days with missing data is different for all the rainfall stations (Table 4.1). RG 600 and RG 360 had the highest number of days with missing data. All missing data for RG 600 was caused by damage to the data logger during and after the fire while for R360 there were days with missing rainfall data even pre-fire because of battery failure. Missing rainfall data at R460, RG 500, RG 700, and RG 800 was due to battery failure. DWA 1214 has no missing rainfall data for the period under consideration. As highlighted in Chapter 3, a fog gauge was placed adjacent rain gauges at 500, 600, 700, 800 and 1214 m.a.s.l. The fog gauges placed at these elevations depended on the same power supply and data loggers as the rain gauges at these stations. Thus, all the fog gauges have identical missing data as rain gauges at these elevations. Fog gauges at 500 and 600 m.a.s.l.were damaged by the fire (9th March 2015) and not re-installed again for monitoring of cloud water data after this date because of budget constraints.

### **4.3 Variation of monthly rainfall with elevation**

The average total rainfall recorded within the observation period (19 May 2014 to 17 June 2015) at the seven stations was 1390.3 mm/a, ranging from 1035.2 -2246.6 mm (Table 4.2). The highest total rainfall of 2246.6 mm was received by the DWA 1214 station located at the highest elevation level, 1214 m.a.s.l., while the lowest total rainfall of 1035.2 mm was received at R360 station located at the lowest elevation level, 360 m.a.s.l. 51-60 % of rainfall fell during the winter months (May-August) at all rainfall stations. The relationship between rainfall and elevation has a high coefficient of determination of  $r^2 = 0.91$  (Figure 4.1). Although, rainfall generally increases with altitude RG500 had lower rainfall total than R460 similarly RG600 had more rainfall than rain gauges at higher elevations namely RG700 and RG800. All these rain gauges are located in similar aspects, thus the decrease of rainfall with an increase in elevation possibly shows influences of other topographic controls. The highest monthly rainfall totals were received in June 2014 while the lowest was in December 2014 (Table 4.2). Interestingly, November had relatively high rainfall for a summer month in this region due to a heavy storm on the 12 November 2014.

**Table 4:2: Monthly rainfall totals (mm/month) recorded by the seven rainfall stations at different elevation levels within Langrivier catchment.**

Month	R360	R460	RG 500	RG 600	RG 700	RG 800	DWA 1214
May-14	49	71	56	78	97	117	187
Jun-14	217	277	283	364	310	289	543
Jul-14	113	144	131	177	162	150	298
Aug-14	147	147	160	222	222	224	400
Sep-14	56	64	58	67	58	57	134
Oct-14	19	21	17	16	19	23	52
Nov-14	132	169	164	170	152	151	226
Dec-14	17	24	18	21	19	20	53
Jan-15	24	34	27	34	37	33	73
Feb-15	17	18	12	14	16	22	39
Mar-15	0	0	3	3	4	3	12
Apr-15	20	19	16	16	18	21	44
May-15	59	66	53	52	81	89	80
Jun-15	166	160	144	160	151.1	161	107
<b>Total</b>	<b>1035</b>	<b>1216</b>	<b>1139</b>	<b>1392</b>	<b>1343</b>	<b>1361</b>	<b>2246</b>

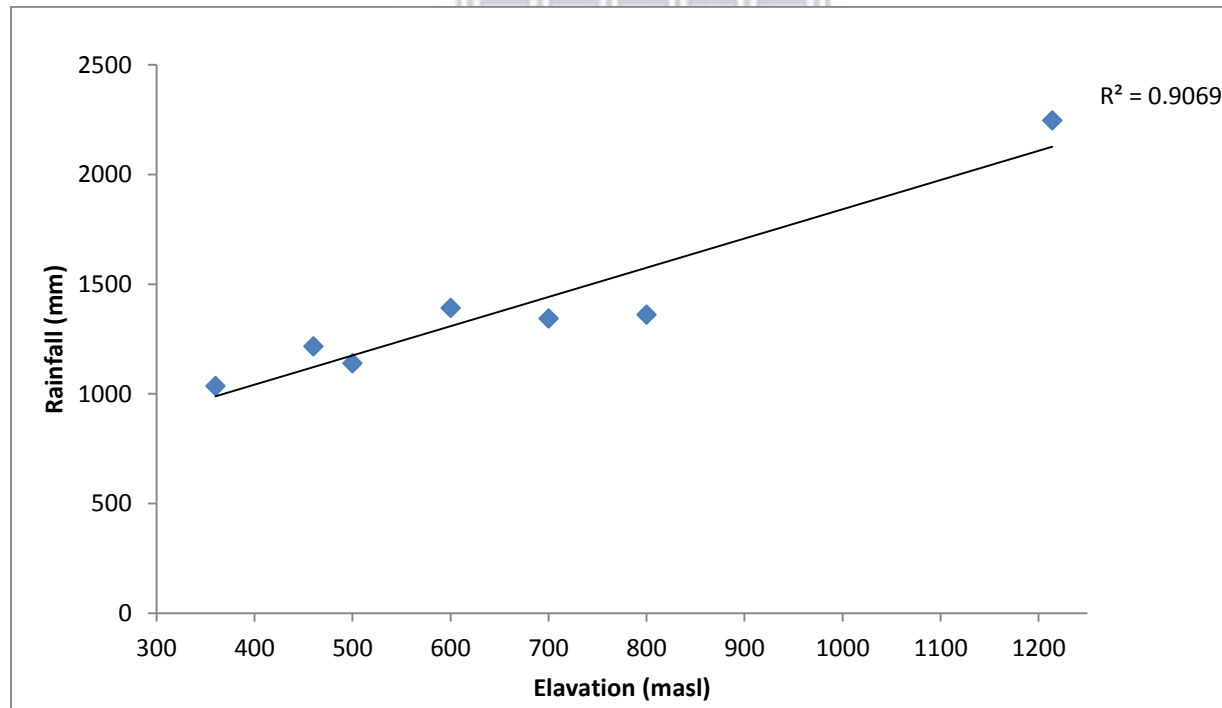


**Figure 4.1: Variation of total rainfall (May 2015- June 2016) with elevation in the Langrivier catchment**

Average rainfall (1390.3 mm/year) and rainfall totals (excluding Dwa 1214) for this study were below average when compared with average monthly and annual rainfall of the catchment. Wicht et al. (1969) using 10 years of data found that rain gauges R360 and R460 were found to have mean annual rainfalls of 1673 mm/year and 1838 mm/year respectively. Also, average winter rainfall (May to August) for rain gauge R360 and 14 B was 980 and 1089 mm respectively, while in summer (December to March), their average rainfalls were 194 mm and 209 mm respectively (Wicht et al. 1969). For the current study, R360 and R460 have rainfall totals of 1035 mm and 1216 mm respectively. Consequently, total summer rainfall for rain gauge R360 and R460 was 58 mm and 76 mm respectively while total winter rainfall for rain gauge R360 and R460 was 535 mm and 639 mm respectively. November is the only month that had more rainfall than average monthly rainfall (Figure 4.2).

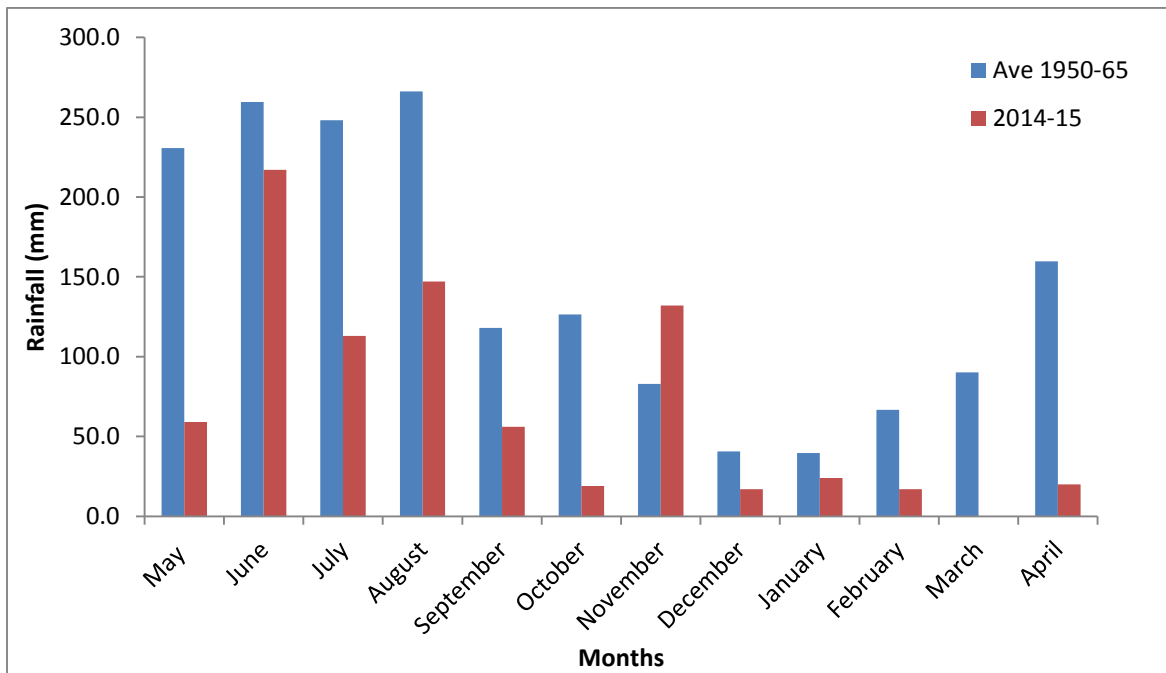


**Figure 4.2: Average monthly rainfall for rain gauge 8B for the Wicht et al. 1969 compared to the current study (R360).**

#### 4.4 Variation of daily rainfall characteristics

Average daily rainfall is generally low ranging from 5.6 mm/day to 13.0 mm/day (Table 4.3). The standard deviations off all stations are relatively high, and as a result, all the stations have a high coefficient of variation. The highest maximum daily rainfall recorded is at DWA 1214 with a value of 104 mm/day and the lowest maximum daily rainfall was at RG 800 with 61 mm/day.

The maximum hourly rainfall intensities do not show a defined trend (increase with elevation or vice versa) between the rain gauges. RG 500 and RG 600 recorded the highest maximum hourly rainfall at 38.1 mm/h<sup>-1</sup> and 39.4 mm/h<sup>-1</sup> respectively.

**Table 4:3: Daily rainfall characteristics of the 7 rainfall stations in Langrivier (May 2014 – June 2015).**

<b>Statistic</b>	<b>R360</b>	<b>R460</b>	<b>RG 500</b>	<b>RG 600</b>	<b>RG 700</b>	<b>RG 800</b>	<b>DWA 1214</b>
Maximum rainfall (mm/day)	64	76	75	83	72	61	104
Mean (mm/day)	5.6	6.8	6.5	8.2	7.7	7.7	13.0
Standard deviation (n)	9.4	12.1	13.4	16.0	12.7	13.0	20.0
Coefficient of Variation	168%	177%	205%	195%	165%	170%	153%
Maximum intensity (mm/h <sup>-1</sup> )	24.3	28.7	38.1	39.4	28.7	21.9	26.9

The seven stations have high correlation coefficients between their daily rainfall totals (Table 4.4). The Shapiro-Wilk test showed that daily rainfall at all the stations is not normally distributed ( $p < 0.0001$ ). Also, the Kolmogorov-Smirnov test showed that all the rainfall station had similar frequency distributions ( $p > 0.05$ ).

**Table 4:4: Correlation matrix of daily rainfall totals of the seven rain gauge stations in Langrivier.**

	R360 (R360)	R460 (R460)	RG 500	RG 600	RG 700	RG 800	DWA 1214
R360 (R360)	1.00	0.97	0.98	0.98	0.97	0.88	0.91
R460 (R460)		1.00	0.97	0.98	0.97	0.88	0.90
RG 500			1.00	0.99	0.97	0.90	0.88
RG 600				1.00	0.99	0.90	0.93
RG 700					1.00	0.92	0.93
RG 800						1.00	0.86
DWA 1214							1.00

#### 4.5 Analysis of number of rainfall days

There is no distinct relationship between elevation and the number of rainy days (Table 4.5). It appears that rainfall generally occurred on the same days at all rain gauges. Rain gauges located between 500-800 m.a.s.l had between 110-113 rainfall days, while rain gauges located at 360,



460 and 1214 m.a.s.l had between 137-149 rainfall days. During the winter months (June to August 2014) period, rainfall occurred over 50% of the time (days), while for the summer months (October, November, December, January, and February) rainfall occurs on about 26% of the time (days) (Table 4.5).

**Table 4:5: Number of rainfall days per month for the seven rainfall stations within Langrivier.**

Date	R360	R460	RG 500	RG 600	RG 700	RG 800	DWA 1214
May-14	9	12	7	8	8	9	8
Jun-14	19	22	14	14	14	14	16
Jul-14	16	24	16	12	13	13	14
Aug-14	16	13	15	15	15	14	18
Sep-14	12	12	7	8	8	9	9
Oct-14	7	7	6	7	6	5	7
Nov-14	10	10	8	8	8	9	12
Dec-14	9	6	2	3	3	3	8
Jan-15	7	8	4	4	4	4	7
Feb-15	8	9	7	7	7	8	8
Mar-15	1	1	1	1	2	1	9
Apr-15	5	6	5	5	5	5	8
May-15	11	11	11	11	11	12	14
Jun-15	7	8	7	7	7	7	8
<b>Total</b>	<b>137</b>	<b>149</b>	<b>110</b>	<b>110</b>	<b>111</b>	<b>113</b>	<b>146</b>

The number of rainy days with rainfall depth ( $\geq 10$ mm) did not vary substantially among the stations except for the rainfall station at the highest elevation point (DWA 1214), which had a relatively higher number of days with 10 mm/day or more (Table 4.6). Out of all the rainfall events that were  $\geq 10$ mm/day, around 38-65% were  $\geq 20$  mm/day and 12-41% were  $\geq 30$  mm/day at all the rainfall stations. Stations with an altitude of 600 m.a.s.l and above (RG 600, RG 700, RG 800, DWA 1214) had relatively higher numbers of rainy days of rainfall quantities in excess of 30 mm/day (31-41%).

**Table 4:6: Classification of rainy days by magnitude of daily rainfall.**

Daily totals	Rainfall stations						
	R360	R460	RG 500	RG 600	RG 700	RG 800	DWA 1214
$\geq 10$ (mm/day)	34	39	37	42	43	45	63
$\geq 20$ (mm/day)	13	21	19	24	25	24	41
$\geq 30$ (mm/day)	4	8	8	13	12	12	26

#### 4.6 Diurnal variation of rainfall

Most of the rainfall in Langrivier catchment falls from 00:00-8:00 am and in the afternoon from 14:00 to 23:00 in the night (Figure 4.3 and Figure 4.4). For the first peak (00:00-8:00 am) most rainfall is collected at 2:00 am for all the stations, while for the second peak, the hours that records the highest rainfall total is 17:00 and 18:00.

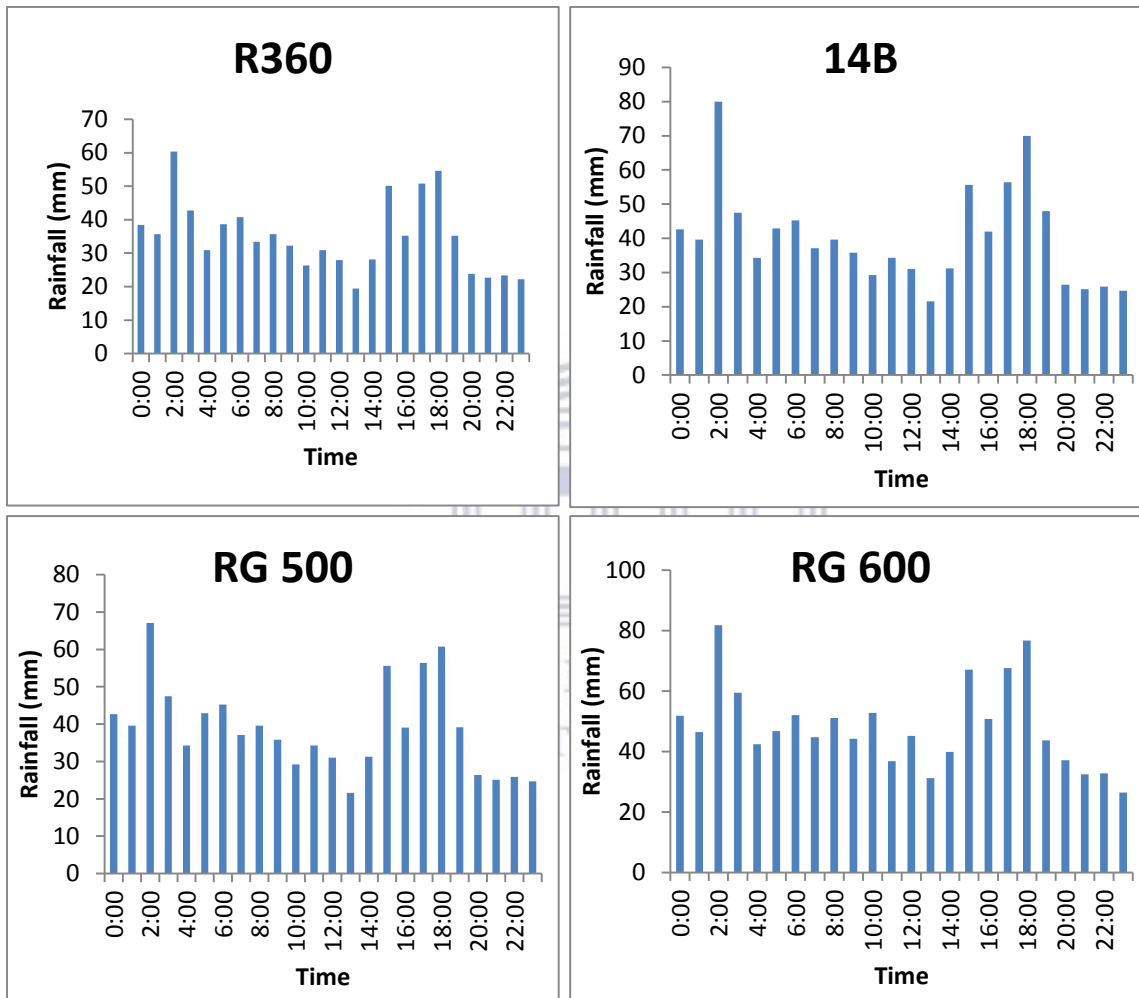
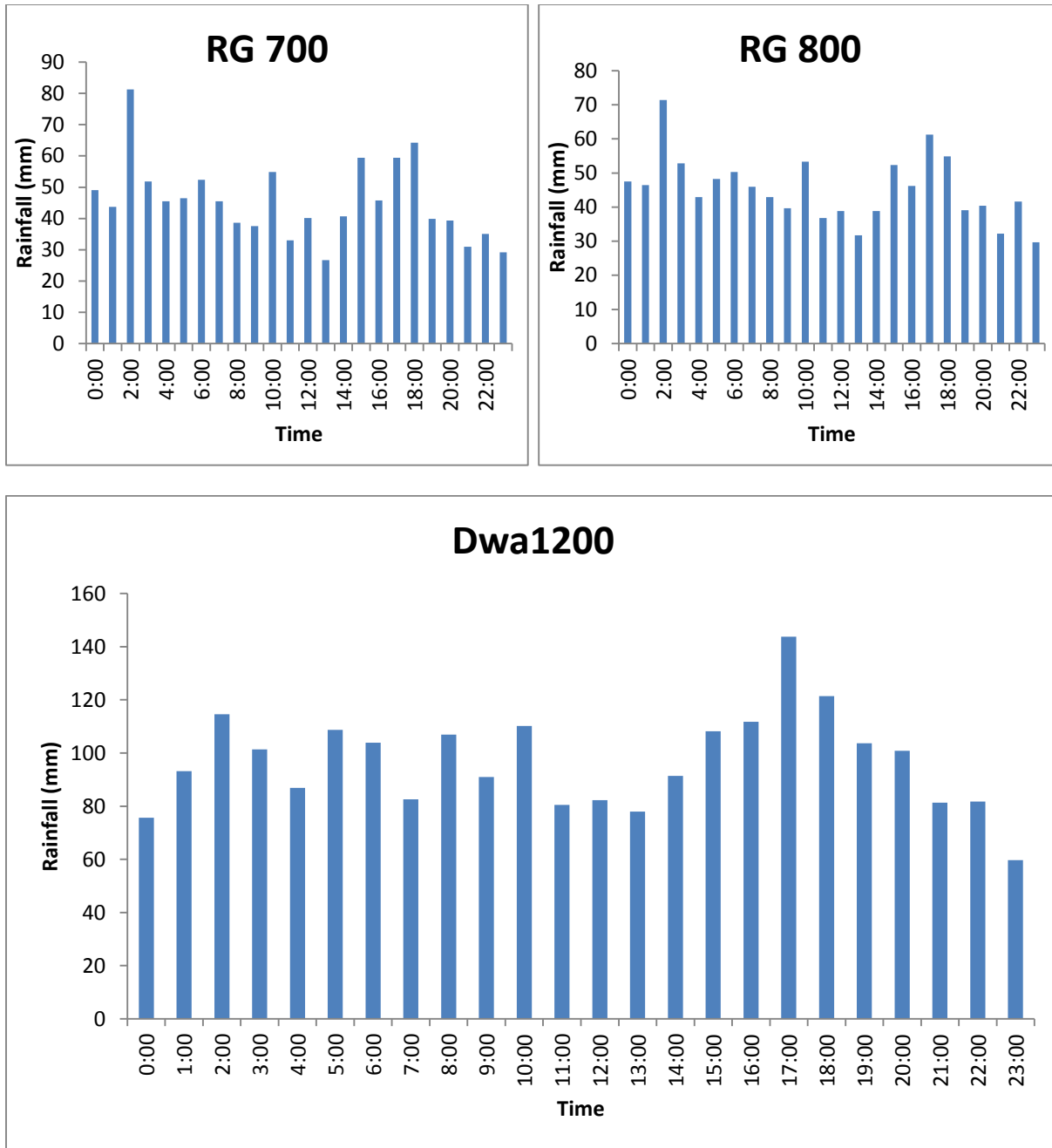


Figure 4.3: Diurnal variation of rainfall for rain gauges RG360, RG460, RG500, and RG600.



**Figure 4.4:Diurnal variation of rainfall for rain gauges RG700, RG800, and DWA1214**

#### **4.7 Number of wet spells**

The number of consecutive days with rainfall rarely extend more than 16 days (Table 4.7). For the current study, a wet spell is defined as whenever a single rain gauge records a rainfall amount of 2.5 mm/day or more for two consecutive days or more. Rain gauge DWA 1214 had the

highest number (40) of wet spells of two days or more, while RG600 has the lowest number of wet (28) spells of two or more days. All the rain gauges have only one wet spell that was more than five days long. RG460 was the only rain gauge that had a wet that was over 16 days long. Overall, these wet spells results indicate that rainfall stations generally have rainfall during the same time.

**Table 4:7: Number of wet spells for the seven rain gauges within Langrivier**

Length of wet spell (days)	R360	R460	RG 500	RG 600	RG 700	RG 800	DWA 1214
>2	35	33	29	28	29	30	40
>5	1	1	1	1	1	1	1
>16	0	1	0	0	0	0	0

#### **4.8 Assessment of the significance of variation of average daily rainfall with elevation**

To test whether the variation of rainfall with altitude is significant, a t-test using average daily rainfall was used. The area of the catchment between 360 to 800 m.a.s.l. receives statistically similar rainfall (Table 4.8). On the other hand, all these rainfall stations (R360, R460, RG 500, RG 600, RG 700, and RG 800) have average daily rainfall significantly different from rainfall station DWA 1214. Also, the average daily rainfall of all the other stations is lower when compared with DWA 1214. Thus, without the inclusion of DWA 1214, rainfall estimated using rainfall stations R360, R460, RG 500, RG 600, RG 700, and RG 800 would be under-estimated for the catchment.

**Table 4:8: Variation of average daily rainfall with elevation in Langrivier.**

T-test using p-values at 0,05 significance level							
	R360	R460	RG 500	RG 600	RG 700	RG 800	DWA 1214
R360	1	0.386	0.471	0.146	0.233	0.167	0.001
R460		1	0,883	0,541	0,766	0.652	0.006
RG 500			1	0,449	0,652	0,543	0.004
RG 600				1	0,738	0,841	0.030
RG 700					1	0,882	0.012
RG 800						1	0.015
DWA 1214							1

Catchment rainfall estimated using rain gauges located between 360 to 800 m.a.s.l. in the catchment is lower than catchment rainfall estimated including the rainfall measured station at 1214 m.a.s.l (Figure 4.5). Cumulative rainfall interpolated for the catchment using Thiessen polygon without the inclusion of the station at 1214 (DWA 1214) is lower than when the DWA 1214 station is included in the interpolation of rainfall (Figure 5.1).

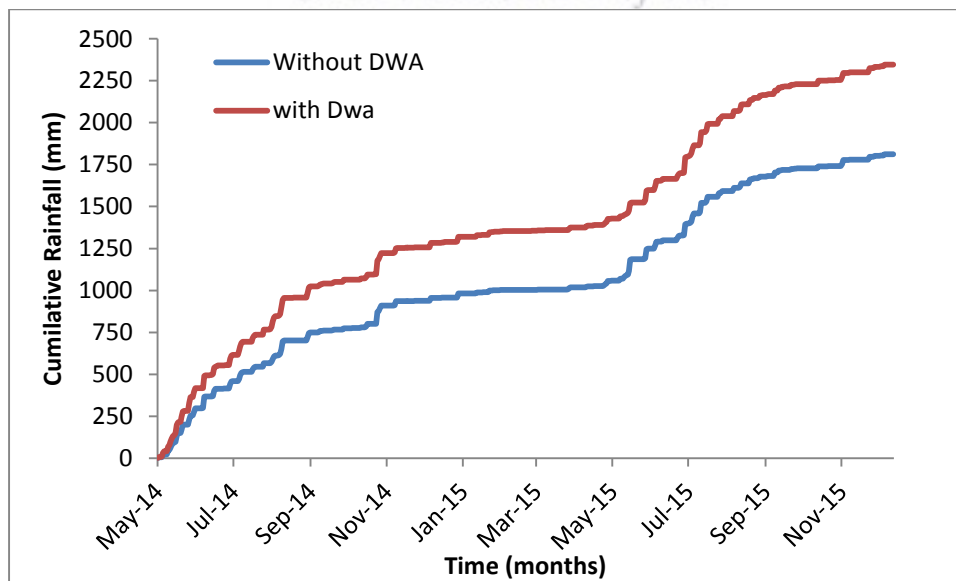


**Figure 4.5: Difference in cumulative rainfall of rainfall when interpolated with and without the inclusion of rainfall monitored at DWA 1214 m.a.s.l**

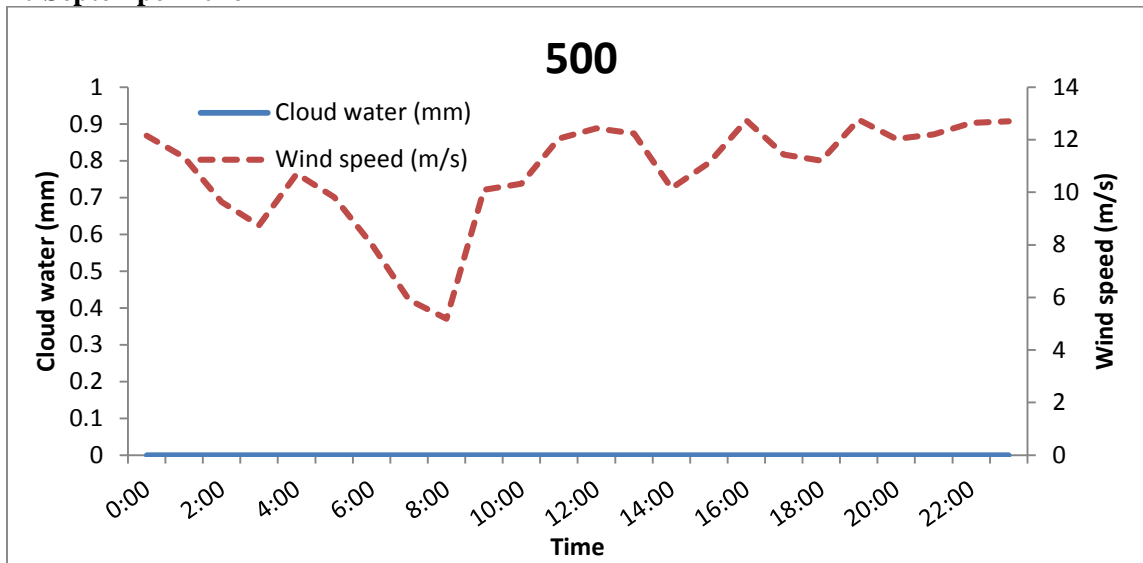
## **4.9 Cloud water contribution to total precipitation**

### **4.9.1 Important weather conditions for cloud water.**

As highlighted in Chapter 2, wind conditions influence cloud water quantities. As such, fog gauges were fitted with wind speed and direction sensors to provide some detail on how wind conditions influence cloud water quantities. The influence of wind conditions on cloud water was examined only on days which had cloud water recording and no rainfall recorded in order to exclude any influence of rainfall on cloud water quantities. There were numerous days that recorded cloud water only and no rainfall and all such day demonstrate a similar wind speed and direction pattern. For illustration, only two days (10 September 2014 and 28 December 2014) were selected to illustrate how wind conditions influence cloud water quantity.

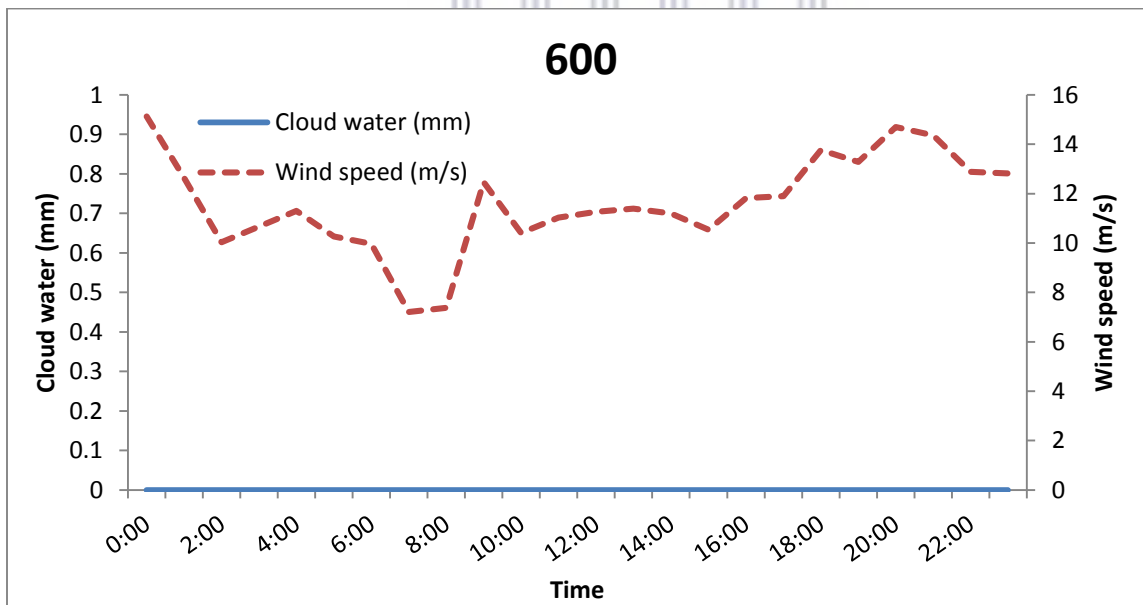
The critical wind direction that produces substantial cloud water quantities is the South East (SE), while the critical wind speed for producing substantial cloud water quantities is 3.8 m/s and above (Figure 4.6a-4.6e and Figure 4.7a-4.7e). When there is no rainfall, cloud water only collected at the fog station at the highest elevation 1214 m.a.s.l. Cloud water at the other fog gauges at 500-800 m.a.s.l is always recorded on the same day as rainfall. In addition, all the fog gauges located at 500-800 m.a.s.l do not record cloud water of more than 0.0254 mm/day throughout the study period. The fog gauge at 1214 m.a.s.l receives as much as 8 mm/hr (hour) of cloud water precipitation with a south-easter wind direction and 10 m/s wind speed (Figure 4.6e). All the fog gauges have comparably different wind speeds and directions possibly as a result of the rugged topography of the catchment.

10 September 2016



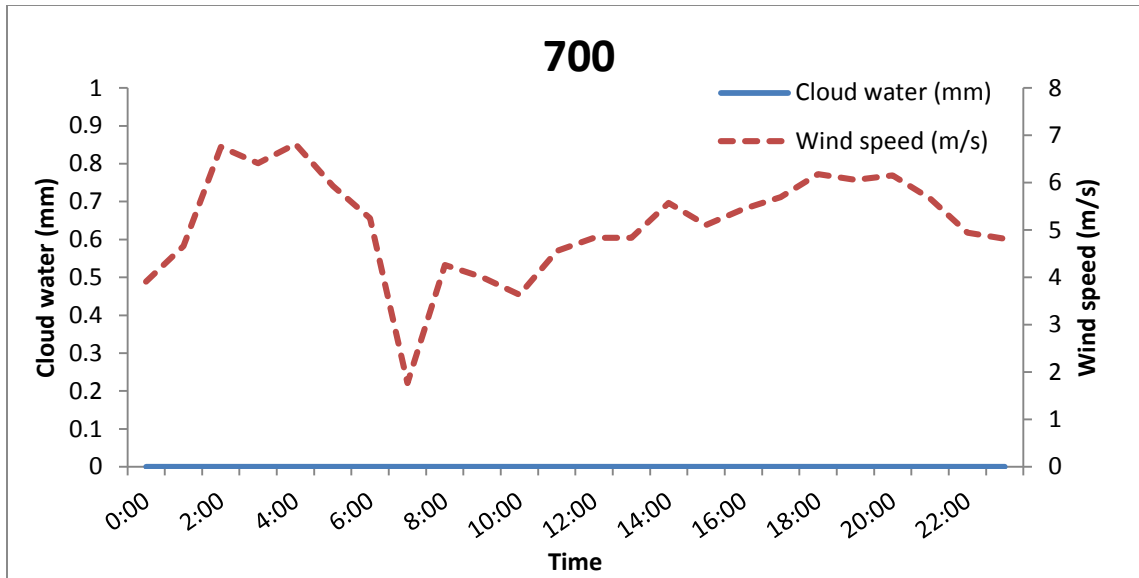
<b>Time</b>	0:00	1:00	2:00	3:00	4:00	5:00	6:00	7:00	8:00	9:00	10:00	11:00
Wind direction	SE	SE	SE	SE	SE	SE	SE	SE	SE	SE	SE	SE
<b>Time</b>	12:00	13:00	14:00	15:00	16:00	17:00	18:00	19:00	20:00	21:00	22:00	23:00
Wind direction	SE	SE	SE	SE	S	SE	SE	SE	SE	SE	SE	SE

**Figure 4.6a: Wind conditions bringing cloud water precipitation at fog gauge located at 500 m.a.s.l on 10 September 2014**



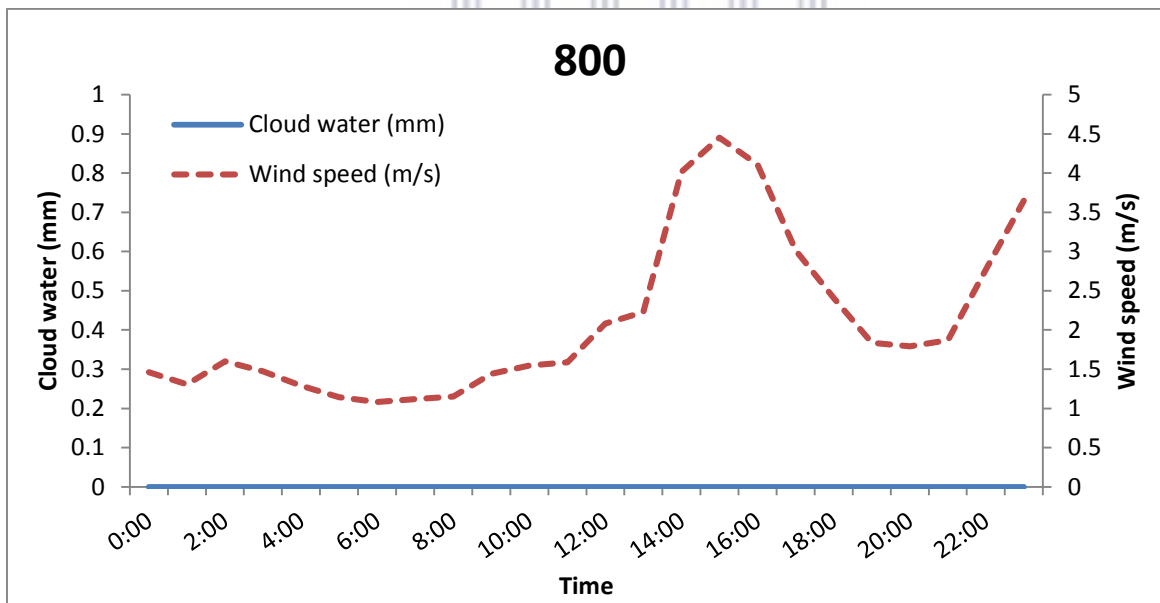
<b>Time</b>	0:00	1:00	2:00	3:00	4:00	5:00	6:00	7:00	8:00	9:00	10:00	11:00
Wind direction	SE	SE	SE	SE	SE	SE	SE	SE	SE	SE	SE	SE
<b>Time</b>	12:00	13:00	14:00	15:00	16:00	17:00	18:00	19:00	20:00	21:00	22:00	23:00
Wind direction	SE	SE	SE	SE	SE	SE	SE	SE	SE	SE	SE	SE

**Figure 4.6b: Wind conditions bringing cloud water precipitation at fog gauge located at 600 m.a.s.l on 10 September 2014**



<b>Time</b>	0:00	1:00	2:00	3:00	4:00	5:00	6:00	7:00	8:00	9:00	10:00	11:00
Wind direction	SE	SE	SE	SE	SE	SE	SE	E	SE	S	S	S
<b>Time</b>	12:00	13:00	14:00	15:00	16:00	17:00	18:00	19:00	20:00	21:00	22:00	23:00
Wind direction	S	S	SE	SE	SE	SE	SE	S	SE	S	S	S

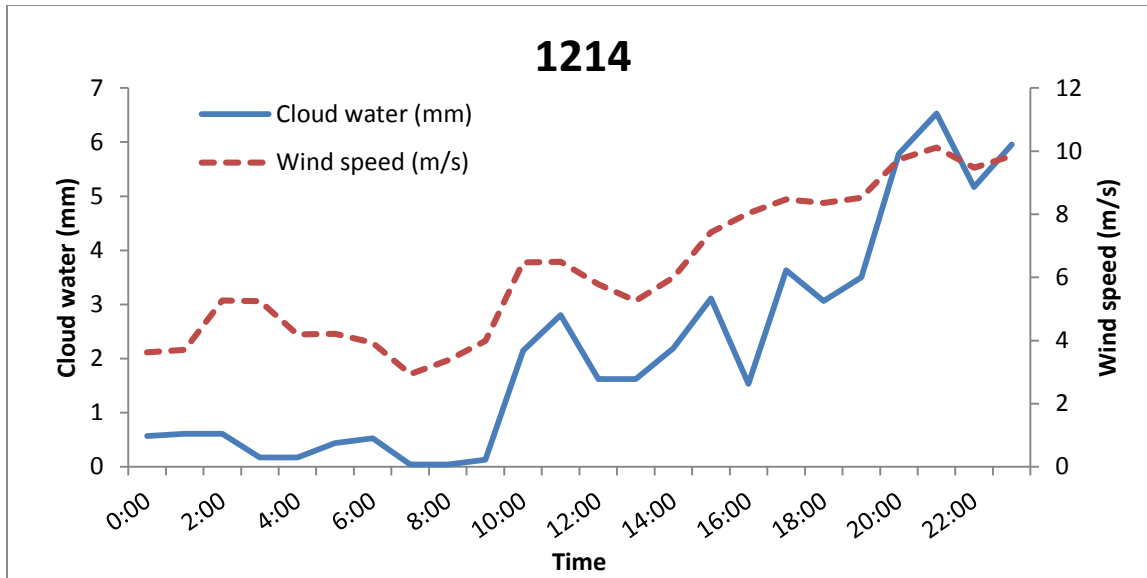
**Figure 4.6c:** Wind conditions bringing cloud water precipitation at fog gauge located at 700 m.a.s.l on 10 September 2014.



<b>Time</b>	0:00	1:00	2:00	3:00	4:00	5:00	6:00	7:00	8:00	9:00	10:00	11:00
Wind direction	NE	E	E	NE	NE	NE	E	NE	N	NE	NE	NE
<b>Time</b>	12:00	13:00	14:00	15:00	16:00	17:00	18:00	19:00	20:00	21:00	22:00	23:00
Wind direction	NE	S	S	S	S	N	NE	E	N	NE	E	E

**Figure 4.6d:** Wind conditions bringing cloud water precipitation at fog gauge located at 800 m.a.s.l on 10 September 2014





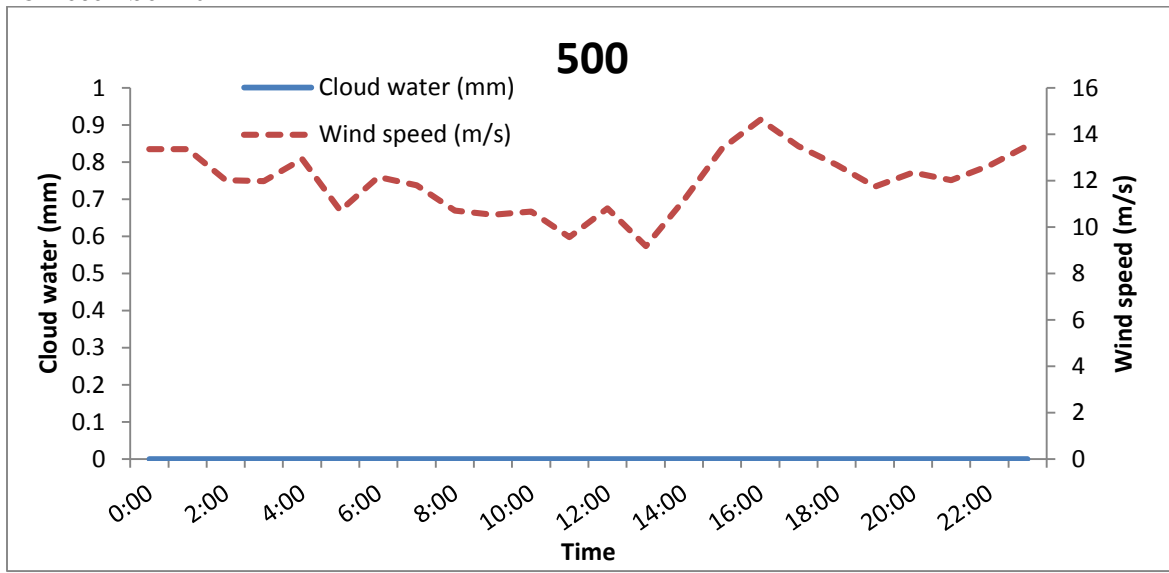
<b>Time</b>	<b>0:00</b>	<b>1:00</b>	<b>2:00</b>	<b>3:00</b>	<b>4:00</b>	<b>5:00</b>	<b>6:00</b>	<b>7:00</b>	<b>8:00</b>	<b>9:00</b>	<b>10:00</b>	<b>11:00</b>
Wind direction	SE	SE	S	S	SE	SE	SE	SE	SE	SE	SE	SE
<b>Time</b>	<b>12:00</b>	<b>13:00</b>	<b>14:00</b>	<b>15:00</b>	<b>16:00</b>	<b>17:00</b>	<b>18:00</b>	<b>19:00</b>	<b>20:00</b>	<b>21:00</b>	<b>22:00</b>	<b>23:00</b>
Wind direction	SE	SE	SE	SE	SE	SE	SE	SE	SE	SE	SE	SE

**Figure 4.6 e: Wind conditions bringing cloud water precipitation at fog gauge located at 1214 m.a.s.l on 10 September 2014.**



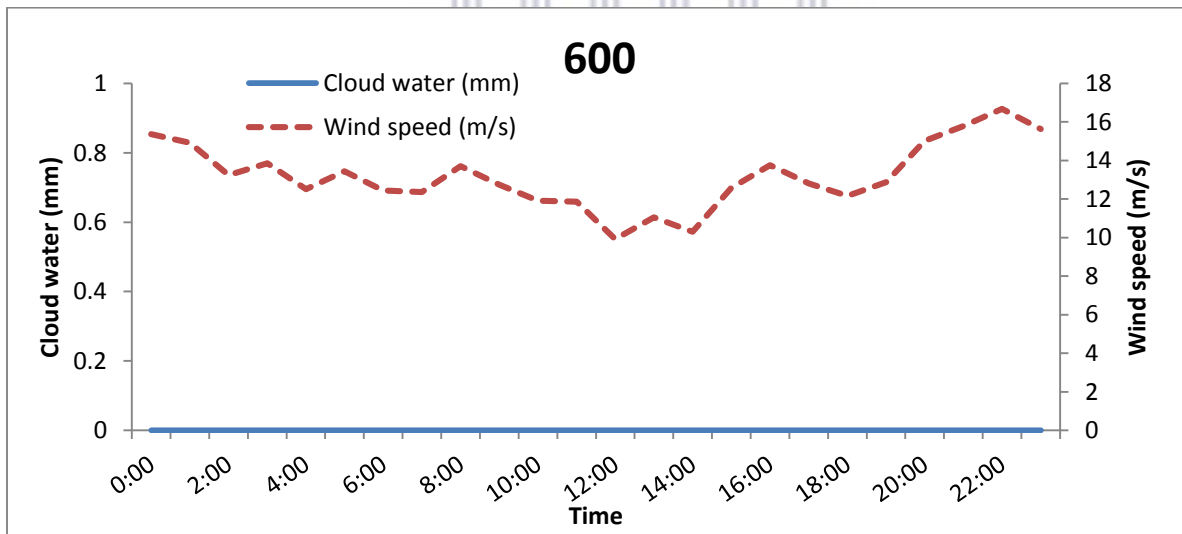
UNIVERSITY of the  
WESTERN CAPE

28 December 2014



<b>Time</b>	0:00	1:00	2:00	3:00	4:00	5:00	6:00	7:00	8:00	9:00	10:00	11:00
Wind direction	SE	SE	SE	SE	SE	SE	SE	SE	SE	SE	SE	SE
<b>Time</b>	12:00	13:00	14:00	15:00	16:00	17:00	18:00	19:00	20:00	21:00	22:00	23:00
Wind direction	SE	SE	SE	SE	SE	SE	SE	SE	SE	SE	SE	SE

**Figure 4.7 a: Wind conditions bringing cloud water precipitation at fog gauge located at 500 m.a.s.l on 28 December 2014**



<b>Time</b>	0:00	1:00	2:00	3:00	4:00	5:00	6:00	7:00	8:00	9:00	10:00	11:00
Wind direction	SE	SE	SE	SE	SE	SE	SE	SE	SE	SE	SE	SE
<b>Time</b>	12:00	13:00	14:00	15:00	16:00	17:00	18:00	19:00	20:00	21:00	22:00	23:00
Wind direction	SE	SE	SE	SE	SE	SE	SE	SE	SE	SE	SE	SE

**Figure 4.7b: Wind conditions bringing cloud water precipitation at fog gauge located at 600 m.a.s.l on 28 December 2014**

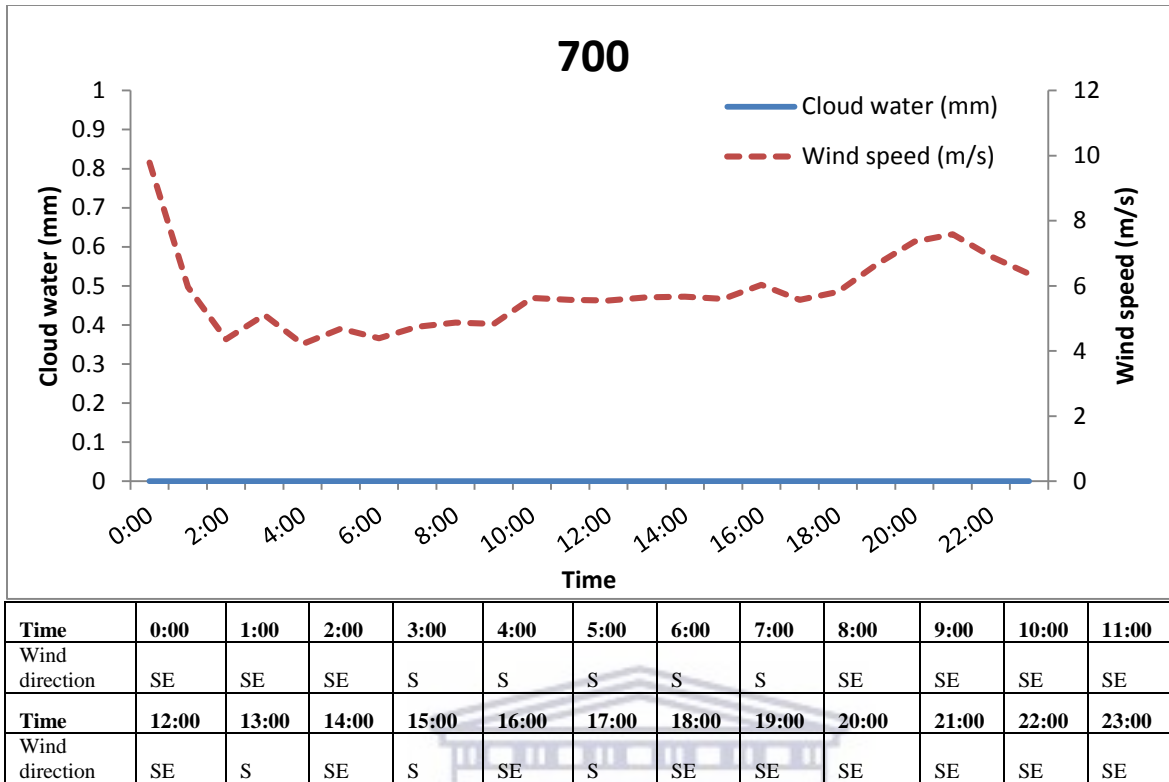


**Figure 4.7c: Wind conditions bringing cloud water precipitation at fog gauge located at 700 m.a.s.l on 28 December 2014**

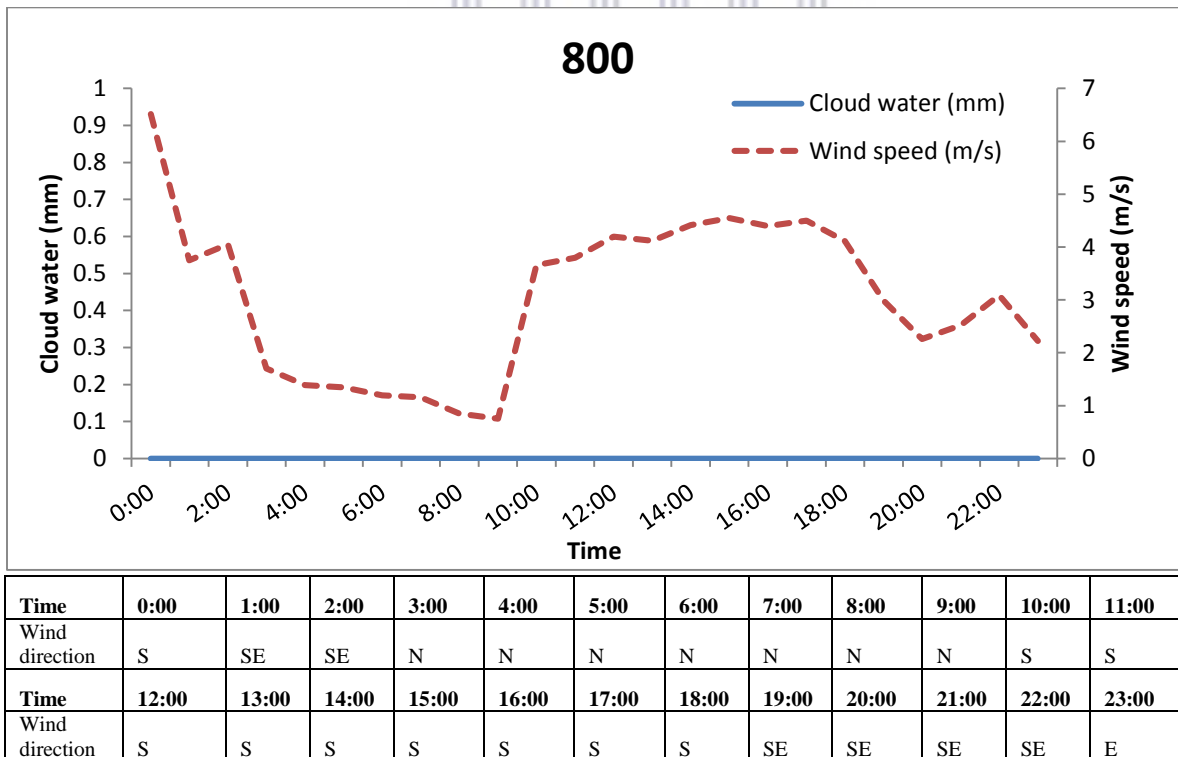
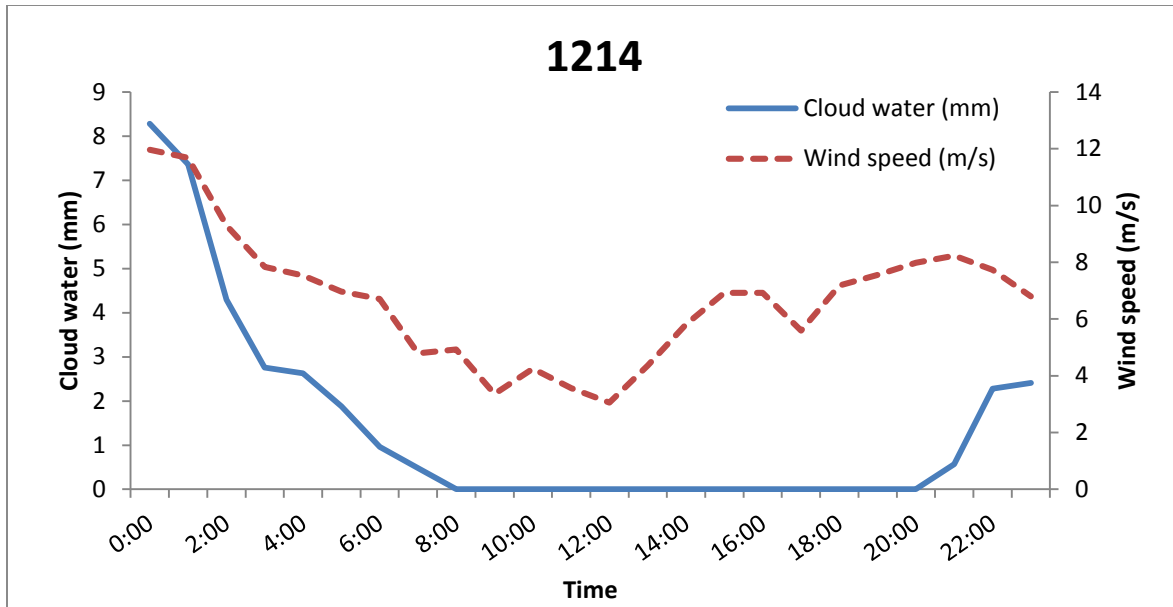


**Figure 4.7 d: Wind conditions bringing cloud water precipitation at fog gauge located at 800 m.a.s.l on 28 December 2014**



<b>Time</b>	0:00	1:00	2:00	3:00	4:00	5:00	6:00	7:00	8:00	9:00	10:00	11:00
Wind direction	SE	SE	S	S	SE	SE	SE	SE	SE	SE	SE	SE
<b>Time</b>	12:00	13:00	14:00	15:00	16:00	17:00	18:00	19:00	20:00	21:00	22:00	23:00
Wind direction	SE	SE	SE	SE	SE	SE	SE	SE	SE	SE	SE	SE

**Figure 4.7 e: Wind conditions bringing cloud water precipitation at fog gauge located at 1214 m.a.s.l on 28 December 2014**

#### 4.9.2 Cloud water diurnal characteristics

Diurnal characteristics of cloud water for all the fog gauges show that cloud water generally occurs throughout the day (Figure 4.5). Cloud water interception is not evenly spread throughout the day although patterns of cloud water interception relative to the time of the day were not identical for the fog gauges at 500-800 m.a.s.l. The LFS at 1214 m.a.s.l has two peaks in the early morning and late evening. The diurnal variation of cloud water of each fog gauge is generally similar with diurnal variation of rainfall (Figure 4.3 and 4.4). Thus, generally cloud water and rainfall occur concurrently particularly for fog gauges LSF 500, LSF 600, LSF 700, and LFS 800.

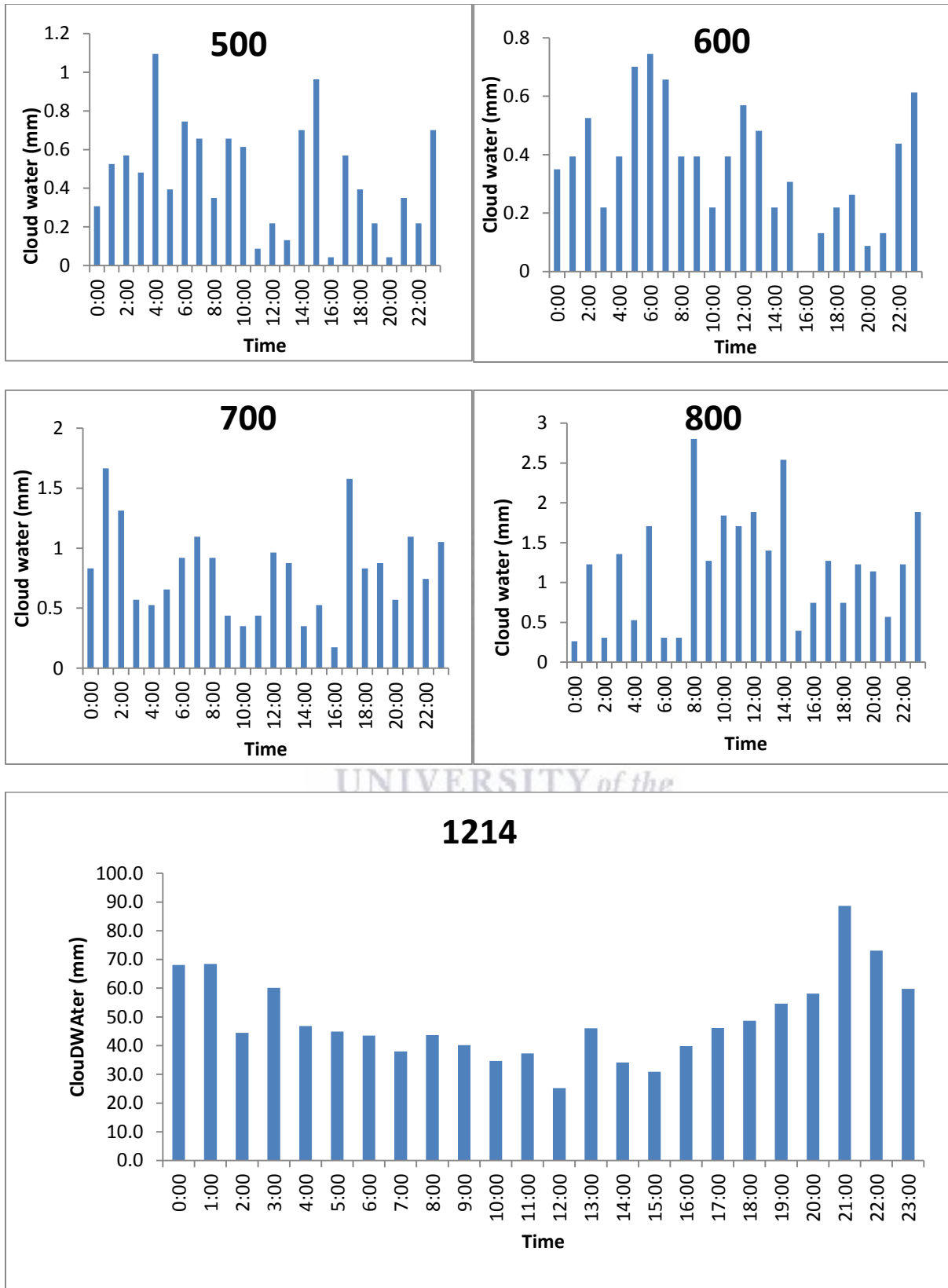
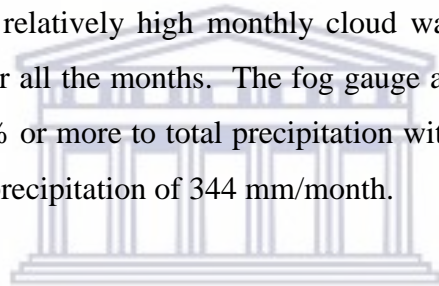


Figure 4.8: Diurnal variation of cloud water (mm) from all the fog gauges.

### 4.9.3 Cloud water contribution to precipitation at different altitudinal zones

Cloud water contribution (quantity and percentage) to total precipitation increased with altitude (Figure 4.9). Fog gauges at the lowest elevation points (LSF 500 and LSF 600) received the lowest cloud water totals contributions at 10.2 and 8.3 mm respectively, albeit they did not have data from April-June 2015. The fog gauge at the highest elevation point LSF 1214 (1214 m.a.s.l), has a substantially higher cloud water total in comparison to the other fog gauges with a total of 1256 mm. Louvred fog screen gauges at 500, 600, 700 and 800 m.a.s.l have low monthly proportional contributions to total precipitation of 0-3% in winter (May to September 2014) (Figure 4.5). In summer (October 2014 and December-March 2015), cloud water interception contributed slightly more with 8-24% at 500, 600, 700 and 800 m.a.s.l, nonetheless these contributions are proportionally low than rainfall contribution to total precipitation. However, the fog gauge at 1214 m.a.s.l has relatively high monthly cloud water contributions; cloud water contributes between 15-85% for all the months. The fog gauge at 1214 m.a.s.l. has eight of the fourteen months contribute 40% or more to total precipitation with December 2014 contributing 292 (85%) mm/month of total precipitation of 344 mm/month.



UNIVERSITY of the  
WESTERN CAPE

(a)

Month	Rainfall (mm)	Cloud water (mm)	% of Cloud water to total precipitation
May-14	56	0.5	1
Jun-14	283	0.9	0
Jul-14	131	1.1	1
Aug-14	160	1.5	1
Sep-14	58	1.1	2
Oct-14	17	3.1	16
Nov-14	164	0.5	0
Dec-14	18	0.8	4
Jan-15	27	0.6	2
Feb-15	12	0.1	1
Mar-15	3	0	0
Apr-15	16		
May-15	53		
Jun-15	144		
Total	1139	10.2	0.9

(b)

Month	Rainfall (mm)	Cloud water (mm)	% of Cloud water to total precipitation
May-14	78	0.4	1
Jun-14	364	0.7	0
Jul-14	177	1.3	1
Aug-14	222	1	0
Sep-14	67	0.2	0
Oct-14	16	2.5	13
Nov-14	170	0.8	0
Dec-14	21	0.8	4
Jan-15	34	0.2	1
Feb-15	14	0.1	1
Mar-15	3	0.3	11
Apr-15	16		
May-15	52		
Jun-15	160		
Total	1392	8.3	0.6

(c)

Month	Rainfall (mm)	Cloud water (mm)	% of Cloud water to total precipitation
May-14	97	1.2	1
Jun-14	310	1.6	1
Jul-14	162	1.7	1
Aug-14	222	2.1	1
Sep-14	58	0.4	1
Oct-14	19	3.2	15
Nov-14	152	1.5	1
Dec-14	19	1.2	6
Jan-15	37	0.8	2
Feb-15	16	0.7	4
Mar-15	4	1.1	24
Apr-15	18	1.1	5
May-15	81	1.7	2
Jun-15	151.1	1	1
Total	1343	19.4	1.4

(d)

Month	Rainfall (mm)	Cloud water (mm)	% of Cloud water to total precipitation
May-14	117	2.5	2
Jun-14	289	2.4	1
Jul-14	150	3.3	2
Aug-14	224	2.1	1
Sep-14	57	1.5	3
Oct-14	23	1.9	8
Nov-14	151	2	1
Dec-14	20	1.6	7
Jan-15	33	2.5	7
Feb-15	22	0.1	1
Mar-15	3	1.1	24
Apr-15	21	0.7	3
May-15	89	4.2	4
Jun-15	161	2.8	2
Total	1361	28.6	2.1

(e)

Month	Rainfall (mm)	Cloud water (mm)	% of Cloud water to total precipitation
May-14	187	133	42
Jun-14	543	98	15
Jul-14	298	100	25
Aug-14	400	107.9	21
Sep-14	134	122.8	48
Oct-14	52	48.3	48
Nov-14	226	128.6	36
Dec-14	53	292.3	85
Jan-15	73	72.1	50
Feb-15	39	36.2	48
Mar-15	12	17.5	60
Apr-15	44	45.4	51
May-15	80	74.2	48
Jun-15	107	43.7	29
Total	2246	1256	35.2

**Figure 4.9: Contribution of cloud water (mm and %) to total precipitation at the different elevation a=500 m.a.s.l; b=600 m.a.s.l; c=700 m; d= 800 m.a.s.l and e=1214 m.a.s.l.**

#### 4.10 Discussion

Rainfall generally increased with altitude in the Langrivier catchment as was found by Wicht et al.(1969). The rainfall totals at different elevations are different from average rainfall estimation achieved by Wicht et al. (1969) using isohyetal maps. For instance, the isohyetal maps showed that rainfall at 460 m.a.s.l differed by 400 mm from rainfall at 800 m.a.s.l. In this study, the difference in rainfall between these two elevation areas is only 145 mm. However, the length of this study (1 year) limits comparison with Wicht et al. (1969) which used 10-year data. A longer period of monitoring rainfall with the new network design used for this study is required to provide conclusiveness of these results.

Rainfall within Langrivier Catchment was highly influenced by elevation, with an  $r^2 = 0.91$ . Rainfall received at highest elevation point (2246 mm) was two times more than rainfall received at the lowest point of the catchment (1035 mm). The large difference in rainfall totals is common in mountain catchments, as mountainous catchments have occasions during which precipitation falling at high altitudes may be 10 or more times higher than low laying areas (Dettinger et al. 2004). In the Ethiopian highlands, slope and aspect not elevation influenced the spatial distribution of rainfall (Nyssen et al. 2005). In this catchment, however, all the rain gauges had the same aspect. The non-linear increase in rainfall between rainfall stations at 460-800 m.a.s.l , may be interpreted as shadowing effect attributed to the slope and high rocky outcrops adjacent to RG 700 and RG 800. In the Stephanie Creek catchment Canada, rain shadowing caused a rain gauge located 880 m.a.s.l to record 260 mm rainfall more than a rain gauge located 950 m.a.s.l (Hrachowitz and Weiler, 2011)

The number of rainfall days equal to or more than 30 mm/day were higher at elevations (600, 700, 800, and 1214 m.a.s.l) points than the lower three stations. Such diurnal characteristics of rainfall in this study conform with findings of Wicht et al. (1969), noting that in the Jonkershoek catchment, the general pattern of rainfall is constant even for light rains of short duration, with variations occurring in the degree of concentration rather than in the form of the pattern. Furthermore, the maximum hourly rainfall intensities for the seven stations are different, and such differences cause variation in rainfall total (Brunneti et al, 2001). Thus, the different numbers of rainy days, different daily rainfall intensities are important factors in the increase of rainfall with altitude in this catchment.



This study has established that there is no significant difference in the average daily rainfall of rain gauges located between 360 and 800 meters above sea level. Thus, increasing the number of stations in this altitudinal range does not improve estimation of catchment rainfall. However, a longer period of study may yield different results as noted above. The rainfall findings of this study contrast those in Goodrich et al. (1995), who found that in a small catchment rain gauges that were 300 meters apart recorded significantly different rainfall total. The results of this study further highlight that the density of a rain gauge network is not important rather than placing rain gauge at representative levels. Catchment rainfall estimated using rain gauges located at the 360-800 m.a.s.l altitudinal range underestimate catchment rainfall. Overall, improved estimation of catchment rainfall for Langrivier is achieved by inclusion of the rain gauge station located at 1214 m.a.s.l. The second part of improving estimation of catchment precipitation by the inclusion of cloud water interception revealed that cloud water may be an important source of moisture in this catchment.

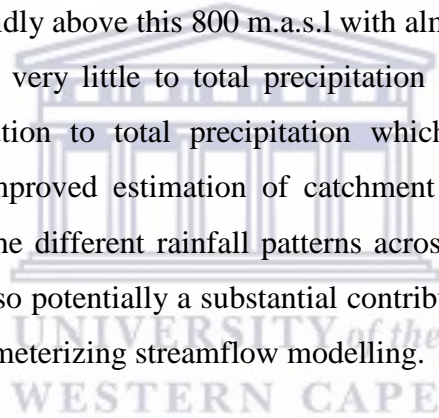
Diurnal cloud water contribution pattern shows that cloud water occurs concurrently with rainfall at 800 m.a.s.l and lower elevations. The concurrent occurrence of cloud water and rainfall characteristic found in this study is contrary to findings of Figuera et al. (2013), who studied rainfall events and identified that cloud interception is common before the onset of rainfall. At the fog gauge located at 1214 m.a.s.l, the only location where cloud water occur even when no rainfall occurred, wind speed and wind direction are critical for cloud water quantity. The South Easter and a wind speed of 3.8 m/s generally lead to substantial cloud water quantities in LFS 1214. Framau et al. (2006) highlighted wind speed as an important aspect the quantity of cloud water interception.

Cloud water interception contributions to total precipitation generally increased with elevation, similar to findings of Holder (2003) in Sierra de las Minas Biosphere Reserve, Guatemala. For the fog gauges at 500, 600, 700, 800 m.a.s.l cloud water interception contributed between 8 to 24% to total precipitation in summer. In winter cloud water interception contributed 1 to 5% of cloud water to total precipitation. The summer contributions from these fog gauges are similar to values from studies around the world (Gomez-Peralta et al. 2008; Holwerda et al. 2011; Prada et al. 2012; Figuera et al. 2013). However, when considering the total precipitation for the two summer months (October and March) of the current study the relatively high contributions of

cloud water interception to total precipitation of 8 to 24% is not substantial as these months had low total precipitation with total precipitation ranging between 2 to 25 mm. The highest cloud water contribution to total precipitation was highest at the fog gauge located at 1214 m.a.s.l.

The fog station at the highest monitoring point had the substantial contribution of cloud water interception throughout the study period. In winter (May- September), cloud water interception in the fog gauge located at 1214 m.a.s.l contributed between 15 to 51% to the total precipitation which is substantial when considering that total precipitation in these months ranged between 90 to 641 mm. Similarly, in summer (October-March) cloud water interception at this fog station contributed between 48 to 85% which is equally substantial when considering that total precipitation during this period ranged between 29 to 354 mm.

Overall, rainfall below 800 m.a.s.l was similar for this catchment throughout the study period. Rainfall seemed to increase rapidly above this 800 m.a.s.l with almost doubling in rainfall total at 1214 m.a.s.l. Fog contributed very little to total precipitation below 800m.a.s.l. but at 1214 m.a.s.l made a 35% contribution to total precipitation which possibly directly influences streamflow characteristics. Improved estimation of catchment rainfall should lead to better predictions of streamflows if the different rainfall patterns across the catchment are taken into account. Fog precipitation is also potentially a substantial contributor to catchment moisture and should also be included in parameterizing streamflow modelling.



## 5 Streamflow modelling

### 5.1 Introduction

In Chapter 4, estimation of catchment precipitation was improved by extending the rain gauge network and accounting for cloud water contribution to total catchment precipitation. Chapter 4 revealed that rainfall and cloud water measured at the highest elevation points (1214 m.a.s.l) contribute significantly towards total catchment precipitation. As stated in Chapter 1, after improving estimation of catchment precipitation, there is a need to assess whether an improved estimation of catchment precipitation leads to improved predictions of streamflow.

In Chapter 3, the ACRU Model was chosen as the appropriate model to predict streamflows for this study. Chapter 3 described in detail the appropriateness of using the model, explained the model's structure, main water budgeting routines, and possible challenges of using the model in this catchment. In this section, model configuration based on how important catchment characteristics are perceived is first described. Thereafter, details of how soils, climate, model parameters and vegetation were derived are described.

### 5.2 Model configuration

The area between 360-850 m.a.s.l of the Langrivier catchment is described as containing soils with high infiltration capacity dominated by subsurface flow and highly vegetated (Midgley and Scott, 1994; New, 1999). This lower area takes up 65-70% (1.59- 1.71 km<sup>2</sup>) when delineated using a 1:50 000 topographic sheet (3318 D). On the other hand, the catchment area 850 to 1423 m.a.s.l is a rock outcrop which has no vegetation, has low infiltration capacity, and has overland flow as the main flow mechanism. The rock outcrop characteristics (overland flow, less or no vegetation, and low infiltration) may significantly influence the hydrological responses and streamflow quantity of Langrivier stream as highlighted in Chapter 3 (McGlynn and McDonnell, 2003). In this study, it is believed that the rock outcrop may be crucial in runoff generation and consequently, accurate representation of the contribution of this zone to total runoff may be significant in improving accuracy streamflow of modelling. The influence of the rock outcrop on hydrograph characteristics will be evaluated in two ways (a) modelling streamflow in lumped mode assuming that the rock outcrop is insignificant to runoff hydrograph characteristics (b)

modelling streamflow in semi-distributed mode assuming that the rock outcrop is a significant factor in streamflow characteristics.

In lumped mode, it is assumed that the upper rock outcrop in the catchment will not have a significant influence on hydrological responses as it occupies a small portion of the catchment. In addition, most rainfall that falls on the rock outcrop will flow into the catchment area between 360-800 m.a.s.l before reaching the stream, thus likely not having a significant influence on streamflow characteristics. In the semi-distributed mode the catchment is divided into two different hydrological response units (HRUs) (Figure 5.1), accounting for the different infiltration rates, subsurface/overland flows and vegetation of the catchment. HRU 2, an impervious rock outcrop (0.86 km<sup>2</sup>) is configured to route runoff directly to the stream (disjunct) and not to the pervious HRU 1 (1.59 km<sup>2</sup>) (Figure 5.1).

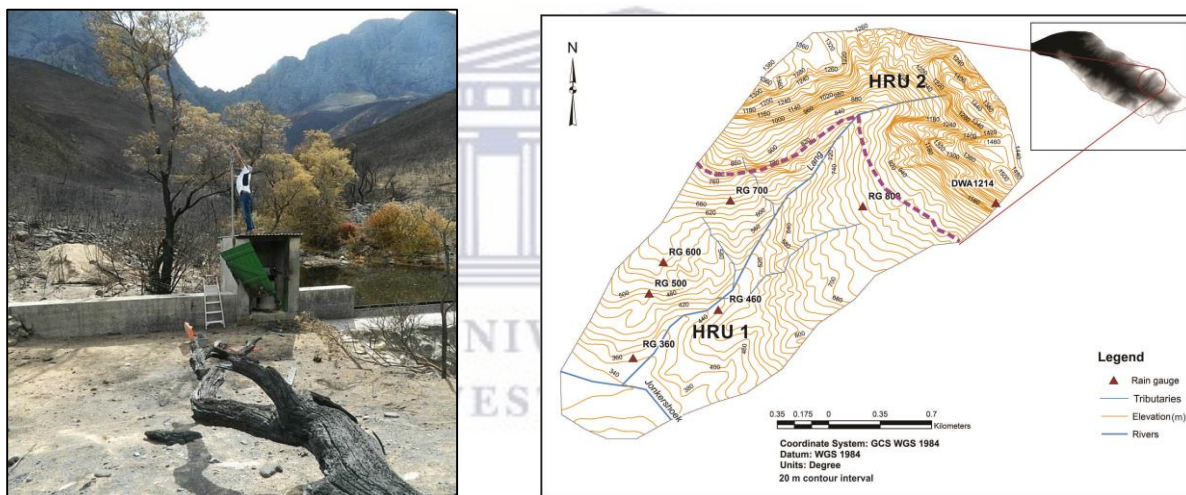


**Figure 5.1: Langrivier catchment as looking from the mouth of the catchment viewed from upstream with the rock outcrop visible (left), catchment division into the two HRUs.**

Model configuration differed mainly on the catchment being simulated as lumped or semi-distributed and different precipitation inputs (Table 5.1). In the lumped mode, precipitation for the catchment is firstly estimated using the old network (R360 and R460), and then using the new rainfall network which estimates rainfall using all the rain gauges, and then using all the rain gauges and all fog gauges. In the semi-distributed mode, HRU 1 has precipitation input (rainfall only) estimated only from rain gauges within this area and HRU 2 has precipitation input estimated using the rain gauge at 1214 m.a.s.l as these two areas receive significantly different precipitation total. For cloud water inclusion in semi-distributed mode, HRU 1 has precipitation

input (rainfall and cloud water) estimate only from the rain gauges and the fog gauges within this area and HRU 2 has precipitation input estimated using the rain gauge and fog gauge at 1214 m.a.s.l. Evaporation for HRU 1 was estimated using the ARC weather station, while for HRU 2 evaporation was estimated using the Dwasberg weather station at DWA 1214 m.a.s.l. Vegetation and soil information is required in all the lumped mode simulations and only HRU 1 when the catchment is simulated in a semi-distributed mode.

**Table 5:1: Model configuration with precipitation and model structure.**

<b>Precipitation input</b>	<b>Lumped</b>	<b>Semi-Distributed</b>
Old rainfall network	x	
New Rainfall network	x	x
New Rainfall network plus Cloud Water contribution	x	x

### 5.3 Soil input information

ACRU requires soil information on soil depths, soil retention constants i.e field capacity (FC), wilting point (WP), and porosity (PO) for the two soil water budgeting layers (A-horizon and B-Horizon). The model is directly linked to detailed soil information for South Africa (Schulze, 1995), and as a result, when no field information is available on the aforementioned soil properties, only the soil texture needs to be defined and the model generates the soil retention constants automatically. For this study, field measurements data for the A-Horizon soil properties (depth of A-Horizon, hydraulic conductivity, soil texture, soil retention curves) exist while the B-Horizon information is obtained from literature and the ACRU database.

Most of the A-horizon soil properties for the catchment were estimated from detailed field measurement in 2015 by Hans (2015). The 2015 study revealed that soil texture of the catchment is mainly sandy loam. The A-horizon depth varied from 0.16 m in the two upper sampling sites (at 700-800 m.a.s.l) to 0.80 m at the lower sampling sites (at 360-400 m.a.s.l) (Figure 3.7). The soil sampling points are spread out in the catchment and representative of the different elevation levels and thus were averaged to give an average depth of the A-horizon. The ACRU manual suggested A-Horizon and B-horizon soil retention constant for sandy loam texture such as those of Langrivier are similar (Table 5.2).

**Table 5:2: Soil water parameters for a typical South African sandy loam texture as determined by Schulze, 1994 (adopted from new 1999).**

WP 1	WP 2	FC 1	FC 2	PO 1	PO 2	ABRESP	BBRESP
0.089	0.084	0.187	0.193	0.486	0.466	0.65	0.65

The A-horizon soil retention curves revealed that the upper part of the catchment (700-800 m.a.s.l) had high draining soil capacity with the soil releasing 8-15% due to gravity which would lead to easy drainage of water during rainfall event in this part of the catchment. In the lower sites (360-400 m.a.s.l ) of the catchment, the drainage of soils was low at 1-5% water released as result of gravity. The catchment has a relatively high porosity as indicated by the bulk densities ranging between 0.89-1.49 g/cm<sup>3</sup> and relatively high organic content with all six sites having at least one sample with 5% organic content. The hydraulic conductivity was variable in the catchment, with a range of 0.1-1 m/day. It is, however, important to note that Hans (2015) conducted the study after the fire of March 2015, and thus the fire may have affected the soil characteristics.

The 2015 field measurements of A-horizon depths (DEPAHO) average 0.51 m contrary to the 0.22 m obtained from digital elevation maps obtained by New (1999). Such a difference highlights the importance of having detailed direct field measurements to improve the accuracy of parameter calibrations. The Hans (2015) did not measure B-horizon depths although there was no B-horizon encountered at the higher elevation sampling sites. The B-horizon depth (DEPBHO) through calibration showed that a depth of 0.7 to 1 m led to adequate simulations (New, 1999). B-Horizon soil retention constants i.e field capacity (FC2), wilting point (WP2), porosity (PO2) will be exclusively estimated using default values of sandy loam soil texture in ACRU as given in Table 5.2, while A-horizon will also use the Hans 2015 field study for calibration.

#### **5.4 Precipitation input**

ACRU requires precipitation (mm) data at daily time scales. Precipitation input (daily rainfall and cloud water) characteristics for the catchment are described in Chapter 4. Thus, this section only describes briefly how precipitation input for the model was derived. For ACRU input, average daily precipitation input was estimated using the Thiessen polygons interpolation

method. Firstly, the old rain gauge network (R360 and R460) was used to estimate daily catchment precipitation (rainfall). Secondly, catchment precipitation input (rainfall) was estimated using all the rain gauges. Lastly, catchment precipitation (rainfall and cloud water) was estimated using all the rain gauges and fog gauges.

## **5.5 Flow routing configuration**

The fraction of total stormflow (QFRESP and is  $\leq 1.0$ ) that will run off from the catchment on the same day as the rainfall event is generally high for small steep catchments (Schulze, 1995). Flow routing for this catchment was setup such that most of the effective rainfall would runoff on the same day. The ACRU groundwater coefficient (COFRU) cannot be measured directly from the field and thus may be adjusted to within reasonable ranges. The model developers recommend a starting value of 0.02 for small catchments, such as Langrivier, with a range of 0.005 to 0.05 (Schulze, 1995). The effective critical depth of soil (m) (SMDDP) from which stormflow generation takes place, is normally deep for catchment dominated by the “push-through method” such as Langrivier. The ACRU manual recommend 0.2 to 0.4 SMDDP value for shallow rooted vegetation, high infiltration soils, with a ‘push through’ flow mechanism catchments such as Langrivier (Schulze, 1995).

## **5.6 Evaporation input**

Daily reference evaporation (A-pan equivalent) was estimated using the Penman-Monteith equation and input directly after being calculated. As stated in Chapter 2, in ACRU total evaporation from vegetation and the soil surface can be modelled either jointly or separately. In this study they were modelled jointly. When the catchment was simulated in lumped mode, evaporation was calculated by using average temperature, wind speed, solar radiation and relative humidity obtained from both the Swartboschkloof and Dwarberg weather stations. When the catchment was simulated in distributed mode, evaporation for HRU 1, temperature, wind speed, solar radiation and relative humidity data was obtained from the Swartboschkloof weather station weather station located at the bottom of the Langrivier catchment. For HRU 2, data on temperature, wind speed, solar radiation and relative humidity from the weather station at Dwarberg (1214 m.a.s.l) was used to estimate potential evaporation. As the temperature, wind speed, solar radiation and relative humidity data was obtained from stations located at the bottom

and at higher elevation from the catchment, no correction factor for elevation was applied. Evaporation from soil and plants was estimated as an entity in the model.

## 5.7 Vegetation input

Vegetation information required by ACRU model includes leaf area index (LAI), root mass distributions in the top and subsoil horizons (by ROOTA and ROOTB), rainfall interception characteristics, the critical fraction (f) of plant available water at which stress occurs, and maximum (effective) rooting depth in the subsoil horizon (EFRDEP). For the Langrivier catchment, there is limited information on the required vegetation characteristics. The Kouga Mesic Proteoid fynbos was chosen as the vegetation type from the ACRU database. The Kouga Mesic Proteoid fynbos was chosen as the closest vegetation analogy of the Protea dominated fynbos found in Langrivier. Both are evergreen sclerophyllous vegetation types dominated by members of the Proteaceae family. The vegetation characteristics monthly values of water use coefficients (CAY), canopy interception per rain day (VEGINT), root mass distribution in the topsoil (ROOTA) and subsoil (ROOTB), coefficient of initial abstractions (COIAM) and index of suppression of soil water evaporation by a litter/mulch layer (PCSUCO) of the Mesic Proteoid fynbos are given in Table 5:3

**Table 5:3: Monthly values of water use coefficients, canopy interception per rain day, root mass distribution in the topsoil, coefficient of initial abstractions and index of suppression of soil water evaporation by a litter/mulch layer of the Mesic Proteoid fynbos**

January	February	march	April	may	June	July	august	September	October	November	December
CAY	0.45	0.45	0.5	0.6	0.6	0.6	0.6	0.6	0.55	0.5	0.45
COIAM	0.3	0.3	0.3	0.3	0.3	0.3	0.3	0.3	0.3	0.3	0.3
VEGINT	0.8	0.8	0.9	0.9	0.9	0.9	0.9	0.9	0.8	0.8	0.8
ROOTA	0.8	0.8	0.8	0.8	0.8	0.8	0.8	0.8	0.8	0.8	0.8
ROOTB	0.2	0.2	0.2	0.2	0.2	0.2	0.2	0.2	0.2	0.2	0.2
PCSUCO	100	100	100	100	100	100	100	100	100	100	100

## 5.8 Model Calibration and Validation

Soil and flow routing parameters were the only aspects of the ACRU model that were subject to calibration. A and B-horizon depths (DEPAHO and DEPBHO), Field capacity (FC), wilting point (WP), porosity (PO), COFRU, QFRESP, and SMDDP of the two soil water budgeting layers were subjected to manual calibration. Calibration revealed that streamflow control



variables (COFRU, QFRESP, and SMDDP) influenced the total simulated flows and peak characteristics differently and in varying degrees. As indicated in Chapter 2, COFRU cannot be measured directly from the field, was initially calibrated at 0.005 to 0.05 as suggested in the ACRU manual. COFRU values between 0.005 to 0.02 led to a substantial underestimation of streamflow i.e both peak flows and low flows. A value of 0.04 was eventually found to be adequate for this small catchment. Quickflow (QFRESP) of small steep mountainous catchments is generally high, and for this catchment, a value less than 0.70 led to simulated peak flows occurring earlier than observed flows, and thus a value of 0.70 led to good simulations. The effective critical depth of soil (m) (SMDDP) from which stormflow generation takes place was initial set at 0.40, closely to the depth of the A-horizon as recommended in the ACRU manual and a value of 0.40 or more led to simulated streamflow peaking quicker than observed. Table 5.4 shows the final parameters deemed to be adequate of streamflow control variables, and soil parameters deemed to be representative of catchment characteristics.

**Table 5:4: Final ACRU model input parameter values for Langrivier modelling**

<u>Locational information</u>				<u>Streamflow simulation control variables</u>					
CIARA	ELEV	ALAT	ALONG	COFRU	SMDDEP	QFRESP			
2.45	950	33.97	18.98	0.04	0.20	0.70			
<u>Soil information</u>									
DEPAHO	DEPBHO	WP1	WP2	FC1	FC2	PO1	PO2	ABRESP	BFRESP
0.51	0.70	0.068	0.093	0.143	0.189	0.432	0.448	0.75	0.95

As the available data is only two and half years, model validation was not performed as the precipitation data, critical in this study, was only collected using the full set (seven rain gauges) for a period of one years. As noted in Chapter 2, there was a fire in the catchment on the 9<sup>th</sup> to 16<sup>th</sup> of March 2015 which burned all the vegetation in the site. As a result, validation of the modelling results was not undertaken as a change in the catchment physiographic characteristics would lead to a different hydrological system than the calibration of the results. The modeling exercise was undertaken from 3 March 2013 to 17 June 2015, the period from 9 March 2015 to 17 June 2015 had minimal rainfall and thus would not significantly affect the results. It is important to note that while the new rain gauge network was only installed in May 2014, the rainfall results indicating that rainfall measured at 360-800 m.a.s.l is similar allows for a longer period (3 March 2013 to 17 June 2015) of simulations. As rainfall is similar at 360-800 m.a.s.l

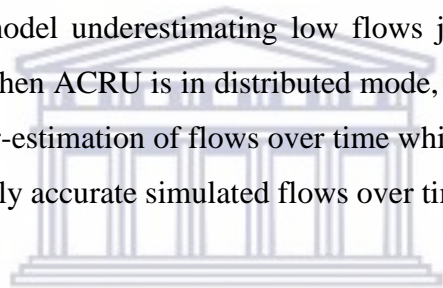
altitudinal range, the precipitation input file from 3 March 2013 to May 2014 has rainfall input only from rainfall station RG 360, RG 460 and DWA 1214. Thereafter, the precipitation file also includes the new rainfall information from rain gauges RG 500, RG600, RG 700, and RG 800.

## **5.9 Hydrographs characteristics of streamflow modelling**

With the model configured in a lumped mode with precipitation input derived from the old rain gauge network only (Lumped + Old network), precipitation derived from the new network (Lumped +New rainfall network) and precipitation derived from the new rain gauge network and cloud water (Lumped + New rainfall and cloud water network) hydrograph characteristics i.e timing of peak, recession curve are generally similar (Figure 5.2 and Figure 5.4). In the three lumped simulations (Lumped + Old network), (Lumped +New rainfall network) and (Lumped + New rainfall and cloud water network) ACRU does not simulate the peak flows well (Figure 5.2 to Figure 5.4). In simulation (Lumped + Old network) and (Lumped +New rainfall network), the simulated flow seems to consistently underestimate flows (particularly peak flows) throughout the two and half years. In addition, the model has a sharp recession curve when compared with the observed flow. This sharp recession curve leads to the model underestimating low flows just after a rainfall event. This sharp recession curve characteristic may not be as a result of incorrect precipitation input as suggested by New (1999); as precipitation input has been improved. The model's linear representation of groundwater contribution (COFRU) to total runoff may be the cause of this pattern in this case. There is a peak in the simulated flow for the rainfall event of 12<sup>th</sup> November 2014 that does not show up in the observed streamflow record, this may be caused by malfunction of the streamflow measurement instrument as an examination of streamflow records during this period shows that streamflows were being recorded. The accumulated flows show that when ACRU is in lumped mode, the inclusion of cloud water to precipitation input leads to over-estimation of flows over time while the exclusion of cloud water to precipitation leads to underestimation of flows over time.

When the model was configured in a semi-distributed state with precipitation input derived from the new network (Distri+ New Rainfall network) and precipitation derived from the new rain gauge network and cloud water (Distri+ New Rainfall network and cloud water) there is an improvement in the peak flow simulations (Figure 5.5 and Figure 5.6). In simulation (Distri+ New Rainfall network), the simulated flow has improved with peak flows being simulated better.

Figure 5.5 shows that the model still has a sharp recession curve when compared with the observed flow. Overall, simulations of daily peak flows of streamflow of the catchment in distributed mode have visually improved in comparison to the catchment simulated in lumped mode. In simulation (Distri+ New Rainfall network and cloud water) the simulated flows give the impression that peak flow simulation has improved throughout the two and half years, albeit the simulated flow seems to over-estimate some observed peaks Figure 5.6. For instance, December 2014 which had 96% of precipitation in the high altitude station DWA 1214 coming from cloud water, has four peaks in the simulated flows that are non-existent in observed streamflow records. In addition, simulations (Distri+ New Rainfall network) and (Distri+ New Rainfall network and cloud water) the model still has a sharp recession curve when compared with the observed flow, as was the case within simulations (Lumped + Old network), (Lumped +New rainfall network) and (Lumped + New rainfall and cloud water network). This sharp recession curve leads to the model underestimating low flows just after a rainfall event. The accumulated flows show that when ACRU is in distributed mode, the inclusion of cloud water to precipitation input leads to over-estimation of flows over time while the exclusion of cloud water to precipitation leads to relatively accurate simulated flows over time.



UNIVERSITY of the  
WESTERN CAPE

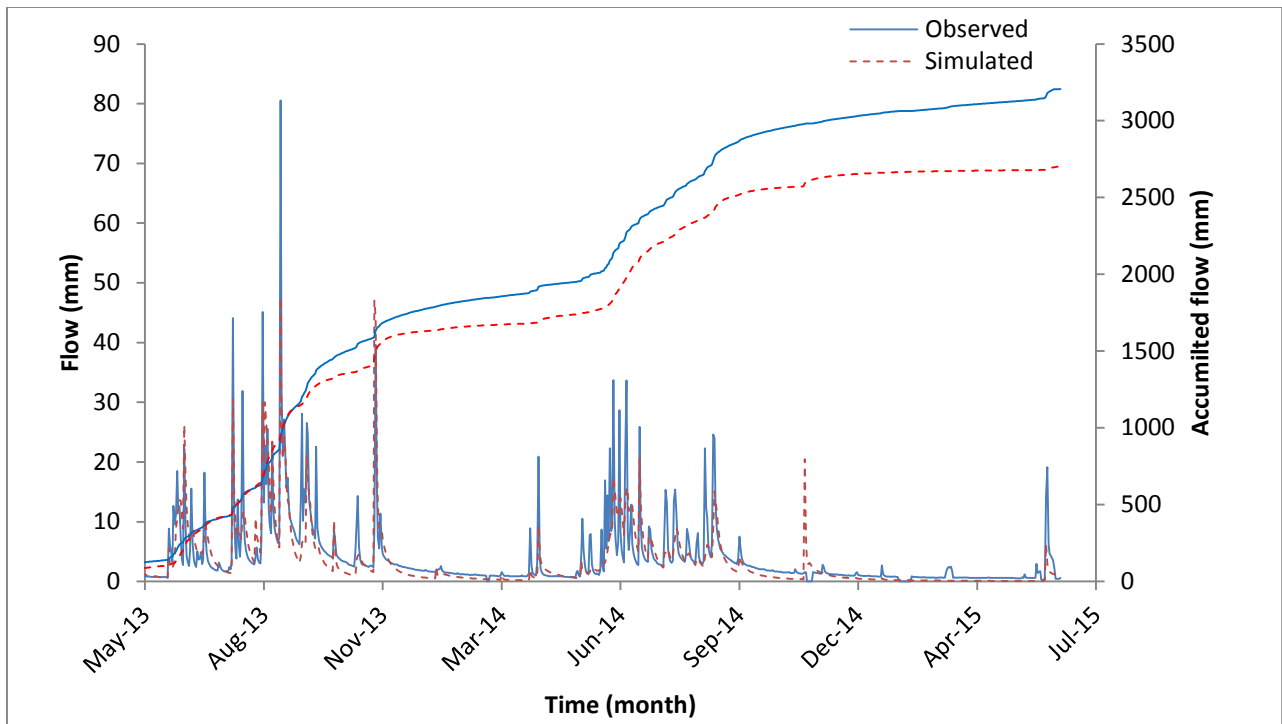


**Figure 5.2: Simulated vs observed flows for the Langrivier stream with ACRU Lumped + precipitation from old rain gauge network.**

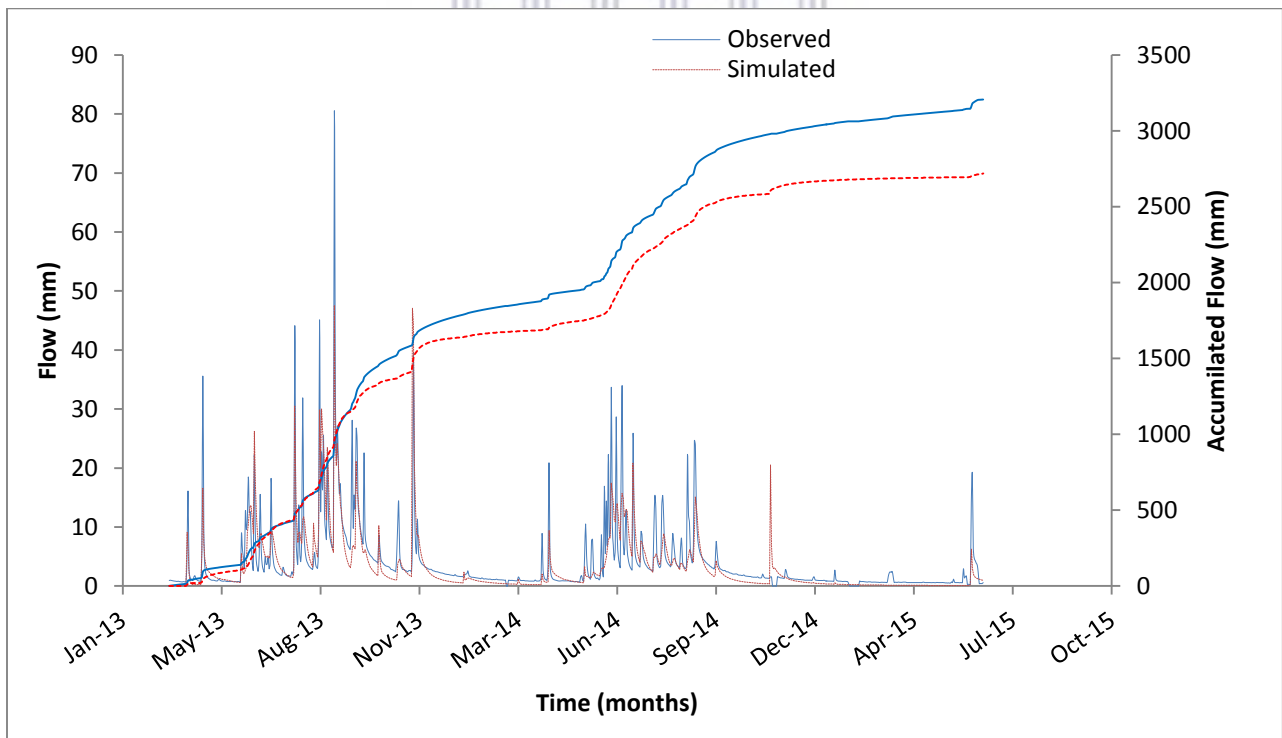


**Figure 5.3: Simulated vs observed flows for the Langrivier stream with ACRU Lumped + precipitation from new rain gauge network**

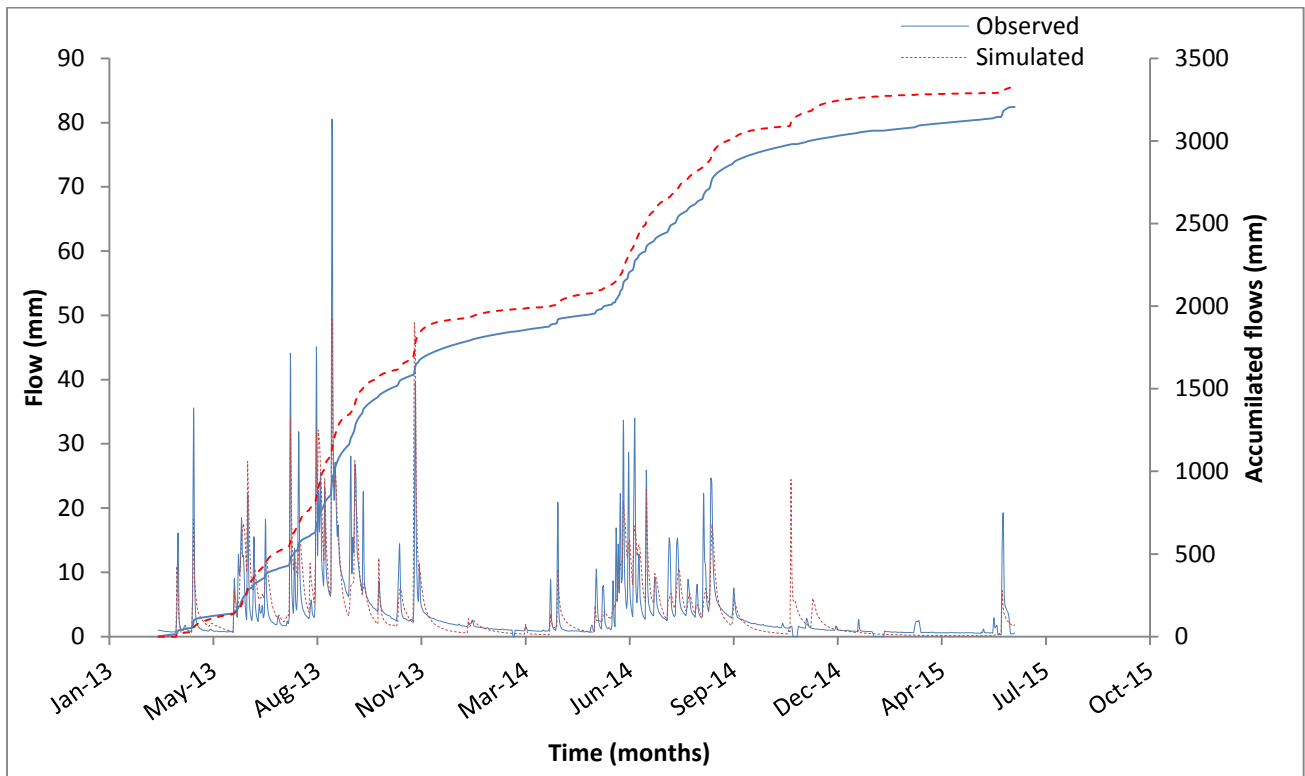


**Figure 5.4: Simulated vs observed flows for the Langrivier stream with ACRU Lumped + Precipitation from rainfall and cloud water**

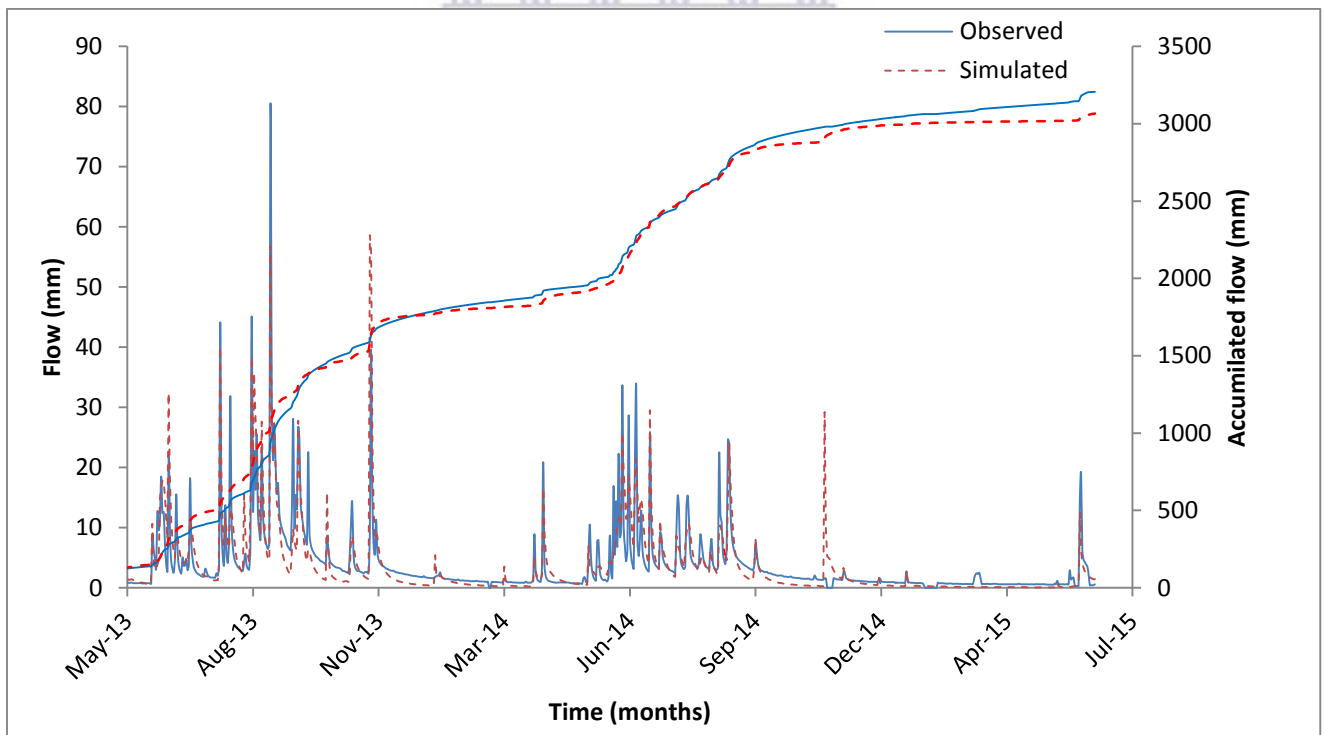


**Figure 5.5: Simulated vs observed flows for the Langrivier stream with semi-distributive + precipitation from new rainfall network.**

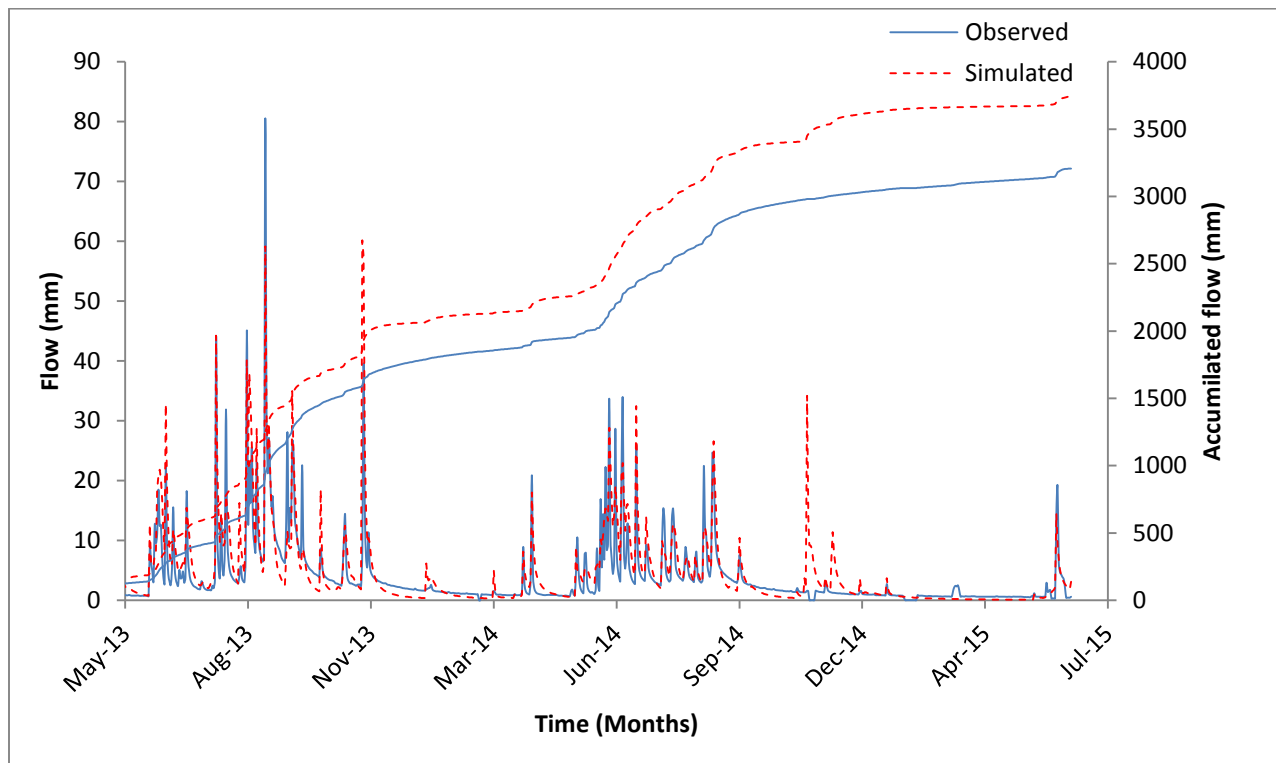


**Figure 5.6: Simulated vs observed flows for the Langrivier stream with semi-distri + precipitation from new rainfall network and cloud water.**

### 5.10 Analysis of flow duration curves

Based on the frequency flow duration curves graphs, one can deduce that ACRU under-simulates low flows for all the simulations in summer (Figure 5.7). ACRU consistently underestimates low flows by around 50% for 5-80% percentage exceedance. Only from 85% to 100% percentage exceedance, does the model overestimate low flows by almost 100%. The tendency of ACRU to underestimate low flows in all configurations (a= Lumped + old rainfall network, b= Lumped + New rainfall network, c= Lumped + Precipitation from rainfall and cloud water, d= Distri+ New Rainfall network, and e= Distri+ New Rainfall network and cloud water) may be caused by the characteristic of the model to consistently underestimate the recession curve after a rainfall event as indicated in Figures 5.2 and 5.6. The characteristic of the model consistently underestimating recession curve possibly indicates that the linear representation of groundwater's contribution to runoff may be the cause of this problem as groundwater contribution to streamflow is not always linear.

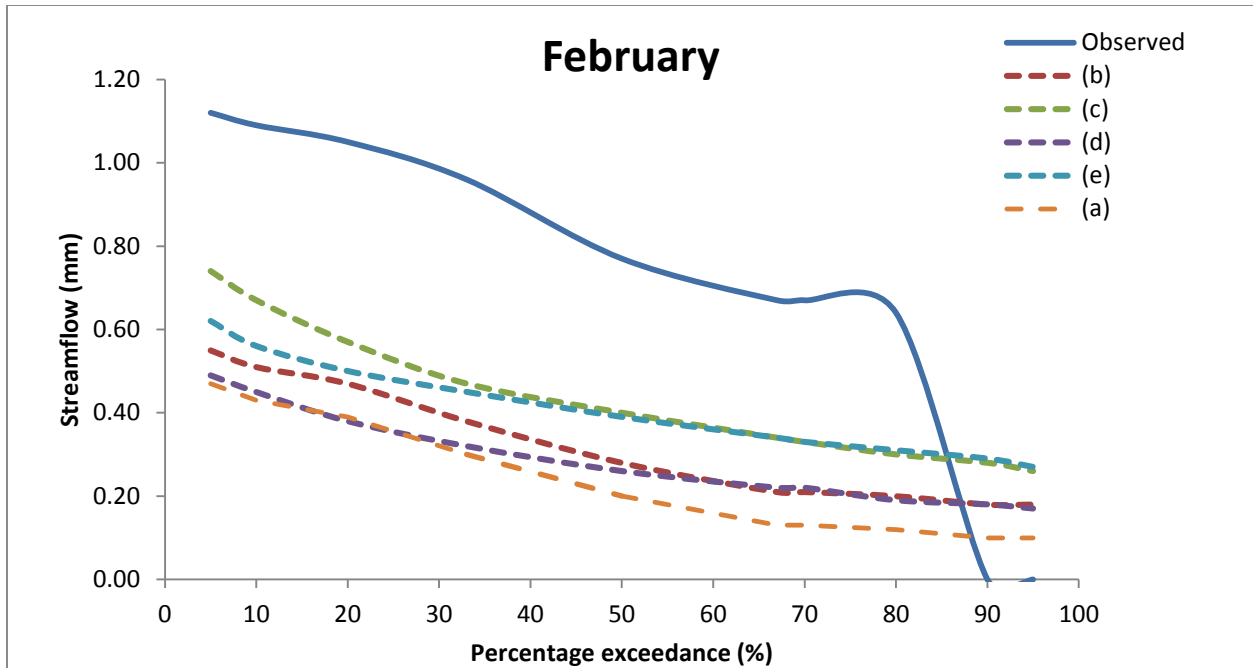


**Figure 5.7: Frequency flow duration curves for a dry month (February) in Langrivier using the five different model configurations.**

In the wet season (August) the model simulates streamflow adequately (Figure 5.8). There are no substantial differences in the frequency flow duration curves in all simulation when compared with the observed. Observed flow duration curves show that the percentage exceedances of the highest flow 26 mm is 5% while the frequency of having flows of 4 mm and less in winter is 65%. In simulation (a) which is Lumped + old rainfall network has the highest underestimation of flows. Simulated flow duration curves of simulation (c) (Lumped + Precipitation from rainfall and cloud water) and (e) (Distri+ New Rainfall network and cloud water) show that the inclusion of cloud water to precipitation input causes the model to overestimates high and low flows. In contrast Simulation (b) (Lumped +New rainfall network), fits generally well with the observed flow duration curve for both high flows. Similarly, simulation (d) (Distri+ New Rainfall network), simulates low flows well, albeit high flows are slightly overestimated. These improved frequency duration curves in winter highlight that groundwater contribution may not be critical to streamflow hydrograph characteristics in winter, with rainfall being more influential.

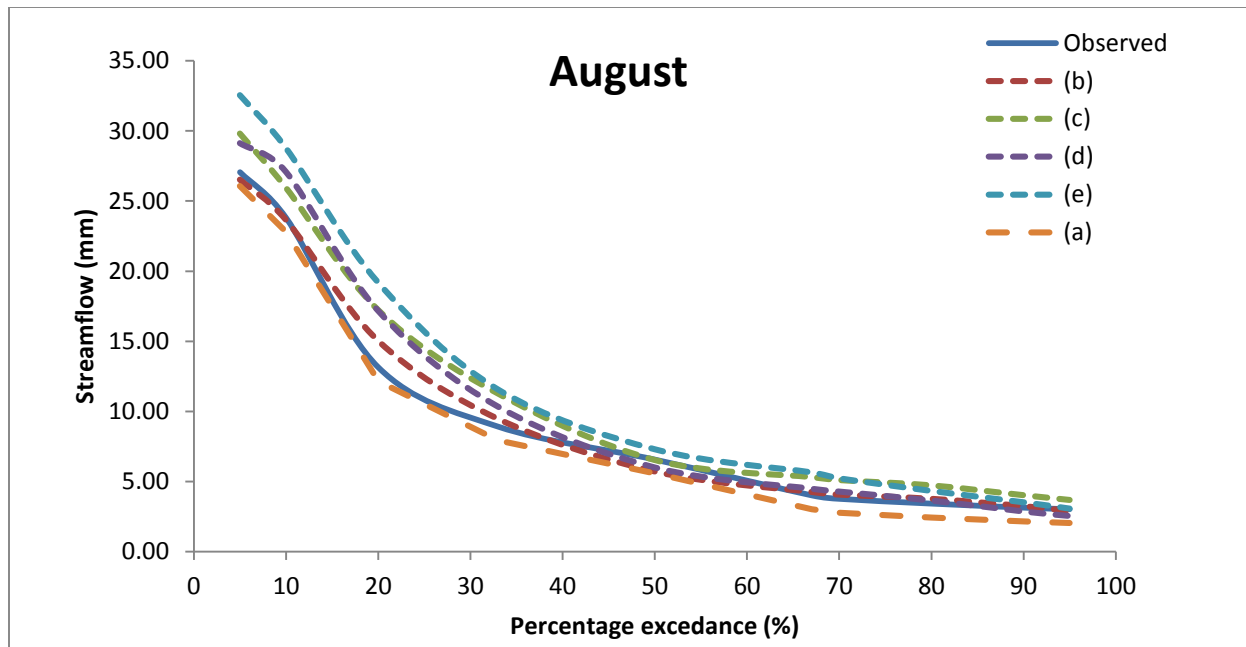


**Figure 5.8: Frequency flow duration curves for wet month (August) in Langrivier using all the five different model configurations**

### 5.11 Statistical results of streamflow modelling

This section presents results of the modeling of streamflows based on the above described model configuration, calibrations and hydrograph characteristics. As stated modelling configuration differ only on whether the model was simulated lumped or semi-distributed and the different precipitation inputs. Average daily observed flow vs average simulated daily flow is adequate as per evaluation criteria of difference between means for only two of the simulations (Lumped + New rainfall and cloud water network) and (Distri+ New Rainfall network) (Table 5.4). The model underestimates average daily streamflow for a simulation where rainfall is the only precipitation input (Lumped+ New Rainfall network), (Lumped+ New Rainfall and cloud water network) and (Distri+ New Rainfall network). When cloud water is included to the precipitation there model overestimates average streamflows.

Total root means square errors (RMSE) are relatively high for all simulations; all RMSEs are not less than half of the standard deviation (StD) of 6.25 as per the evaluation criteria (Table 5.4). The desired RMSE value should be close to zero and based on that, one can deduce that simulation (Distri+ New Rainfall network) has the best value in comparison to the other simulations although there does not appear to be a significant difference between the RMSE



values of the simulations. However, the PBIAS have significant differences in the level of over/underestimation of average daily streamflows. For instance, PBIAS simulation (Lumped+ New Rainfall network) underestimates observed flows by 15.21 % while simulation (Distri+ New Rainfall network and cloud water) overestimates by a similar value at -16.84, a difference of 32.50% between the two simulations. Overall the PBIAS values show that the model is predicting streamflow adequately and all simulations are within the evaluation criteria which state that a PBIAS of 25 is good. The simulations with the best PBIAS values are simulations (Lumped+ New Rainfall and cloud water network) and (Distri+ New Rainfall network).

Simulating streamflow of Langrivier catchment with precipitation input file comprising of improved rainfall only (simulation Distri+ New Rainfall network ) leads to the best simulation results of all the five simulation results with the goodness of fit results for the coefficient of determination of 0.70, correlation coefficient 0.84 and Nash E 0.67 (Table 5.5). However, simulating streamflow with improved precipitation data (rainfall and cloud water) with ACURU in semi-distributed mode (Simulation Distri+ New Rainfall network and cloud water); a simulation that was expected (as it accounted for all possible precipitation in the catchment as well as the rock outcrop) to produce even better results when compared to simulation (Distri+ New Rainfall network) had the poorest simulation results. The goodness of fit simulation values for Distri+ New Rainfall network and cloud water simulation for correlation coefficient and Nash E were 0.70 and 0.62, the lowest while the coefficient of agreement was the highest for all scenarios with a value of 0.91. Simulation (Distri+ New Rainfall network) indicate that streamflows are overestimated consistently i.e accumulated flows. Thus, some of the precipitation (cloud water) may not be reaching the stream directly as indicated in the time series of simulation (Distri+ New Rainfall network and cloud water) Figure 5e, possibly suggesting that cloud water may be important for other processes.

**Table 5:5: Summary of model evaluation statistics results for the five different simulations.**

Evaluation statistic	Lumped + precipitation from old rain gauge network (a)	Lumped + precipitation from new rain gauge network (b)	Lumped + Precipitation from rainfall and cloud water (c)	Semi-distri + precipitation from rainfall new network (d)	Semi-distri + precipitation from rainfall and cloud water (e)
Observed Mean (mm)	3.89	3.89	3.89	3.89	3.89
Simulated mean (mm)	3.05	3.30	4.04	3.72	4.55
% between means	30	15.21	-3.88	4.39	-16.8
Standard Dev. (orbse)	6.25	6.25	6.25	6.25	6.25
RMSE	3.93	3.74	3.74	3.57	3.84
PBIAS	25.32	15.21	-22.51	4.39	-16.84
r	0.68	0.80	0.81	0.84	0.7
NSE	0.60	0.64	0.64	0.67	0.62
R <sup>2</sup>	0.61	0.65	0.66	0.77	0.71

### 5.12 Influence of cloud water on evaporation rates

As substantial quantities of cloud water interception that were recorded by the fog station at 1214 m.a.s.l do not seem to influence streamflow hydrograph characteristics (Lumped+ New Rainfall and cloud water network, Distri+ New Rainfall network and cloud water), such cloud water amounts may be critical for evaporation rates in the catchment. As such, climate variables (daily average temperature, relative humidity, solar radiation, wind speed using the Dwarsberg weather station data) on days (10 Sep 2014, 3 Dec 2014 and 28 Dec 2014) that had substantial cloud water amounts and days (1 Sept 2014, 16 Sept 2016, 7 Dec 2014 and 2 Feb 2015) without substantial cloud water amounts were compared in order to determine the influence of cloud water on evaporation rates. The comparison of the climate variables shows that average temperature, solar radiation, wind speed do not have a distinct pattern, while cloud water increases relative humidity (Table 5.6). The evaporation (mm) results calculated using the Penman-Monteith equation suggest that that cloud water increases relative humidity and decreases air temperature which ultimately leads to low daily evaporation rates on days that have cloud water presence (Table 5.6).

**Table 5:6: Influence of cloud water on evaporation rates in the Langrivier catchment.**

Date	Average Temp (Deg Cels)	% Average Rel. Humidity	Solar Radiation, MJ/m <sup>2</sup>	Wind Speed, m/s	Rainfall (mm)	Cloud Water Interception (mm)	Evaporation (mm)
1-Sep-2014	16.51	25.08	39.61	1.11	0.00	0.00	3.88
10-Sep-2014	6.39	99.90	12.56	6.27	0.00	51.20	0.53
16-Sep-2014	15.39	41.80	33.15	1.34	0.00	0.00	4.10
3-Dec-2014	9.18	100.00	15.48	11.97	0.51	93.89	0.92
7-Dec-2014	21.56	54.40	72.78	2.93	0.00	0.00	11.07
28-Dec-2014	12.51	95.70	56.31	6.71	0.00	33.90	3.59
2-Feb-2015	14.65	59.79	63.15	6.07	0.00	0.00	7.10

### 5.13 Discussion: Streamflow modelling

Based on the hydrographs characteristics, flow duration curves, and goodness of fit statistics of the five different modeling configurations adequately predicted streamflows as per the criteria defined in Chapter 3. When the catchment was simulated in a lumped mode, with precipitation input being either rainfall only (simulation Lumped+ Old Rainfall network and Lumped+ New Rainfall network) or both rainfall and clouds (simulation Lumped + New rainfall and cloud water network), there was no marked improvement and no marked difference between the simulations in terms of NSE and RMSE. In simulations (Lumped+ Old Rainfall network) and (Lumped+ New Rainfall network), observed flows consistently had higher values when compared to simulated flows. In contrast, simulation (Lumped + New rainfall and cloud water network) had the opposite of simulation (Lumped+ Old Rainfall network) and (Lumped+ New Rainfall network), with simulated flows consistently having higher values of daily mean flows. The identical model evaluation characteristics for simulation (Lumped+ New Rainfall network) and (Lumped + New rainfall and cloud water network) indicate that inclusion of cloud water leads to overestimation of streamflows. The over-simulations in simulation (Lumped + New rainfall and cloud water network) when precipitation input includes cloud water suggest that cloud water does not directly contribute to streamflows. Simulating streamflow in semi-distributed mode, simulations improved.

The observed flows compared to simulated flows hydrographs, accumulated flows, PBIAS, and flow duration curves demonstrate that the most accurate simulation of all the five simulations

was simulation (Distri+ New Rainfall network). Simulation (Distri+ New Rainfall network) showed that improved catchment rainfall and accounting for the rocky outcrop improved streamflow prediction, and flow duration curves of this showed that ACRU slightly over-estimated wet season high flows while substantially underestimating low flows in the dry season. The low flows under-estimation of streamflow suggests that the model consistently had a sharp recession curve in comparison to observed flows. Also, the accumulated flows of simulation (Distri+ New Rainfall network) are the most closely matching of all simulations.

Simulation (Distri+ New Rainfall network and cloud water), similar to simulation (Lumped + New rainfall and cloud water network) in configurations except for delineation of the catchment to account for the rock outcrop, had highest over-estimation in all simulations. Simulation (Distri+ New Rainfall network and cloud water) had the highest precipitation quantity, with the inclusion of cloud water at the highest elevation point as part of the precipitation input into HRU2. Thus, simulation of peak flows was expected to be improved drastically. Consequently, peak flows simulation was improved considerably nevertheless the model also simulated peaks that were non-existent in observed flows. For instance, in figure 5.6, December 2014 has two peaks that are pronounced while there is no change in observed flows. Looking closely at the precipitation data, on two occasions in this month the fog gauge at 1214 m.a.s.l recorded over 90 mm of precipitation captured as cloud water interception but this does not show in observed streamflow. This possibly indicates that cloud water interception may not be reaching the stream. Furthermore, a comparison of comparative statistics of observed flows versus simulated flows in simulation (Distri+ New Rainfall network and cloud water) revealed that observed flows consistently had lower values than simulated flows, and flow duration curves showed that simulated flows over-estimated high flows.

Flow duration curves demonstrate that ACRU simulates flows better on wet season month (August) and dry season month (February). In a dry month (February), ACRU under-estimated low flows for all simulations. Underestimation of low flows might be as a result of the ACRU model's inability to simulate baseflow adequately, the model has a baseflow control function that cannot be directly measured and is constant which is not the case in reality. In contrast, the wet month of August showed that the model generally over-estimated high flows for simulation Lumped + New rainfall and cloud water network, simulation Distri+ New Rainfall network and

Distri+ New Rainfall network and cloud water. Overestimation of the wet period has also been reported by (Everson, 2001). Everson (2001) noted that ACRU did not adequately simulate baseflow dominant catchments such as Langrivier. New (1999) partly attributed overestimation of wet months by ACRU to be caused by the models inability to simulate adequately the ‘wetting up’ of the catchment.

The current study had poorer results when compared with New (1999) streamflow predictions of streamflows. New (1999) simulated streamflow in a lumped mode, and had better simulation results when compared with this study for both when the model was configured in a lumped or semi-distributed form. However, there were few differences in the model versions used New (1999) and this study. The main difference between the two studies is that the model version used in New (1999) had an interflow parameter and the model version used in this study does not have the interflow parameter. Thus, the interflow parameter may have influenced the simulation results of New (1999) significantly, as it probably led to flow mechanism that is similar to the Langrivier catchment. Also, a study by Reed et al. (2006) highlights that, although lumped models generally outperformed distributed models, factors such as model formulation, parameterization, and the skill of the modeler can have a bigger impact on simulation accuracy.

Cloud water presence, which is dependent on wind direction and wind speed, is important for reducing evaporation rates. The presence of cloud water at the highest elevation point increases relative humidity which leads to decrease in evaporation rates. Figuera et al. (2013) also found that the presence of orographic clouds and fog increases the relative humidity, decreases the insolation and temperature, thereby decreasing water use by plants. Thus, cloud water presence in the highest elevation point possibly decreases water use by plants in the Langrivier catchment.

Overall, the five simulations involving improved estimation catchment precipitation (rainfall and cloud water interception) showed that improved estimation of catchment rainfall improves prediction of streamflows. Simulating the catchment in lumped mode (simulation a, b) and semi-distributed mode (Simulation d) also highlighted that the rock outcrop in Langrivier is important for the catchment hydrological responses, although previous studies indicated that the catchment flow mechanisms is predominantly subsurface. However, the inclusion of cloud water interception (Simulation Lumped + New rainfall and cloud water network and Distri+ New

Rainfall network and cloud water) caused overestimation on observed streamflows, indicating that cloud water is not contributing directly to streamflow

## **6 Conclusions and recommendations**

Improving accurate estimation of catchment rainfall characteristics (quantity, intensity, duration, and storm direction) has been at the heart of the science of hydrology for decades (Singh 1997, Buytaert et al. 2006). Accurate information about rainfall characteristics, which vary spatially and temporally, is critical particularly in mountain catchments (Buytaert et al. 2006, Bitew and Gebremichael 2010; Anctil et al. 2006; Goodrich et al. 1995). Mountain catchments provide valuable amounts of water to the human populations particularly in South Africa where 83.3 % of water used in South Africa comes from surface water i.e rivers (Colvin, et al. 2013).

The specific objectives of this thesis were to improve estimation of catchment precipitation of the Langrivier catchment to ultimately accurately predict streamflows. The rain gauge network monitoring rainfall at the Langrivier was assumed to be the reason for poor predictions of streamflows in the Langrivier (New, 1999; Manamathela, 2012). As a result, the rain gauge network was expanded to include higher elevation points in the catchment. The results indicated that rain gauges R360 and R460 were only representative for catchment rainfall from about 360 to 800 m.a.s.l, and not representative of rainfall at elevation point 1214 m.a.s.l. The expansion of rain gauge network to higher elevations (1214 m.a.s.l) improved estimation of catchment rainfall. Thus, such results albeit a longer period of monitoring is desirable; suggest that one rain gauge placed at the lower area (360- 800 m.a.s.l) of Langrivier catchment is sufficient for adequate estimation of rainfall for that part of the catchment.

Cloud water contribution to total precipitation results revealed that cloud water contributes substantially to total precipitation at elevation point 1214 m.a.s.l (over 1250 mm). Further examination of cloud water data revealed that wind speeds 3.8 m/s or more and a south east wind direction is critical for cloud water quantity. The presence of cloud water generally increased relative humidity which led to a decrease in evaporation rates. Through the expansion of the rain gauge network and monitoring cloud water, this study successfully improved the estimation of catchment precipitation. Ultimately improved the estimation of catchment precipitation (rainfall

and cloud water) was used to predict streamflows of the Langrivier stream using the ACRU hydrological model with five different model configurations.

The best streamflow modeling results were achieved by simulating the catchment in semi-distributed mode and accounting for variable rainfall input and different runoff generating mechanisms of the Langrivier catchment. Modeling streamflow with the inclusion of cloud water contribution to total precipitation led over-estimation of streamflows. Overestimation of streamflow with inclusion cloud water as precipitation input suggested that cloud water does not directly contribute to streamflow hydrograph characteristics in the Langrivier catchments. Overall, streamflow modeling results demonstrated that the ACRU model simulated streamflows successfully as per evaluation criteria

In conclusion, the study achieved its aim to contribute towards an improved understanding of the spatial and temporal variation of different forms of precipitation in the Langrivier and Jonkershoek mountain catchment and their influence on hydrological responses. The study has improved the understanding of the spatial and temporal variation of rainfall by determining that rainfall does not vary significantly in the 360-800 m.a.s.l altitudinal range. Furthermore, the rainfall results suggest that a rain gauge network has to monitor highest elevation points in a catchment as such points significantly influence the accuracy of rainfall estimation. Cloud water contribution to total precipitation in the Langrivier catchment is only substantial at higher elevations (1214 m.a.s.l) and not in the 360-800 m.a.s.l altitudinal range.

The streamflow modelling results revealed that the configuration of the model into a lumped or distributed model has a profound influence on the accuracy of predicting streamflows. Furthermore, streamflow modelling suggested that although cloud water contribution to total precipitation may be substantial at higher elevations, cloud water does not directly contribute to streamflow characteristics. Cloud water may be important for reducing evaporation rate in the Langrivier catchment. In addition, although not investigated in this study, cloud water may be important for soil moisture content.

It is recommended that a longer monitoring period is needed for the results of improved estimation of catchment rainfall and cloud water contribution to total precipitation to be conclusive. As cloud water does not seem to contribute directly to streamflow, an isotopic study

to trace the flow paths of cloud water to further enhance the understanding of cloud water in the hydrological processes of the Langrivier catchment is recommended. The ACRU model had a deficiency in representing groundwater by a linear constant. This catchment has been shown to have throughflow as the main runoff generation mechanism (Midgley and Scott 1994). However, there is limited information on groundwater and throughflow information. As a result, modeling streamflow without comprehensive throughflow and groundwater information would be a challenge no matter which type of model was used to predict streamflows. Therefore, it is recommended that detailed studies of throughflow and groundwater characteristics be conducted in order to allow for use of a hydrological model more representative of throughflow and groundwater characteristics such as the MIKE-SHE model.



UNIVERSITY *of the*  
WESTERN CAPE



## 7 References

- Abbott M.B., Bathurst J.C., Cunge J.A., O'Connell P.E., and Rasmussen J. 1986. An introduction to the European Hydrological System — Systeme Hydrologique Europeen, “SHE”, 1: History and philosophy of a physically-based, distributed modelling system. *Journal of Hydrology* 87 (1-2): 45-49
- Allen R.G. Pruitt W.O., Wright J.M., Howell T.A., Ventura F., Snyder R., Itenfisu D., Steduto P., Berengena J., Yrisarry J.B., Smith M., Pereira L.S., Raes D., Perrier A., Alves I., Walter I., and Elliott R. 2006. A recommendation on standardized surface resistance for hourly calculation of reference ETo by the FAO56 Penman-Monteith method. *Agricultural Water Management* 81: 1–22
- Anderson A.E., Weiler M., Alila Y., and Hudson R.O. 2009. Subsurface flow velocities in a hillslope with lateral preferential flow. *Water Resources Research* 45
- Andreassian V., Perrin C., Michel C., Usart-Sanchez I., and Lavabre J. 2001. Effect of imperfect rainfall knowledge on the efficiency and the parameters of catchment models. *Journal of hydrology* 250: 206-223
- Anctil F., Lauzon N., Andreassian V., Oudin L., and Perrin C. 2006. Improvement of rainfall-runoff forecasts through mean areal rainfall optimization. *Journal of Hydrology* (328): 717– 725
- Arnold J.G., Moriasi D.N., Gassman P.W., Abbaspour K.C., White M.J., Srinivasan R., Santhi C., Harmel R.D., van Griensven A., Van Liew M.W., Kannan N., and Jha M.K. 2012. SWAT: model use, calibration, and validation. *American Society of Agricultural and Biological Engineers* 55(4): 1491-1508
- Bain L. J. and Engelhardt M. 1992. Introduction to probability statistics and mathematical statistics 2nd edition. Duxbury press, an imprint of Wadsworth publishing company. Belmont, California.
- Bales R.C., Molotch N.P., Painter T.H., Dettinger M.D., Rice R., and Dozier J. 2006. Mountain hydrology of the western United States. *Water resources research*, 42: 08432
- Bell V.A., and Moore R.J. 2000. The sensitivity of catchment runoff models to rainfall data at different spatial scales. *Hydrology and earth science systems* 4 (4): 653-667

- Bellerby T., Todd M., Kniveton D., Kidd C. 2005. Rainfall Estimation from a Combination of TRMM Precipitation Radar and GOES Multispectral Satellite Imagery through the Use of an Artificial Neural Network. *Journal of applied meteorology* 39:2115-2128
- Bennett, B. M., and Kruger, F. J. 2013. Ecology, forestry and the debate over exotic trees in South Africa. *Journal of Historical Geography* 42: 100 – 109
- Berndtsson R., and Niemczynowicz J. 1988. Spatial and temporal scales in rainfall analysis - Some aspects and future perspectives. *Journal of Hydrology* 100: 293-313
- Beven, K.J. 2001. Rainfall-Runoff modelling: The Primer, John Wiley and Sons Ltd, England.
- Bergström S. and Graham L.P. 1998. On the scale problem in hydrological modelling. *Journal of Hydrology* 211: 253–265
- Beyene E.G. and Meissner B. 2010. Spatio-temporal analyses of correlation between NOAA satellite RFE and weather stations' rainfall record in Ethiopia. *International Journal of Applied Earth Observation and Geoinformation* 12: 69–75
- Bezuidenhout C. N. 2005. Development and Evaluation of Model-Based Operational Yield Forecasts in the South African Sugar Industry, Ph.D. thesis, University of KwaZulu-Natal, South Africa.
- Bitew M.M., and Gebremichae M. 2010. Spatial variability of daily summer rainfall at a local-scale in a mountainous terrain and humid tropical region. *Atmospheric Research* 98: 347–352
- Blocken B., Carmeliet J., and Poesen J. 2005. Numerical simulation of the wind-driven rainfall distribution over small-scale topography in space and time. *Journal of Hydrology* 315: 252–273
- Booyesen, P.V., and Tainton, N.M. 1984. Ecological Effects of Fire in South African Ecosystems Ecological Studies, Springer Verlag, Berlin. 48
- Bonell M. 1998. Selected challenges in runoff generation research in forests from the hillslope to headwater drainage basin scale. *Journal of the American Water Resources Association* 34 (4): 765-785

- Butterworth J.A., Schulze R.E., Simmonds L.P., Moriarty P., and Mugabe F. 1999. Hydrological processes and water management in a dry land environment IV: Long-term groundwater level fluctuations due to variation in rainfall. *Hydrology and Earth system sciences* 3(3): 353-361
- Buytaert W., Celleri R., Willems P., De Bièvre B., and Wyseure G. 2006. Spatial and temporal rainfall variability in mountainous areas: A case study from the south Ecuadorian Andes. *Journal of Hydrology* 329: 413– 421
- Bruijnzeel L., Eegster W., and Burkard R. 2005. Fog as a hydrologic input. Encyclopedia of Hydrological Sciences. Edited by M G Anderson. John Wiley & Sons, Ltd.
- Bradley R.S. and Jones P.D. (1995). Climate since A.D.1500. II New fether lane, London, EC4D
- Britton, D. L. 1991. The benthic macroinvertebrate fauna of a South African mountain stream and its response to fire. *South African Journal of Aquatic Science* 17: 51–64
- Brunetti M., Maugeri M., and Nanni T. 2001. Changes in total precipitation, rainy days and extreme events in northeastern Italy. *International Journal of Climatology* 21: 861–871
- Chen F., and Liu C. 2012. Estimation of the spatial rainfall distribution using inverse distance weighting (IDW) in the middle of Taiwan. *Paddy Water Environ* 10:209–222
- Cheng K., Lin Y., and Liou J. 2008. Rain-gauge network evaluation and augmentation using geostatistics. *Hydrological processes* 22: 2554–2564
- Cheng C., Cheng S., Wen J., and Lee J. 2012. Effects of raingauge distribution on estimation accuracy of areal rainfall. *Water Resource Manage* 26: 1–20
- Ciach G.J., and Krajewski W.F. 2006. Analysis and modeling of spatial correlation structure in small-scale rainfall in Central Oklahoma. *Advances in Water Resources* 29:1450–1463
- Colvin C., Nobula S., Haines I., Nel J., Le Maitre D., and Smith J. 2013. An introduction to South Africa's source areas. WWF South Africa report.

- Dawson T.E. 1998. Fog in the California redwood forest: Ecosystem inputs and use by plants. *Oecologia* 117: 476–485.
- Dettinger M., Redmond K., and Cayan D. (2004). Winter Orographic Precipitation Ratios in the Sierra Nevada—Large-Scale Atmospheric Circulations and Hydrologic Consequences. *Journal of Hydrometeorology* 5: 1102-1116
- Didszun J. and Uhlenbrook S. 2008. Scaling of dominant runoff generation processes: Nested catchments approach using multiple tracers. *Water Resources Research*, (44)
- Dye P.J. and Croke B.F.W. 2003. Evaluation of streamflow predictions by the IHACRES rainfall runoff model in two South African catchments. *Environmental Modelling & Software* 18: 705–712
- Everson C.S. 2001. The water balance of a first order catchment in the montane grasslands of South Africa. *Journal of Hydrology* 241:110–123
- Forbes K.A., Kienzle S.W., Coburn C.A., Byrne J.M., and Rasmussen J. 2011. Simulating the hydrological response to predicted climate change on a catchment in southern Alberta, Canada. *Climatic Change* 105: 555–576
- Franchini M. Wendling J., Obled C., and Todini E. 1996. Physical interpretation and sensitivity analysis of the TOPMODEL. *Journal of Hydrology* 175: 293-338
- Frumau K.F.A., Burkard R., Schmid S., Bruijnzeel L.A., Tobon-Marin C., and Calvo J. 2006. Fog gauge performance under fog and wind-driven rain conditions. To be published in L.A. Bruijnzeel (ed.), *Mountains in the Mist: Science for Conserving and Managing Tropical Montane Cloud Forests*
- Figueira C., Manazes de Sequeira M., Vasconcelos R., and Prada S. 2013. Cloud water interception in the temperate laurel Forest of Madeira Island. *Hydrological sciences journal* 58: 152-161
- Gan T.Y., Dlamini E.M., and Biftu G.F. 1997. Effects of model complexity and structure, data quality, and objective functions on hydrologic modeling. *Journal of Hydrology* 192: 81-103

- Gomez-Peralta D., Oberbauer S.F., McClain M.E, and Philippi T.E. 2008. Rainfall and cloud-water interception in tropical montane forests in the eastern Andes of Central Peru. *Forest Ecology and Management* 255: 1315–1325
- Goodrich D. C. 1990. Geometric simplification of a distributed rainfall-runoff model over a range of basin scales. Ph.D. thesis. The University of Arizona.
- Goodrich D.C., Faures J.M., Woolhisera D.A., Lanea L.J., and Sorooshian S. 1995. Measurement and analysis of small-scale convective storm rainfall variability. *Journal of Hydrology* 173: 283-308
- Goovaerts P. 2000. Geostatistical approaches for incorporating elevation into the spatial interpolation of rainfall. *Journal of Hydrology* 228: 113–129
- Gumindoga W., Rwasoka D.T. and Murwira A. 2011. Simulation of streamflow using TOPMODEL in the Upper Save River catchment of Zimbabwe. *Physics and Chemistry of the Earth* 36: 806–813
- Gumindoga W., Rientjes T.H.M., Haile A.T., and Dube T. 2015. Predicting streamflow for land cover changes in the Upper Gilgel Abay River Basin, Ethiopia: A TOPMODEL based approach. *Physics and Chemistry of the Earth* article in press
- Gurtz J., Zappa M., Jasper K., Lang H., Verbunt V., Badoux A., and Vitvar T. 2003. A comparative study in modelling runoff and its components in two mountainous catchments. *Hydrological Processes* 17: 297–311
- Gurtz J. Zappa M., Jasper K., Lang H., Verbunt M., Badoux A., and Vitvar T. 2003. A comparative study in modelling runoff and its components in two mountainous catchments. *Hydrological Processes* 17: 297–311
- Hans D. 2015. Spatial variation of soil physical properties and soil water characteristics of the Langrivier catchment in Jonkershoek nature reserve. Honours project, Unpublished. University of the Western Cape, South Africa.
- Helsel D.R. and Hirsch R.M. 2002. Statistical methods in water resources. Techniques of Water-Resources Investigations of the United States Geological Survey. Book 4, Hydrologic Analysis and Interpretation.

- Holder C.D. 2003. Fog precipitation in the Sierra de las Minas Biosphere Reserve, Guatemala. *Hydrological processes* 17: 2001–2010
- Holwerda F., Bruijnzeel L.A., Muñoz-Villers L.E., Equihua M. and Asbjornsen H. 2011. Rainfall and cloud water interception in mature and secondary lower montane cloud forests of central Veracruz, Mexico. *Journal of Hydrology* 384: 84–96
- Hughes D. A. 2004. Incorporating groundwater recharge and discharge functions into an existing monthly rainfall–runoff model/Incorporation de fonctions de recharge et de vidange superficielle de nappes au sein d’un modèle pluie-débit mensuel existant. *Hydrological Sciences Journal* 49(2): 297-311
- Hughes D. A. 200). Comparison of satellite rainfall data with observations from gauging station networks. *Journal of Hydrology* 327: 399– 410
- Hughes D. A., Andersson L., Wilk J., and Savenije H.H.G. (2006). Regional calibration of the Pitman model for the Okavango River. *Journal of Hydrology* 331: 30– 42
- Hughes D.A and Slaughter A. 2015. Daily disaggregation of simulated monthly flows using different rainfall datasets in southern Africa. *Journal of Hydrology: Regional Studies* (4): 153–171
- Hrachowitz M. and Weiler M. 2011. Uncertainty of precipitation estimates caused by sparse gaging networks in a small, mountainous watershed. *Journal of Hydrologic Engineering* 16(5): 460-471.
- Jayakrishnan R., Srinivasan R., Santhi C., and Arnold J.G. 2005. Advances in the application of the SWAT model for water resources management. *Hydrological processes* 19: 749–762
- Kapangaziwiri E. 2007. Revised parameter estimation methods for the pitman monthly rainfall-runoff model. MSc dissertation. Rhodes University, South Africa.
- Kapangaziwiri E., and Hughes D.A. 2008. Towards revised physically based parameter estimation methods for the Pitman monthly rainfall-runoff model. *Water SA* (34)
- Kidd C, Kniveton D.R., Todd M.C., and Bellerby T.J. 2003. Satellite rainfall estimation using combined passive microwave and infrared algorithms. *Journal of hydrometeorology* 4: 1088-1104

- Kienzle S.W. 2011. Effects of area under-estimations of sloped mountain terrain on simulated hydrological behaviour: a case study using the ACRU model. *Hydrological processes* 25: 1212–1227
- Koren V.I., Finnerty B.D., Schaake J.C., Smith M.B, Seo D.J., and Duan Q.Y. 1999. Scale dependencies of hydrologic models to spatial variability of precipitation. *Journal of Hydrology* 217: 285–302
- Krause P., Boyle D.P., and Base F. 2005. Comparison of different efficiency criteria for hydrological model assessment. *Advances in Geosciences* 5: 89–97
- Lentz R.D., Dowdy R.H., and Rust R.H. 1995. Measuring wind and low-relief topographic effects on rainfall distribution. *American Society of Agricultural Engineers* 11 (2): 241-248
- Lerwarne M. 2009. Setting up ArcSwat hydrological model for the Verlorenvlei catchment. MSc dissertation. University of Stellenbosch, South Africa.
- Madsen H. 2000. Automatic calibration of a conceptual rainfall–runoff model using multiple objectives. *Journal of Hydrology* 235: 276–288
- Manamathela S. 2012. Hydrological Response of a fynbos and Pine afforested catchment. Honours project, unpublished. University of the Western Cape, South Africa.
- Marloth R. 1903. Results of experiments on Table Mountain for ascertaining the amount of moisture deposited from the South-East clouds. Transactions of the South African philosophical society. Plate IV
- Marloth R. 1905. Results of further experiments on Table Mountain for ascertaining the amount of moisture deposited from the South-East clouds. Transactions of the South African philosophical society. Plate I
- Mazvimavi D. 2003. Estimation of flow characteristics of ungauged catchment. PhD Thesis. Wageningen University, Netherlands.
- McGlynn B.L. and McDonnell J.J. 2003. Quantifying the relative contributions of riparian and hillslope zones to catchment runoff. *Water resources research*, 39 (11): 1310

- McJannet D., Wallace J., and Reddell P. 2007. Precipitation interception in Australian tropical rainforests: II. Altitudinal gradients of cloud interception, stemflow, throughfall and interception. *Hydrological Processes* 21: 1703–1718
- Midgley J.J. and Scott D.F. 1994. The use of stable isotopes of water (D and <sup>18</sup>O) in hydrological studies in the Jonkershoek valley. *Water SA* 20:2
- Moriasi D.N., Arnold J.G., Van Liew M.W., Bingner R.L., Harmel R.D., and Veith T.L. 2007. Model evaluation guidelines for systematic quantification of accuracy in catchment simulations. *American Society of Agricultural and Biological Engineers* 50(3): 885–900
- Moses G. 2008. The establishment of the long-term rainfall trends in the annual rainfall patterns in the Jonkershoek valley, Western Cape, South Africa. MSc dissertation, University of the Western Cape, South Africa.
- Mugabe F.T., Chitata T., Kashaigili J., and Chagonda I. 2011. Modelling the effect of rainfall variability, land use change and increased reservoir abstraction on surface water resources in semi-arid southern Zimbabwe. *Physics and Chemistry of the Earth* 36: 1025–1032
- Nandargi S., and Mulye S.S. 2012. Relationships between Rainy Days, Mean Daily Intensity, and Seasonal Rainfall over the Koyna Catchment during 1961–2005. *The Scientific World Journal*. ID 894313, doi:10.1100/2012/894313
- Navas A., Machi'n J., and Soto J. 2005. Assessing soil erosion in a Pyrenean mountain catchment using GIS and fallout <sup>137</sup>Cs. *Agriculture, Ecosystems and Environment* 105: 493–506
- Nespor V. and Sevruks B. 1998. Estimation of wind-induced error of rainfall gauge measurements using a numerical simulation. *Journal of atmospheric and oceanic technology* 16: 450-464
- New M.G. 1999. Hydrologic sensitivity to climate variability and change in the south Western Cape Province, South Africa. PhD dissertation. University of Cambridge, United Kingdom.



- Ncube M. 2006. The impact of land cover and land use on the hydrological response in the Olifants. MSc thesis. University of the Witwatersrand, South Africa.
- Ndiritu J.G. 2014. A multiplier-based method of generating stochastic areal rainfall from point rainfalls. *Physics and Chemistry of the Earth* 67–69 64–70
- Nullet D., and Juvik J.O. 1994. Generalised mountain evaporation profiles for tropical and subtropical latitudes. *Singapore Journal of Tropical Geography* 15 (1): 17–24.
- Nyssen J., Vandenreyken H., Poesen J., Moeyersons J., Deckers J., Haile M., Salles C., and Govers G. (2005). Rainfall erosivity and variability in the Northern Ethiopian highlands. *Journal of Hydrology* (311):172–187
- Perrin C, Michel C., and Andre´assian V. 2003. Improvement of a parsimonious model for streamflow simulation. *Journal of Hydrology* 279: 275–289.
- Prada S., Menezes de Sequeira M., Figueira C., and Oliveira da Silva M. 2009. Fog precipitation and rainfall interception in the natural forests of Madeira Island (Portugal). *Agricultural and Forest Meteorology* 149: 1179–1187
- Prada S., Menezes de Sequeira M., Figueira C., and Vasconceles R. 2012. Cloud water interception in the high altitude tree heath forest (*Erica arborea* L.) of Paul da Serra Massif (Madeira, Portugal). *Hydrological processes* 26: 202-212
- Razali N.M. and Wah Y.B. 2011. Power comparisons of Shapiro-Wilk, Kolomogorov-Siminov, Lilliefors and Anderson-Darling tests. *Jornal of statistical modeling and analytics* 2(1): 21-33
- Reed S., Koren V., Smith M., Zhang Z., Moreda F., Seo D., and DMIP Participants. 2006. Overall distributed model intercomparison project results. *Journal of Hydrology* 298: 27–60
- Refsgaard J.C. 1999. Parameterisation, calibration and validation of distributed hydrological models. *Journal of Hydrology* 198: 69–97
- Royappen, M. 2002. Towards improved parameter estimation in streamflow predictions using the ACURU model. MSc Thesis. University of KwaZulu-Natal, South Africa.

- Sanborn S.C. and Bledsoe B.P. 2006. Predicting streamflow regime metrics for ungauged streams in Colorado, Washington, and Oregon. *Journal of Hydrology* 325: 241–261
- Sawilowsky S.S. 2005. Misconceptions leading to choosing the t test over the Wilcoxon Mann-Whitney test for Shift in location parameter. *Journal of Modern Applied Statistical Methods* 4 (2): 598-600
- Sawunyama T. 2008. Evaluating uncertainty in water resource estimation in Southern Africa: a case study of South Africa. PhD thesis. Rhodes University, South Africa.
- Scholl M.A., Giambelluca T.W., Gingerich S.B., Nullet M.A., and Loope L.L. 2007. Cloud water in windward and leeward mountain forests: The stable isotope signature of orographic cloud water. *Water resources research* 43: W12411
- Scholl M., Eugster W., and Burkard R. 2011. Understanding the role of fog in forest hydrology: stable isotopes as tools for determining input and partitioning of cloud water in montane forests. *Hydrological Processes* 25: 353–366
- Schmidt E.J., and Schulze, R.E. 1987. SCS-based design runoff. ACRU Report No. 24. Department of Agricultural Engineering, University of Kwazulu-Natal, South Africa.
- Scott D.F., and Prinsloo F.W., Moses G., Mehlomakulu M., and Simmers A.D.A. 2000. A re-analysis of the South African catchment afforestation experimental data. Water research commission report no. 810/1/00
- Scott DF., and Prinsloo W.F. 2008. Longer-term effects of pine and eucalypt plantations on streamflow. *Water resources research*, 44, W00A08
- Schulze R.E. 1995. Hydrology and Agrohydrology: A text to accompany the ACRU 3.00 . Agrohydrological Modelling System.
- Seact J.K. 1969. Flow-Duration Curves. Manual of Hydrology: Part 2. Low-Flow Techniques. Geological survey water-supply paper 1542-A.
- Seyfried M.S. and Wilcox B.P. 1995. Scale and the nature of spatial variability: field examples having implications for hydrological modelling. *Water resources research* 31: 173-184

- Singh V.P. 1997. Effect of spatial and temporal variability in rainfall and watershed characteristics on streamflow hydrograph. *Hydrological processes* 11: 1649-1669.
- Singh J., Knapp H. V., and Demissie M. 2004. Hydrologic modeling of the Iroquois River Catchment using HSPF and SWAT. ISWS CR 2004-08. Champaign, Ill.: Illinois State Water Survey.
- Shah S.M.S., O'Connell P.E., Hosking J.R.M. 1996. Modelling the effects of spatial variability in rainfall on catchment response. 2. Experiments with distributed and lumped models. *Journal of Hydrology* 175: 89- 111
- Stonehouse J.M., and Forrester G.J. 1998. Robustness of the t and U tests under combined assumption violations. *Journal of Applied Statistics* 25 (1): 63-74
- Strangeway I. 2010. A History of Rain gauges. TerraData Ltd
- de Castro Teixeira A.H., Bastiaanssen W.G.M., Ahmad M.D., Moura M.S.B., and Bos M.G. 2008. Analysis of energy fluxes and vegetation-atmosphere parameters in irrigated and natural ecosystems of semi-arid Brazil. *Journal of Hydrology* 362: 110– 127
- Gomez-Plaza A., Martinez-Mena M., Albaladejo J., and Castillo V.M. 2001. Factors regulating spatial distribution of soil water content in small semiarid catchments. *Journal of Hydrology* 253: 211- 226
- Tennant W.J., and Hewitson B.C. 2002. Intra-seasonal rainfall characteristics and their importance to the seasonal prediction problem. *International Journal of Climatology* 22: 1033-1048
- Van Wyk D.B. 1987. Some effects of afforestation on streamflow in the Western Cape Province, South Africa. *Water SA* 13: 1
- Viessman jr W., Lewis G.L. and Knapp J.W. 1989. Introduction to hydrology 3rd edition. Harper and Row, Publishers, New York.
- Vicente-Serrano S.M., Saz-Sánchez M.A. and Cuadrat J.M. 2003. Comparative analysis of interpolation methods in the middle Ebro Valley (Spain): application to annual precipitation and temperature. *Climate research* 24: 161–180

- Vischel T., and Lebel T. 2007. Assessing the water balance in the Sahel: Impact of small scale rainfall variability on runoff. Part 2: Idealized modeling of runoff sensitivity. *Journal of Hydrology* 333: 340– 355
- Viviroli D. and Weignartner R. 2004. The hydrological significance of mountains: from regional to global scale. *Hydrology and Earth System Sciences* 8(6): 1016-1029
- Volkman T.H.M., Lyon S.W., Gupta H.V., and Troch P.A. 2010. Multicriteria design of rain gauge networks for flash flood prediction in semiarid catchments with complex terrain. *Water resources research* 46: 1-16
- Warburton M.L. 2012. Challenges in modelling hydrological responses to impacts and interactions of land use and climate change. Ph.D. thesis. University of KwaZulu-Natal, South Africa.
- Weiler M. and McDonnell J.J. 2007. Conceptualizing lateral preferential flow and flow networks and simulating the effects on gauged and ungauged hillslopes. *Water resources research* 43: W03403
- Wicht C.L. 1940. A preliminary account of rainfall in Jonkershoek. *Transactions of the Royal Society of South Africa* 28 (2): 161-173
- Wicht C.L. 1941. Diurnal fluctuations in the Jonkershoek streams due to evaporation and transpiration. *Journal of the South African Forestry Association* 7: 34-39
- Wicht C.L., Meyburgh J.C., and Bousted P.G. 1969. Rainfall at the Jonkershoek forest hydrological research station. University of Stellenbosch (44) series A
- World meteorological organization. 2008. Guide to Hydrological Practices: Volume I Hydrology – From Measurement to Hydrological Information. WMO-No. 168
- Xu C.Y. and Singh V.P. 1998. A Review on monthly water balance models for water resources investigations. *Water Resources Management* 12: 31–50
- Young I.T. 1977. Proof without prejudice: Use of the Kolmogorov-Smirnov test for the analysis of histograms from the flow systems and other systems. *The Journal of histochemistry and cytochemistry* 25 (7): 935-941

Zehe E. and Blöschl G. 2004. Predictability of hydrologic response at the plot and catchment scales: Role of initial conditions. *Water resources research*, (40), W10202, doi:10.1029/2003WR002869



UNIVERSITY *of the*  
WESTERN CAPE